PEROXIDE-CURABLE MACROMONOMER DERIVATIVES OF ISOBUTYLENE-RICH ELASTOMERS

by

Jackson McGuire Dakin

A thesis submitted to the Department of Chemical Engineering

In conformity with the requirements for the

Degree of Master of Applied Science

Queen's University

Kingston, Ontario, Canada

(January, 2014)

Abstract

Macromonomers bearing oligomerizable C=C functionality have been prepared by the nucleophilic displacement of allylic bromide functionality on brominated poly(isobutylene-co-isoprene) (BIIR). Whereas commercial grades of isobutylene-rich elastomers do not cure under the action of peroxides, these materials undergo simultaneous cross-linking and degradation when activated by radical initiators, with the competitive balance dictated by the reactivity of the oligomerizable group. Vinyl benzoate, vinyl imidazolium, and acrylate functionalities cure rapidly to high cross-link density whereas the maleimide graft is too reactive and unstable for any utility. Methacrylate and itaconate macromonomers cure to moderate extent while maleate esters and unactivated terminally unsaturated groups are unable to significantly counteract the degradation mechanism and do not afford any appreciable cross-link density to BIIR.

The most reactive macromonomers display the potential for scorch, an effect that is efficiently mitigated with the introduction of (2,2,6,6-tetramethyl-piperidin-1-yl)oxyl (TEMPO) to quench free radical cure activity. Furthermore, an acrylated adduct, AOTEMPO, is able to recover more of the cross-link density that would otherwise be lost to irreversible free radical coupling. These nitroxyls display longer than expected induction times, likely due to the catalytic nature of TEMPO when alkoxyamine decomposition is significant.

A suite of elastomeric ionomers bearing N-functional imidazolium bromide functionality have been prepared in order to investigate the N-alkylation dynamics with brominated poly(isobutylene-*co*-para-methylstyrene) (BIMS) as well as the subsequent peroxide cure activity of the reactive ionomer. A functional imidazole bearing a methacrylate group displayed moderate alkylation rate and good cure activity whereas a 4-vinylbenzyl analogue provides fast alkylation at the expense of storage stability. N-Allylimidazole is rapidly alkylated by BIMS in both

solution and solvent free processes and the resulting ionomer displays unique cure dynamics. This phenomenon is investigated by model compound polymerization and is likely due to the unique free radical reactivity of allyl imidazolium moieties. The cross-linked ionomer displays many of the beneficial physical properties associated with a hybrid ionic/covalent network including good resistance to stress relaxation and thermal stability.

Acknowledgements

First and foremost I would like to thank my supervisor and mentor, Dr. Scott Parent, for his frank, insightful, and pragmatic guidance throughout my undergraduate and graduate degrees. His advice and teaching in all things chemistry, career, and life not only made working on this project enjoyable but much more rewarding and valuable. In the same regard I would like to thank my co-supervisor, Dr. Ralph Whitney, in particular for his help with the finer side of model compound chemistry and synthesis.

I would like to acknowledge my lab-mates past and present. In particular Adam, for teaching me the basics of ionomer chemistry during my undergraduate project and forming the basis for my master's project. Your instruction and mentorship allowed me to hit the ground running in my master's and I am truly thankful for that. To my other lab-mates, Dave, Mo, Brian, Antonio, Chris, thank you for making life in the lab a pleasure and shutting off the oil bath when I forgot.

Thank you to Brenda Willis, my volleyball coach, for allowing me to excel on the court while balancing this academic undertaking. Thank you as well to my team-mates who made life at Queen's, in the gym or otherwise feel like home.

Finally, a last thank you to my family, including Flurry, who have supported me in every aspect of my life, academic or otherwise, without whom this project would never have been possible.

Table of Contents

List of Figures

List of Tables

List of Schemes

List of Abbreviations

δ – chemical shift

μmol - micromoles

AlIm - 1-allylimidazole

AOTEMPO – 4-acryloyloxy-2,2,6,6-tetramethylpiperidine-N-oxyl free radical

ATRP – atom transfer radical polymerization

BDE – bond dissociation energy

BHT – butylated hydroxytoluene

BIIR- brominated poly(isobutylene-co-isoprene)

BIMS – brominated poly(isobutylene-*co*-para-methylstyrene)

BuIm - 1-butylimidazole

Bu_4NOH – tetrabutylammonium hydroxide

$CDCl_3$ – deuterated chloroform

cm^3 – cubic centimeters

DCP – dicumyl peroxide

DDIm - 2-dodecyl-1*H*-imidazole

DMSO-d_6 – deuterated dimethyl sulfoxide

EtAlIm - 1-allyl-2-ethyl-1H-imidazole

EtBuIm - 1-butyl-2-ethyl-1H-imidazole

EtVIm - 1-vinyl-2-ethyl-1H-imidazole

eq. - equivalents

g – grams

G' – storage modulus

G'' – loss modulus

h - hours

HRMS – high resolution mass spectroscopy

Hz - Hertz

IIR – poly(isobutylene-co-isoprene)

IIR-AA – acrylate derivative of BIIR

IIR-AlImBr – N-allylimidazolium bromide derivative of BIIR

IIR-DDI – dodecyl itaconate derivative of BIIR

IIR-DDMA – dodecyl maleate derivative of BIIR

IIR-MAA – methacrylate derivative of BIIR

IIR-MBA – maleimidobenzoate derivative of BIIR

IIR-UA – undecenoate derivative of BIIR

IIR-VBA – vinylbenzoate derivative of BIIR

IIR-VImBr – N-vinylimidazolium bromide derivative of BIIR

ImEMA - 2-(1*H*-imidazol-1-yl)ethyl methacrylate

IMS - poly(isobutylene-*co*-para-methylstyrene)

IMS-AlImBr - N-allylimidazolium bromide derivative of BIMS

IMS-AlImBr-XL – cross-linked N-allylimidazolium bromide derivative of BIMS

IMS-BuImBr - N-butylimidazolium bromide derivative of BIMS

IMS-DDImBr - N-dodecylimidazolium bromide derivative of BIMS

IMS-EtAlImBr – 2-ethyl N-allylimidazolium bromide derivative of BIMS

IMS-EtBuImBr – 2-ethyl N-butylimidazolium bromide derivative of BIMS

IMS-EtVImBr– 2-ethyl N-vinylimidazolium bromide derivative of BIMS

IMS-ImEMABr - 2-(1*H*-imidazol-1-yl)ethyl methacrylate bromide derivative of BIMS

IMS-ImEMABr-XL – cross-linked 2-(1*H*-imidazol-1-yl)ethyl methacrylate bromide derivative of BIMS

IMS-UDImBr - N-undecene imidazolium bromide derivative of BIMS

IMS-VImBr – N-vinylbenzyl imidazolium bromide derivate of BIMS

IP – isoprene

Kg - kilograms

kPa - kilopascals

min - minutes

mL - milliliters

mmHg – millimeters of mercury

mmol - millimoles

mol - moles

MPa - megapascals

PhAlImBr - 3-benzyl-1-allyl-1H-imidazol-3-ium bromide

PhEtAlImBr - 3-benzyl-2-ethyl-1-allyl-1H-imidazol-3-ium bromide

PhVImBr - 3-benzyl-1-vinyl-1H-imidazol-3-ium bromide

PIB – poly(isobutylene)

ROOR - peroxide

rpm – revolutions per minute

S_N2 – bimolecular nucleophilic substitution

tanδ – loss tangent (G''/G')

TBAB – tetrabutylammonium bromide

T_g – glass transition temperature

THF - tetrahydrofuran

TEMPO - 2,2,6,6-tetramethylpiperidine-N-oxyl free radical

TEMPOH – hydroxy TEMPO

UDIm - 1-(10-undecen-1-yl**)**-1*H*-imidazole

UV – ultraviolet

VBIm – 1-(4-vinylbenzyl)-1*H*-imidazole

VIm - 1-vinylimidazole

Chapter 1

Introduction and Literature Review

1.1 Isobutylene-Rich Elastomers

Poly(isobutylene) (PIB) is an amorphous elastomer that, when cationically polymerized to molecular weights between 70 and 225 kg/mol, retains elasticity down to -50°C. Uncross-linked PIB displays several unique and valuable properties including excellent thermal and oxidative stability due to the high C-H bond dissociation energy (BDE) of the sterically accessible methyl groups [1]. Furthermore, PIB displays unique vibration dampening properties and superior gas impermeability due in part to its unusually high density, relative to other polyolefins, of 0.917 g/cm^3 [2]. Because of these properties, PIB finds use coatings, adhesives, sealants and chewing gum.

Scheme 1: The structure of common isobutylene-rich elastomers

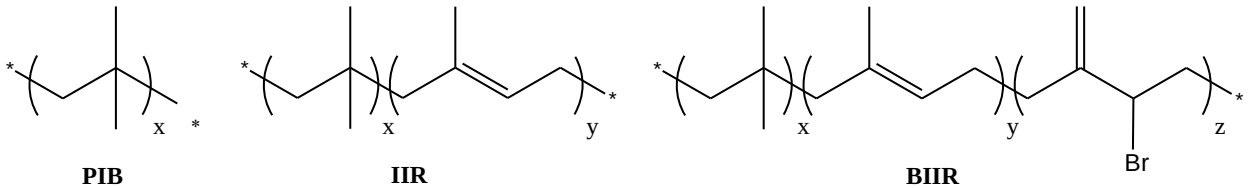

PIB **IIR** **BIIR**

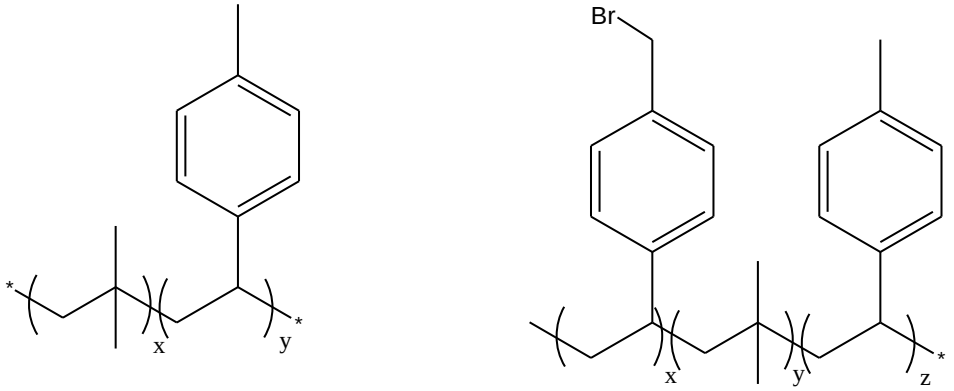

IMS **BIMS**

The main limitation of PIB is its poor reactivity towards cross-linking. Uncross-linked elastomers are viscoelastic materials whose entangled polymer chains are able to move past each other under applied stress. As such, they can deform irreversibly which limits their utility as engineering materials. The phenomenon in which an elastomer deforms permanently under constant strain is called stress relaxation, or creep if the stress is constant, both of which are major shortcomings in uncross-linked elastomers. The ability of an amorphous elastomer above its T_g to resist deformation is proportional to chain entanglements, but without covalent cross-linking these entanglements are not permanent [3]. Vulcanization, also known as curing or cross-linking, is the process by which polymer chains are covalently connected such that the chains can no longer relax under sustained load [1]. This process not only improves the elastomer's resistance to stress relaxation and creep, but also increases modulus and tensile properties.

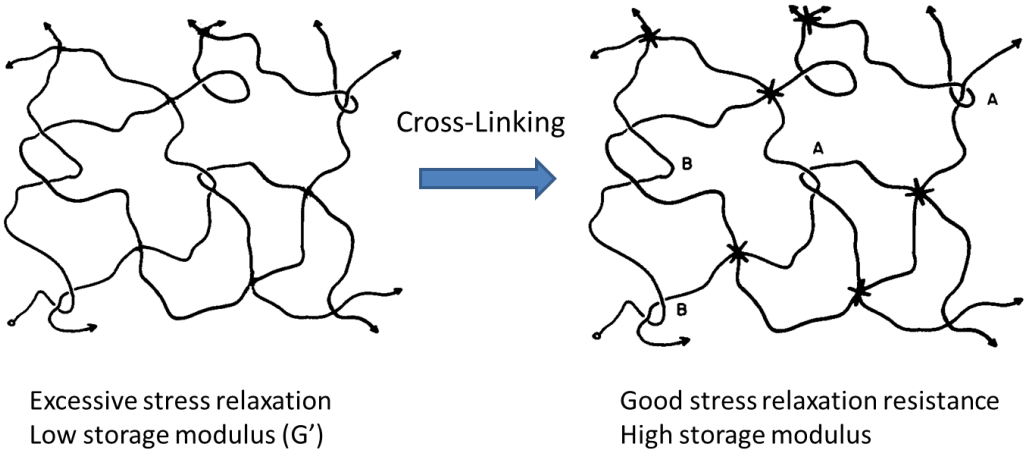

Figure 1: Elastomer cross-linking

Modulus is a measure of stiffness that is separated into two components based on the stress response to an applied sinusoidal strain [4]. The storage modulus (G') corresponds to the in phase portion of the stress response and represents energy stored elastically whereas the loss modulus (G'') is the out of phase portion and represents energy dissipated as heat. Both components

contribute to the overall physical and mechanical properties of the material. The ratio of the loss and storage moduli is labelled the loss tangent and is calculated by:

$$\tan \delta = \frac{G''}{G'}$$

Given these definitions, it follows that an ideally elastic material would have a loss tangent of 0, and an ideally viscous material's loss tangent would approach infinity. According to the kinetic theory of rubber, storage modulus is particularly useful as a measure of cross-link density, also referred to as extent of cure [5].

The deficiencies of uncross-linked PIB were first overcome in 1940 with the invention of a random copolymer with isoprene by the Standard Oil Development Company [6]. Small amounts (1-2 mol%) of isoprene mers were incorporated randomly in the cationic polymerization of isobutylene by 1,4-addition to make poly(isobutylene-co-isoprene) (IIR) [7]. IIR, which eventually became known as butyl rubber, was invented during the Second World War when feedstocks of natural rubber were limited. The small amount of unsaturated isoprene mers are amenable to further chemical modification, in particular sulfur vulcanization, which makes butyl rubber ideal for tire inner tube applications, a market in which butyl rubber still dominates. Although butyl rubber is able to cross-link with sulfur formulations similar to those used in natural rubber vulcanization, it does so at a slower rate compared to the natural rubber and poly(butadiene) materials used in other parts of the tire. In order to cure each part of the tire concurrently, the vulcanization rate of IIR needed to be accelerated [8]. This was done by brominating the isoprene mers to make brominated poly(isobutylene-co-isoprene) (BIIR) whose allylic bromide functionality is more reactive to sulfur vulcanization [8].

Another option for a rapidly curing isobutylene-rich elastomer was first explored in 1961 by copolymerizing isobutylene with vinyl benzyl chloride [8]. The benzylic chloride functionality

was introduced as an alternative reactive site to brominated isoprene mers and was expected to be more stable than BIIR. Although this technology was patented in 1975, problems with branching during polymerization as well as the high cost of the vinyl benzyl chloride starting material reduced its commercial appeal [9].

In 1989, an alternative route towards a halogenated benzylic copolymer of isobutylene was invented by copolymerizing isobutylene with para-methylstyrene [10]. This produced poly(isobutylene-*co*-para-methylstyrene) (IMS), an elastomer with better oxidative and thermal stability than butyl rubber but equally good impermeability [10]. Furthermore, up to 60% of the para-methylstyrene mers can be brominated via a single step free radical bromination [11]. The product, brominated poly(isobutylene-*co*-para-methylstyrene) (BIMS) , is comparable to BIIR in that the reactive benzylic sites are amenable to cross-linking or other chemical modification.

1.2 Chemical Modification of BIIR and BIMS

The allylic and benzylic bromide functionality of BIIR and BIMS respectively are reactive to a wide range of nucleophiles which makes them attractive for chemical modification towards functional isobutylene-rich elastomers. This process is complicated in BIIR by the susceptibility towards isomerization and dehydrohalogenation shown in Scheme 2 [12].

Scheme 2: Isomerization and elimination reactions of BIIR

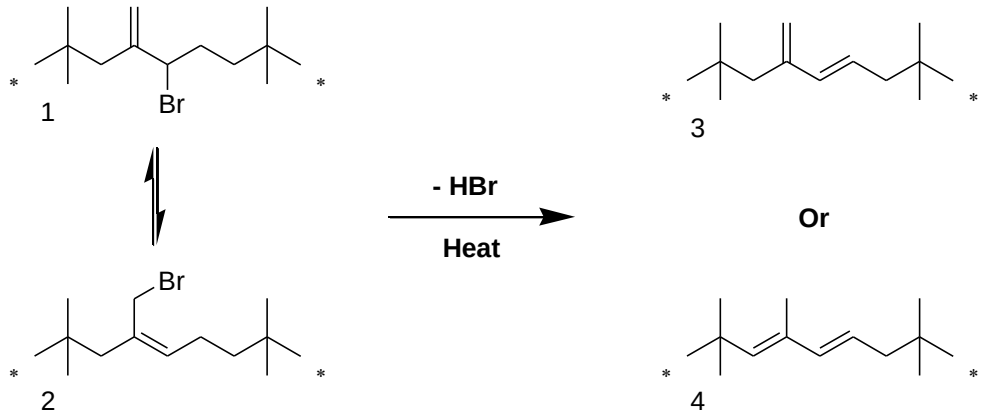

The exomethylene isomer (**1**) is the kinetically favoured halogenation product but can be isomerized at high temperature to the more thermodynamically stable endo isomer (**2**). Furthermore, in the absence of acid scavengers, thermal dehydrohalogenation leads to degradation of the rubber [13], and in the presence of acid scavengers forms conjugated dienes (**3**) and (**4**) [14]. As it has been found that the E,Z-BrMe endo isomers are more reactive to nucleophilic substitution, the exomethylene isomer can be isomerized by treatment with a Lewis acid such as zinc stearate or a bromide nucleophile such as TBAB [12] [15]. The latter proceeds via the well known S_N2' concerted allylic rearrangement [16] [17] and is very selective for the Z-endo isomer due to a preferred reactive conformation [12]. The versatility of the allylic bromide of BIIR, as seen in the literature, is illustrated in Scheme 3.

Scheme 3: The functionalization of the allylic bromide functionality in BIIR

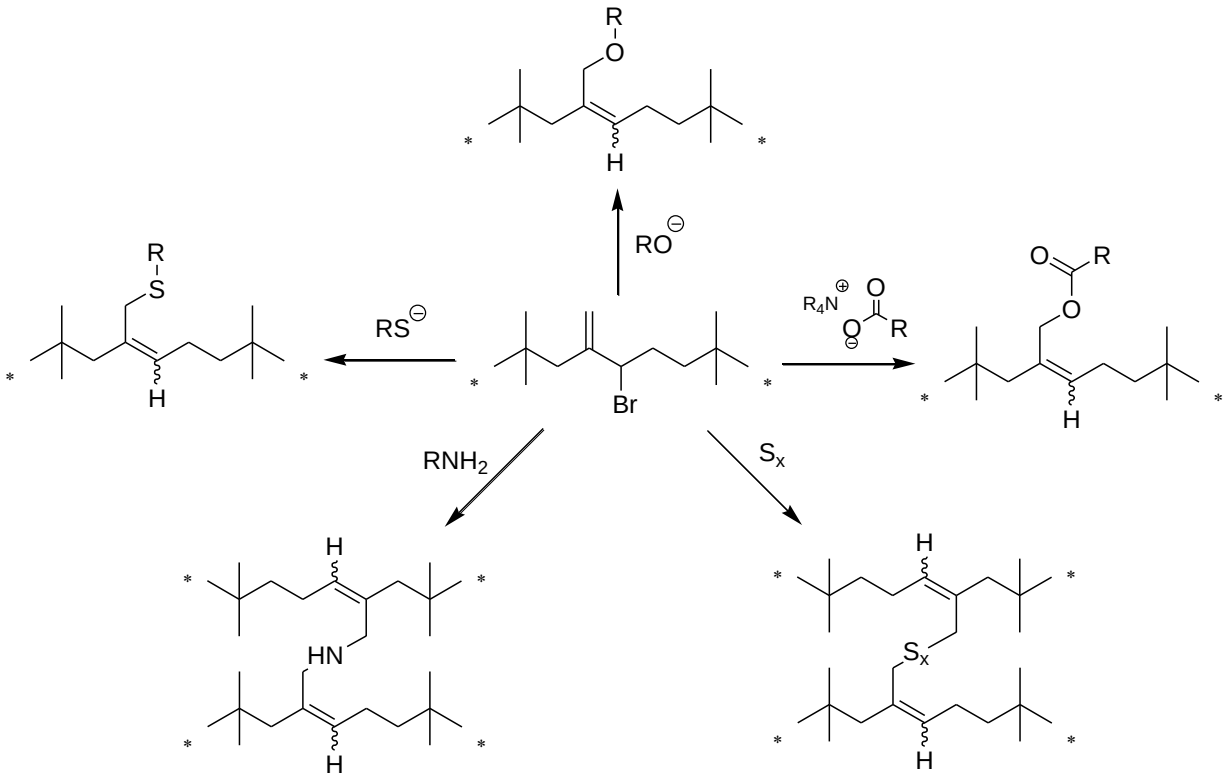

The first functionalization of butyl rubber developed, and still the most common, was sulfur cross-linking. This process has been well studied and produces covalent cross-link made up of

one (monosulfide), two (disulfide), or three or more (polysulfide) sulfur atoms per cross-link [17]. Sulfide bonds, especially of higher order, can break apart and reform during dynamic stress affording sulfur cured articles with superior dynamic mechanical properties [18]. The efficient sulfur vulcanization of rubber for tire applications, though, requires many additives such as mercaptobenzothiazoles, sulfonamides, dithiocarbamates, and thiuram polysulfides, which act as accelerators, activators, retarders, and stabilizers [19]. Not only do these additives present health and safety concerns during compounding and vulcanization itself [20], but they remain in the thermoset article as leachables and extractables. This reduces the appeal of sulfur cures in applications that require clean curing technology such as pharmaceutical or food packaging.

Oxygen nucleophiles have been used to functionalize both BIIR and BIMS. Poly(ethylene-oxide) has been grafted to BIIR using the Williamson reaction, as have aromatic alcohols by the in situ formation of tetrabutylammonium salts of phenol [21]. Tetrabutylammonium salts of carboxylic acids have also been used to form ester derivatives of BIIR by nucleophilic substitution using TBAB as a phase transfer catalyst [22] [23]. Similar methacrylate and acrylate esters were synthesized by researchers at Exxon again using TBAB salts of the acrylates in solution [24].

Thioether derivatives of BIIR have been prepared by nucleophilic substitution with thiolate ions formed in situ from thiols in the presence of a strong base [16]. Their synthesis, though, is complicated by air oxidation of thiols to disulfides which reduces yield. These functional thioether grafts have been used to covalently couple silica to BIIR, significantly improving dispersion of siliceous filler.

The nucleophilic substitution of BIIR by amines has also been studied [25]. It was shown that both primary and secondary amines can alkylate twice to form covalent cross-links in BIIR and

BIMS, although secondary amines do so more slowly. Tertiary amines are quaternized by BIIR and BIMS to form ionomers which have been shown to provide novel properties in elastomers [26].

The Suzuki-Miyaura coupling reaction was also used to graft 4-vinylphenylboronic acid to BIIR with C-C bonds [27]. This was done in solution using a palladium (II) dimer catalyst which produced endo cis and trans adducts in high yield. This method was pursued because it was argued that C-C bonds would not be susceptible to hydrolysis and therefore improve the stability of the final article.

1.3 Peroxide-Curable Derivatives of BIIR and BIMS

Cross-linking of commercially important polymers can be classified into two main classes; sulfur or peroxide vulcanization [28]. Sulfur vulcanization was first invented by Charles Goodyear in 1841 in order to cross-link natural rubber [29], leading to a rapid influx of vulcanized rubber parts in industry. Although sulfur vulcanization is ubiquitous, the mechanism is not well understood, particularly for butyl rubber which does not respond well to conventional cure accelerators [17]. The main advantage of sulfur vulcanization is the good dynamic mechanical properties afforded by labile poly(sulfide) bonds.

Peroxide cures, first discovered by Ostromislensky in 1915 [30], form carbon-carbon bonds which are much stronger than sulfur cross-links making peroxide cured elastomers less prone to stress relaxation and compression set [18]. Unlike sulfur vulcanization, peroxide can be used to cross-link fully saturated polymers like poly(ethylene) as well as those with residual unsaturation. In comparison to sulfur vulcanization, the chemistry involved in peroxide cures is well understood and has been well described [18] [31] [30]. Peroxides are often used to cure fully

saturated elastomers such as hydrogenated nitrile-butadiene rubber and ethylene-propylene copolymers by the mechanism shown in Scheme 4.

Scheme 4: A simplified mechanism for the peroxide cross-linking of saturated elastomers

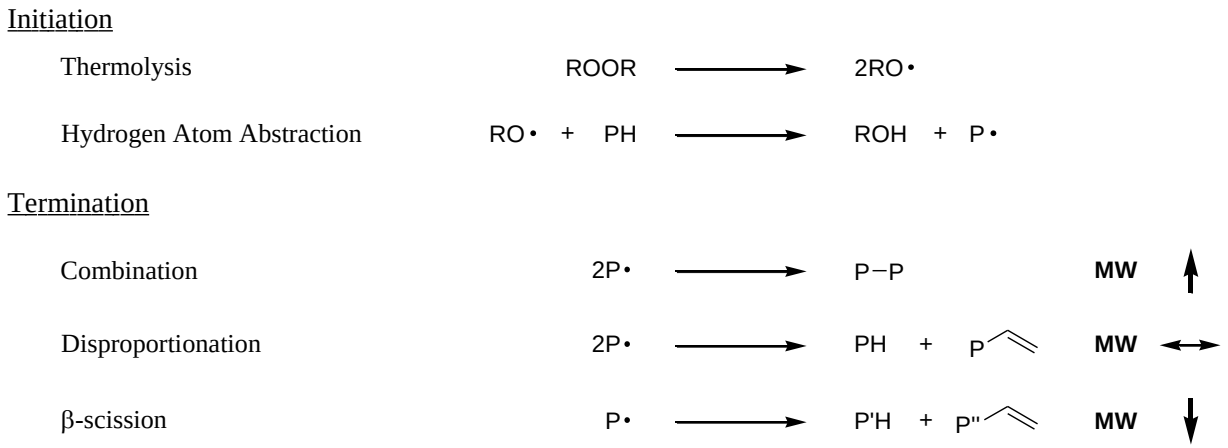

Organic peroxides decompose by first order thermolysis to form two oxygen centered radicals. The rate of thermolysis is highly dependent on temperature and the nature of the peroxide. For example, dicumyl peroxide, which is commonly used for rubber curing, has a decomposition half-life in alkane solutions of 5.5 minutes at 160°C and 43 minutes at 140°C [32]. Oxygen centered radicals are able to abstract hydrogen atoms from available sites along the polymer chain. The macroradicals formed by hydrogen atom abstraction can then undergo one of three reactions; combination to build molecular weight, disproportionation (negligible change in molecular weight), or β-scission which degrades the polymer. The propensity towards each one depends on the nature of the macroradical. The peroxide cross-linking of saturated polymers is stoichiometric, meaning that each initiating radical can form a maximum of one cross-link although in practice efficiency is less than that due to inefficiencies in hydrogen atom abstraction and disproportionation [33].

Although peroxide vulcanization is able to cure many unsaturated elastomers, β-scission is the dominant reaction for PIB leading to degradation of the polymer [34]. Hydrogen atom abstraction

occurs from the methyl groups in PIB due to steric hindrance to form unstable primary radicals which rearrange via the mechanism shown in Scheme 5.

Scheme 5: β-Scission of primary poly(isobutylene) macroradicals

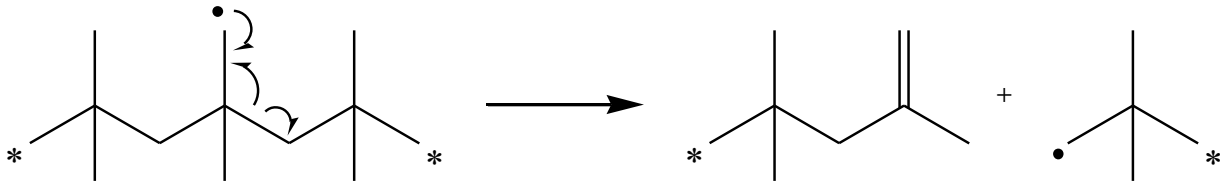

Adding isoprene to PIB, as is the case with IIR, can reduce the amount of degradation by providing a site for more efficient cross-linking, but the 1-2 mol% isoprene is not enough to counteract degradation completely and butyl rubber also degrades in the presence of peroxide [35].

Although peroxide has been used to cross-link unsaturated polymers for decades, the mechanism by which it does so is still unclear. It was originally thought that allylic hydrogen abstraction followed by combination was the only mechanism possible but extensive model compound work found that this only contributes to approximately 85% of the overall cross-link density [36] [37] [38]. The rest is attributed to C=C oligomerization by vinyl addition. This kinetic chain length explains why polybutadiene cross-links much more efficiently than polyisoprene [39].

Although oxygen centered radicals are generally good at hydrogen atom abstraction, they can also fragment into methyl radicals by a similar β-scission mechanism to that shown in Scheme 5. The balance between these reactions is heavily dependent on temperature as well as the nature of available abstractable hydrogens [40]. Note that, in general, oxygen centered radicals prefer abstraction while alkyl radicals prefer addition [41].

In the case of butyl rubber, the improved reactivity provided by the unsaturated isoprene mers is not enough to counteract degradation. In order for this balance to be overcome, at least 3 mol% isoprene needs to be incorporated to make what is known as high IP butyl rubber [35]. Introducing more isoprene is difficult because isoprene acts as a chain transfer agent in the cationic copolymerization of isobutylene and isoprene, and as such molecular weight decreases dramatically with increasing IP content [42]. Furthermore, high IP butyl rubber produces peroxide cross-linking activity at the expense of polymer stability and long-term aging properties [11], and still requires the use of co-curing agents to cure [43].

The first peroxide curable isobutylene rich elastomer was prepared by Oxley and Wilson by the copolymerization of isobutylene, isoprene, and divinylbenzene to create the terpolymer shown in Scheme 6 [44]. This approach makes use of the potential for oligomerization of pendant vinyl groups by radical addition to form cross-links and has been termed ‘macromonomer’ peroxide cross-linking. These cures produce appreciable kinetic chain length as each initiating molecule can now create several cross-links. As such, isobutylene-rich macromonomers can be cured to high extent with relatively little peroxide.

Scheme 6: The structure of an isobutylene, isoprene, and divinylbenzene terpolymer

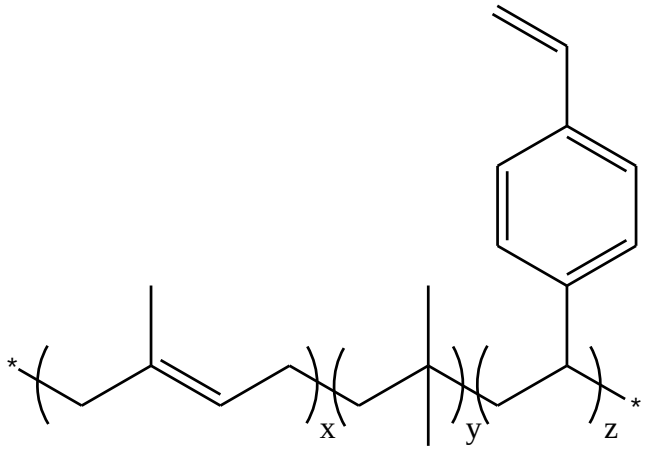

Unfortunately, the cationic polymerization of the difunctional divinylbenzene gives a polymer with significant initial cross-link density and up to 85% gel content. Although the polymer was found to cure even further with peroxide, initial gel content made this terpolymer difficult to compound and dissolve. Polysar rubber adopted this technology to produce a terpolymer with approximately 1.3 mol% cross-linked divinylbenzene, known by the trade name XL-10,000. The lowered gel content improved workability of the polymer but was still enough to render the product insoluble in many solvents and make processing difficult [45].

Most recently, the macromonomer approach has been used to make peroxide curable acrylate and vinylbenzoate grafts of BIIR [23] shown in Scheme 7. These have been shown to easily overcome the degradation reaction and provide good cross-link density without the use of coagents.

Scheme 7: Peroxide initiated cross-linking of vinylbenzoate grafted butyl rubber

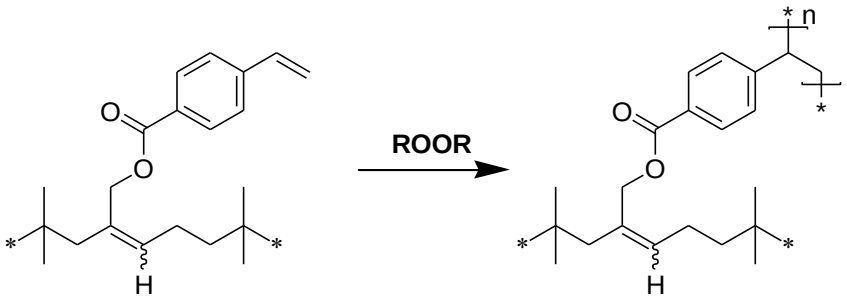

1.4 Isobutylene-Rich Ionomers

An ionomer is a thermoplastic polymer containing a small amount of ionic groups (< 15 mol%) dispersed throughout a polymer matrix of low dielectric constant [46]. The introduction of small amounts of ionic functionality in non-polar polymers leads to the formation of ionomers with improved mechanical and adhesive properties to their parent materials. Aggregation of the ion pairs into multiplets produces a material with similar physical properties to those of conventional covalently cross-linked thermoset elastomers [26] [47]. Two to eight ion pairs form aggregates,

which with enough ionic functionality can amass further to form clusters [48]. Restricted chain mobility afforded by the ionic network can result in an extended rubbery plateau and in some cases broadening of T_g or even the appearance of a second glass transition [48]. Up to now, several ionomers have been well studied, especially those containing carboxylate and sulfonate anions which are produced commercially [49] [50]. The ionic network, although significant, is labile and as such the major shortcoming of elastomeric ionomers is stress relaxation, a deficiency that essentially eliminates any commercial utility [47] [51] [52].

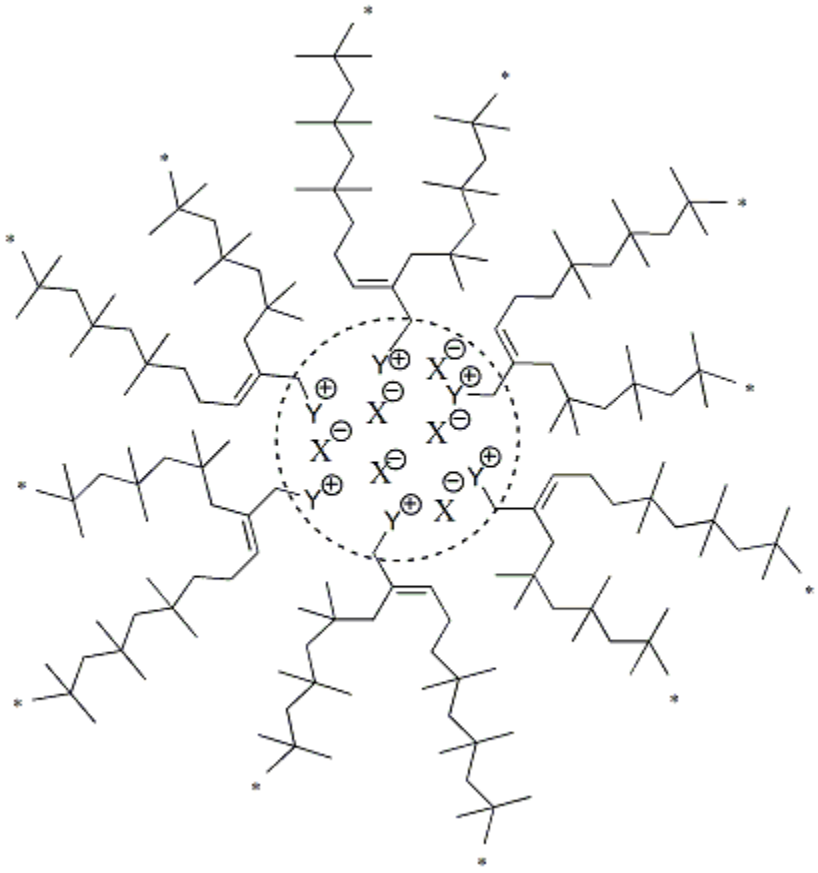

Figure 2: Ionic aggregation in a generic butyl rubber ionomer

Isobutylene-rich ionomers have the potential to provide the superior properties of isobutylene-rich elastomers with the unique properties of ionomers. To this end, the first sulfonated ionomer of PIB was developed in 1987 bearing ionic terminal groups [53]. More recent research into

isobutylene-rich ionomers has focused on inert alkylammonium and triphenylphosphonium bromide derivatives of BIIR bearing ionic functionality on the isoprene mers [54]. These ionomers have shown the potential for good adhesion, dispersion of siliceous filler, and anti-microbial properties [55] [56] [57] [58].

Scheme 8: Recent ionomer derivatives of BIIR developed in the Parent group

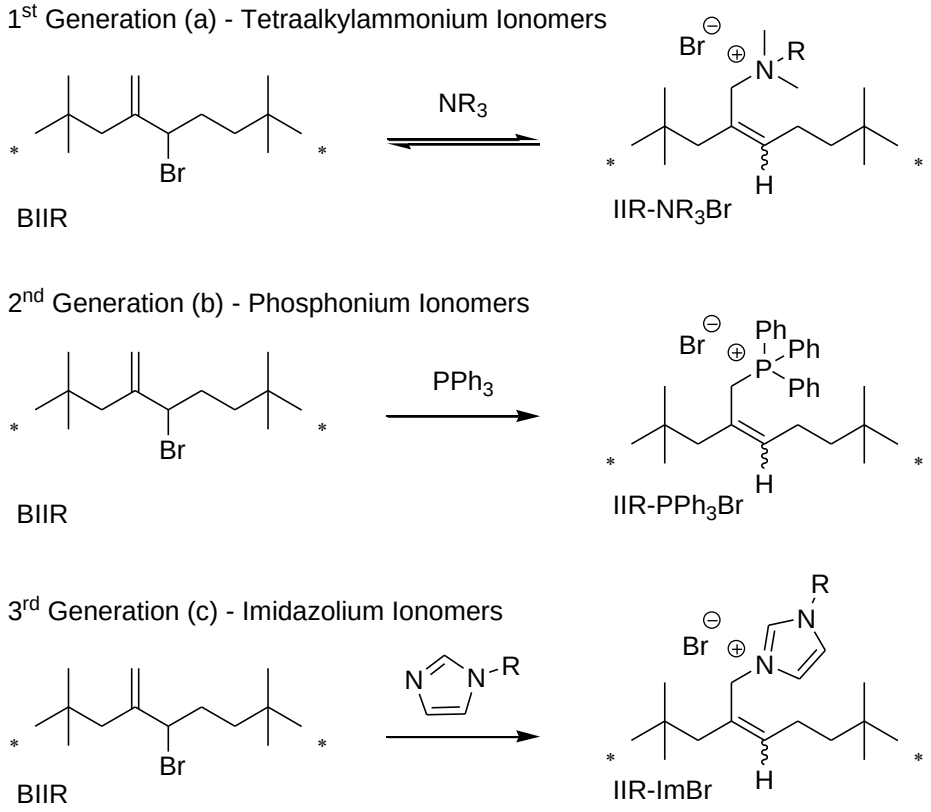

Scheme 8 shows the progression of isobutylene-rich ionomers developed in recent years in the Parent group. The triphenylphosphine derivative garnered the most attention due to facile solvent-free preparation and thermal stability [54]. Furthermore, phosphonium ionomers of BIMS have been prepared and the potential for anion metathesis has been described [59].

Tetraalkylammonium ionomers are attractive because of the wide variety of functional amines commercially or synthetically available [60]. The main issue is reversibility of the quaternization reaction by the reverse Menschutkin reaction shown in Scheme 9 [25] [61].

Scheme 9: Reverse Menschutkin reaction for a generic tetra-N-alkylammonium bromide

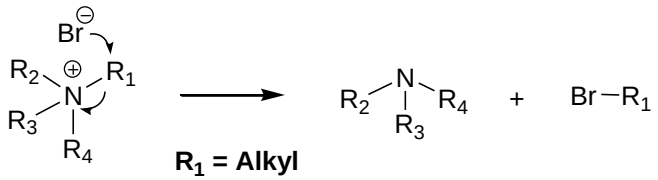

R_1 = Alkyl

R_2, R_3, R_4 = H or Alkyl

Like amines, a wide variety of functional imidazoles are commercially available. Imidazoles have been previously grafted onto polyfluorene polymers to provide conductivity [62] via a S_N2 bromide displacement reaction that is well known for brominated polymers [63]. 1-Butyl imidazole was first alkylated by BIIR in solution to produce an isobutylene-rich N-butylimidazolium bromide ionomer [64]. It was found that the N-alkylation of imidazole nucleophiles by halide displacement of BIIR proceeds irreversibly in high yield to produce a stable ionomeric product. No reversibility was observed up to 160°C and heating of the imidazolium bromide ionomer in solution with tetrabutylammonium acetate showed no exchange of acetate nucleophile after 2 hours. This reaction was also extended to solvent-free conditions to providing both environmental and economic benefits [65]. Furthermore, bis-imidazoles, as well as the double alkylation of imidazole itself, have been used to produce covalently cross-linked ionomers in a one-step solvent free process [47]. The robustness of imidazolium ionomers of BIIR at typical rubber compounding temperatures make functional imidazole an attractive starting point for further functionalization of isobutylene-rich elastomers.

Because N-butylimidazole does not provide a site for covalent cross-links when grafted to BIIR or BIMS, the main deficiency of the 3rd generation N-butylimidazolium bromide ionomer is its

susceptibility to stress relaxation and creep. Covalent cross-linking is required to counteract this deficiency but grafting imidazoles to form the ionomer consumes the reactive site needed for conventional vulcanization. Most recently, the possibility of introducing ion-pairs bearing moieties reactive to peroxide oligomerization has been explored [66], an area that has otherwise been largely overlooked. This new chemistry has demonstrated the potential to create a new class of engineering material containing both ionic and covalent networks. The aforementioned phosphine and tertiary amine ionomer derivatives could be functionalized to produce peroxide-initiated covalent cross-linking reactivity but are ill-suited for this purpose due to poor conversion [67] [25] and the air-instability of functional phosphines [68]. This leaves N-functional imidazolium bromide derivatives as the most logical choice for isobutylene-rich, peroxide curing reactive ionomers.

The first generation of peroxide curing isobutylene-rich ionomers employed N-vinylimidazolium bromide derivatives of both BIMS and BIIR [66]. N-vinylimidazolium ionic liquids have displayed good activity toward free radical polymerization to form poly(ionic liquids) (PILs) [69] [70] [71] [72] and have been the focus of much research due to their unique conductivity and temperature stability [73] [74] [75]. Vinylimidazolium ionic liquids are known to homopolymerize under peroxide initiation at moderate temperature, a property that has been exploited to peroxide vulcanize a vinylimidazolium bromide ionomer as shown in Scheme 10 [66].

Scheme 10: Synthesis and peroxide initiated cross-linking of an N-vinylimidazolium bromide ionomer derivative of BIIR

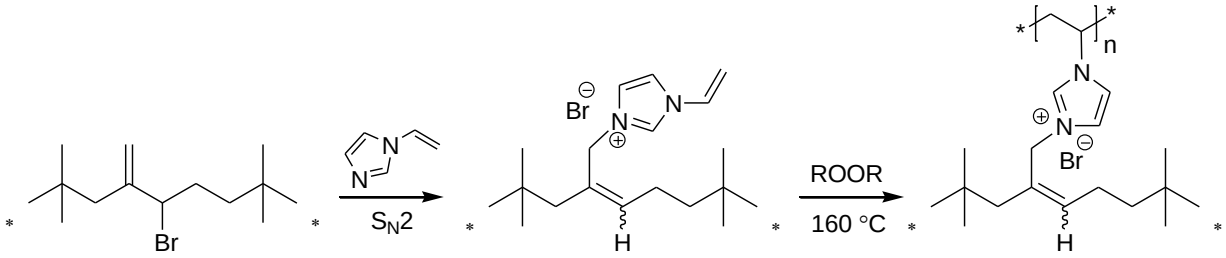

Imidazoles have displayed the fastest alkylation reactions compared to other heterocycles such as pyridine, oxazole or thiazole [76] [77] but N-functionalization of the ring produces a large effect on alkylation rate. It was discovered that the alkylation reaction of VIm compared to BuIm is several times slower, a limitation that inhibits the commercial value of this technology [78]. Part of this research will aim to find a faster alkylating functional imidazole able to cross-link BIMS with minimal peroxide.

1.5 Research Objectives

The objective of this research is to expand on two distinct previous projects in the group; reactive ionomers of BIMS, and BIIR macromonomer reactivity.

1. BIMS reactive ionomers:
    a. Develop a functional imidazole able to be rapidly alkylated by BIMS in both solution and solvent-free syntheses.
    b. Explore other synthetic methods to accelerate N-functional imidazole quaternization by BIMS.
    c. Study the cure dynamics and final mechanical properties of the novel ionomers and assess them for commercially practicality.
2. BIIR macromonomer reactivity:
    a. Synthesize a suite of BIIR macromonomers bearing peroxide-active functionality to test the effect of functional group reactivity on cure dynamics.

b. Assess and characterize the scorch protecting ability of functional nitroxyls on BIIR macromonomers.

Chapter 2

Isobutylene-Rich Macromonomers:

Peroxide-Initiated Cross-Linking Dynamics

Disclaimer:

The work presented in the following chapter is based upon unpublished preliminary studies as reported in chapter 4 of the Ph.D. dissertation entitled "Peroxide Curable Butyl Rubber Derivatives" by Karthik Vikram Siva Shanmugam[1]. Shanmugam's chapter focused on the relationship between stability of BIIR derived macromonomers versus their peroxide reactivity. The stability issues encountered by Dr. Shanmugam were subsequently resolved, forming the basis of the material presented here. Some of Dr. Shanmugam's original data, the specifics described below, survived this transition and is gratefully used in this thesis.

DCP-initiated cures for each macromonomer (Figure 4) were originally conducted by Dr. Shanmugam but were repeated and confirmed by me, with the exception of the vinylimidazolium ionomer which was based on previous research conducted by Adam Ozvald[2], and the novel allylimidazolium ionomer. Furthermore, the syntheses and characterization reported herein for the non-ionic macromonomers, although confirmed experimentally by me, were used as written by Dr. Shanmugam with only minor changes. The plot of maximum cure rate versus cure extent (Figure 5) was originally generated from Dr. Shanmugam's data, and the original ionomer data was added to it. Finally, data for the DCP-initiated cures of IIR-MAA with increasing peroxide

[1] Karthik V. S. Shanmugam, "Peroxide Curable Butyl Rubber Derivatives", Ph.D. dissertation, Dep. Chem. Eng., Queen's Univ., Kingston, ON, 2012

[2] A. Ozvald, J. S. Parent and R. A. Whitney, "Hybrid ionic/covalent polymer networks derived from functional imidazolium ionomers", *Journal of Polymer Science: Part A: Polymer Chemistry*, vol. 51, pp. 2438-2444, 2013

loading (Figure 6b) was conducted by Dr. Shanmugam. All other data and written work appearing in the following chapter is original to this thesis.

I would like to thank Dr. Shanmugam for laying a strong experimental foundation in the field of BIIR-derived macromonomers, and for allowing me to use the preliminary data he collected to complete my master's thesis.

2.1 Introduction

Poly(isobutylene-*co*-isoprene) (IIR) is a copolymer prepared by cationic polymerization of isobutylene and 1-2 mol% isoprene. This elastomeric material owes its superior oxidative stability and gas impermeability to its isobutylene-rich polymer backbone [11], while the residual unsaturation provided by isoprene mers supports the sulfur vulcanization reactivity needed to transform IIR into thermoset articles [1]. Cure reactivity is greatly improved by halogenating isoprene-derived unsaturation to yield brominated poly(isobutylene-*co*-isoprene) (BIIR) [8], whose allylic halide functionality is highly reactive to sulfur nucleophiles. Unfortunately, sulfur-cure formulations require accelerators and co-curing agents, resulting in a vulcanized product containing leachable and extractable residues [19].

Although peroxide-based cure formulations are generally much cleaner, IIR incurs radical degradation when activated by organic peroxides [28] [35]. This limitation can be overcome by introducing small amounts (between 0.05 and 0.20 mmol/g) of polymerizable functionality to the material to generate macromonomer derivatives that cross-link by radical homopolymerization of pendant groups, as opposed to the hydrogen abstraction + macro-radical combination mechanism that underlies peroxide-cures of saturated polymers [23]. It should be noted that macromonomers are often defined as materials bearing polymerizable end groups [79] [80] [81], whereas in the present context, BIIR-derived macromonomers contain many polymerizable groups distributed randomly along the polymer chain.

An early example of an isobutylene-rich macromonomer was described by Oxley and Wilson, who polymerized isobutylene, isoprene, and divinylbenzene to give an elastomer that cured by radical oligomerization of residual styrenic functionality [44]. However, the activation of divinylbenzene during the cationic polymerization process yielded a gel content of 85% that

compromised the material's processing characteristics. Wang et al. prepared gel-free analogues by post-polymerization modification of brominated poly(isobutylene-*co*-para-methylstyrene), yielding acrylate derivatives that cured to high extent when activated by peroxide thermolysis, UV-initiation, and electron beam bombardment [24]. More recently, BIIR-derived macromonomers have been prepared by the Suzuki-Miyaura coupling reaction using 4-vinylphenylboronic acid, [27] and through bromide displacement by acrylate and vinylbenzoate nucleophiles [23].

The present work is concerned with the relationship between the structure of a macromonomer's functionality and the material's cross-linking dynamics and yields. Scheme 11 illustrates the macromonomers of interest, which range from highly reactive acrylates and styrenics [82], to relatively unreactive maleate diesters [83] [84] [85] and unactivated allylic monomers [86] [87]. Some of these functional groups have been studied extensively in the context of low temperature homopolymerization, with reliable estimates of the propagation rate constants providing insight into the potential reactivity of a given macromonomer system. For example, rate constants measured at 60°C suggest that macromonomer reactivity may decline in the order acrylates > methacrylates > styrenics > itaconates [82]. However, reaction conditions used in elastomer curing are substantially different, with temperatures in the range of 160°C and polymerizable functionalities rarely exceeding concentrations of 0.25 mmoles / g polymer. Moreover, several of the functional groups of interest have received little attention, such as vinyl and allyl imidazolium bromide ionic liquids.

Scheme 11: Reactive functional groups within BIIR-derived macromonomers

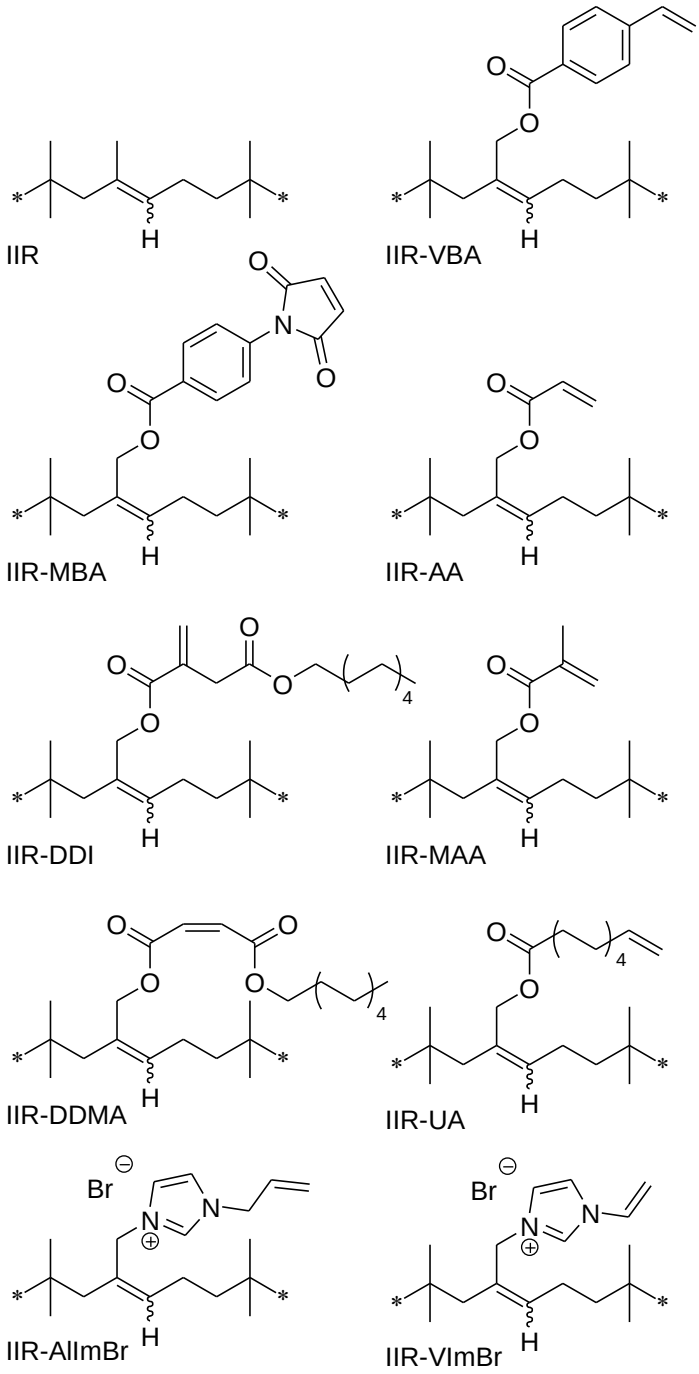

This report describes the synthesis of a wide range of IIR-based macromonomers (Scheme 11), and characterizes their reactivity toward peroxide-initiated cross-linking under conditions that are relevant to industrial practice. Reaction dynamics and yields are measured by dynamic shear

rheometry, and results are discussed in the context of underlying polymer cross-linking and scission mechanisms. The study concludes with a demonstration of new chemistry for delaying the onset of reactive macromonomer cross-linking without compromising ultimate cure yields.

2.2 Experimental

Materials: Acrylic acid (99%), vinylbenzoic acid (VBA, 97%), methacrylic acid (MAA, 99%), 10-undecenoic acid (UA, 98%), maleic anhydride (99%), 4-aminobenzoic acid (99%), sodium acetate (anhydrous, 99%), acetic anhydride (99%), itaconic anhydride (95%), dodecanol (95%), tetrabutylammonium bromide (TBAB, 98%), tetrabutylammonium hydroxide (Bu_4NOH, 1M solution in methanol, 98%), dicumyl peroxide (DCP, 98%), triethyl amine (Et_3N 99%), N,N'-m-phenylene maleimide (98%), 2,2,6,6-tetramethylpiperidin-1-oxyl (TEMPO, sublimed 99%), 4-hydroxy-2,2,6,6-tetramethylpiperidin-1-oxyl (TEMPOH, 97%) and 1-vinylimidazole (VIm, 99+%) were used as received from Sigma-Aldrich. 1-Allylimidazole (AlIm, 99%) was used as received from Alfa Aesar. Butyl rubber (IIR, 2.8 mol% isoprene, RB-301) and BIIR (Bromobutyl 2013, allylic bromide content ~0.15 mmol/g) were used as received from LANXESS Inc. (Sarnia, ON).

Synthesis of IIR-g-methacrylate (IIR-MAA): Methacrylic acid (0.322 g, 3.7 mmol) was treated with a 1M solution of Bu_4NOH in methanol (3.7 ml, 3.7 mmol Bu_4NOH) to yield the desired Bu_4N carboxylate salt, which was isolated by removing methanol under vacuum. BIIR (11 g) and Bu_4NBr (0.53 g, 1.65 mmol) were dissolved in toluene (100 g) and heated to 85°C for 180 min. The Bu_4N carboxylate salt (1.2 g, 3.7 mmol) was added before heating the reaction mixture to 85°C for 60 min. The esterification product was isolated by precipitation from excess acetone, purified by dissolution/precipitation using THF /acetone, and dried under vacuum to give IIR-g-methacrylic acid (IIR-MAA) in near quantitative yield. **^{1}H-NMR** ($CDCl_3$): δ 6.03

(s,C**H**$_2$=C(CH$_3$)-COO-, 1H), δ 5.47 (s,C**H**$_2$=C(CH$_3$)-COO-,1H), δ 3.36 (s, (CH$_2$=C(C**H**$_3$)-COO-, 3H) ,δ 4.51 (E-ester, =CH-**C**H$_2$-OCO-, 2H, s), δ 4.56 (Z-ester, =CH-**C**H$_2$-OCO-, 2H, s).

Synthesis of IIR-g-maleimido benzoate (IIR-MBA): Maleic anhydride (3 g, 0.03 mol) and 4-aminobenzoic acid (4.2 g, 0.03 mol) were dissolved in acetone (10 g) and the mixture was stirred for 12 h at room temperature. The insoluble amidic acid precipitate was filtered off and dried in vacuum. The amidic acid (6 g, 0.025 mol) was treated with acetic anhydride (8 g, 0.078 mol) and sodium acetate (1 g, 0.012 mol) at 80°C for 15 min. Maleimidobenzoic acid was isolated by precipitating through successive precipitation-dissolution in water/THF and dried in vacuum. **^{1}H-NMR** (DMSO-d$_6$): δ 7.21 (s,-C**H**=C**H**-, 2H), δ 7.50 (d, Ar-**H**, 2H), δ 8.02 (d, Ar-**H**, 2H). HRMS calculated for $C_{11}H_7NO_4$: 217.0371, found 217.0375.

BIIR (10 g), TBAB (0.48 g, 1.5 mmol), maleimidobenzoic acid (0.651 g, 3.0 mmol) and triethyl amine (0.3g, 3.0 mmol) were dissolved in THF (100g) and refluxed in a 250 ml vessel for 600 min. The esterification product was isolated by precipitation from excess acetone, purified by dissolution/precipitation using THF/acetone, and dried under vacuum to give IIR-g-maleimido-benzoate (IIR-MBA).

Synthesis of IIR-g-dodecyl itaconate (IIR-DDI): Monododecyl itaconate was prepared as previously described [88].1-Dodecanol (8.0 mmol, 1.5 g) and itaconic anhydride (24 mmol, 2.7 g), were dissolved in toluene (10 g) and heated to 80°C for 4 h. Residual starting materials and solvent were removed by Kugelrohr distillation (T = 80°C, P = 0.6 mmHg). The resulting acid-ester was isolated and dried. **^{1}H-NMR** (DMSO-d$_6$): δ 6.14 (d, HOOC-C**(=C**H$_2$**)**-CH$_2$-COO-, 1H), δ 5.74 (d, HOOC-C**(=C**H$_2$**)**-CH$_2$-COO-, 1H), δ 3.28 (s, HOOC-C**(=**CH$_2$**)**-C**H**$_2$-COO-, 1H) δ 3.98 (t, -CH$_2$-COO-C**H**$_2$-, 2H), δ 1.52 (m, -COO-CH$_2$-C**H**$_2$-, 2H), δ 1.36 (m, -COO-(CH$_2$)$_{10}$-C**H**$_2$-CH$_3$,

2H), δ 1.25 (m, -CH_2-(C**H**$_2$)$_9$- CH_2-CH_3, 18H), δ 0.87 (t, CH_2-C**H**$_3$, 3H). HRMS calculated for $C_{17}H_{31}O_4$: 299.2225, found 299.2222.

Monododecyl itaconate (0.98 g, 3.3 mmol) was treated with a 1M solution of Bu_4NOH in methanol (3.3 ml, 3.3 mmol Bu_4NOH) to yield the desired Bu_4Ncarboxylate salt, which was isolated by removing methanol under vacuum. BIIR (11 g) and Bu_4NBr (0.53 g, 1.65 mmol) were dissolved in toluene (100 g) and heated to 85°C for 180 min. The Bu_4N carboxylate salt (1.78 g, 3.3 mmol) was added before heating the reaction mixture to 85°C for 60 min. The esterification product was isolated by precipitation from excess acetone, purified by dissolution/precipitation using THF/acetone, and dried under vacuum to give IIR-g-dodecyl itaconate (IIR-DDI) in near quantitative yield. **^{1}H-NMR** ($CDCl_3$): δ 6.24 (s, C**H**$_2$=C(CH_2)-COO-, 1H), δ 5.62 (s, C**H**$_2$=C(CH_2)-COO-, 1H), δ 3.36 (s, CH_2=C(C**H**$_2$)-COO-, 2H), δ 4.54 (E-ester, =CH-**C**H$_2$-OCO-, 2H, s), δ 4.60 (Z-ester, =CH-**C**H$_2$-OCO-, 2H, s).

Synthesis of IIR-g-undecenoate (IIR-UA): 10-Undecenoic acid (0.88 g, 3.7 mmol) was treated with a 1M solution of Bu_4NOH in methanol (4.8 ml, 4.8 mmol Bu_4NOH) to yield the desired Bu_4N carboxylate salt, which was isolated by removing methanol under vacuum. BIIR (16 g) and Bu_4NBr (0.77 g, 2.4 mmol) were dissolved in toluene (100 g) and heated to 85°C for 180 min. The Bu_4N carboxylate salt (2.04 g, 4.8 mmol) was added before heating the reaction mixture to 85°C for 60 min. The esterification product was isolated by precipitation from excess acetone, purified by dissolution/precipitation using THF/acetone, and dried under vacuum to give IIR-g-undecenoate (IIR-UA) in near quantitative yield. **^{1}H-NMR** ($CDCl_3$): δ 5.68 (m,-CH_2=C**H**-CH_2-, 1H), δ 4.85 (d, C**H**$_2$=CH-, 1H), δ 4.79 (d, C**H**$_2$=CH-, 1H), δ 4.51 (E-ester, =CH-**C**H$_2$-OCO-, 2H, s), δ 4.56 (Z-ester, =CH-**C**H$_2$-OCO-, 2H, s).

Synthesis of IIR-g-dodecyl maleate (IIR-DDMA): 1-Dodecanol (1.5 g, 8.04 mmol) and maleic anhydride (0.98 g, 10.05 mmol) were dissolved in toluene (10 g) and heated to 80°C for 4 h. Residual starting materials and solvent were removed by Kugelrohr distillation (T = 80°C, P = 0.6 mmHg). The resulting acid-ester was isolated. **^{1}H-NMR** ($CDCl_3$): δ 6.46 (d, HOOC-C**H**=CH-COO-, 1H), δ 6.36 (d, HOOC-CH=C**H**-COO-, 1H), δ 4.27 (t, =CH-COO-C**H_2**-, 2H), δ 1.71 (m, -COO-CH_2-C**H_2**-, 2H), δ 1.36 (m, -COO-$(CH_2)_{10}$-C**H_2**-CH_3, 2H), δ 1.25 (m, -CH_2-(C**H_2**)$_9$-CH_2-CH_3, 18H), δ 0.87 (t, CH_2-C**H_3**, 3H). HRMS calculated for $C_{16}H_{29}O_4$: 285.2078, found 285.2065.

Monododecyl maleate (0.94 g, 3.3 mmol) was treated with a 1M solution of Bu_4NOH in methanol (3.3 ml, 3.3 mmol Bu_4NOH) to yield the desired Bu_4N carboxylate salt, which was isolated by removing methanol under vacuum. BIIR (11 g) and Bu_4NBr (0.53 g, 1.65 mmol) were dissolved in toluene (100 g) and heated to 85°C for 180 min. The Bu_4N carboxylate salt (1.7 g, 3.3 mmol) was added before heating the reaction mixture to 85°C for 60 min. The esterification product was isolated by precipitation from excess acetone, purified by dissolution/precipitation using THF/acetone, and dried under vacuum to give IIR-g-dodecyl maleate (IIR-DDMA) in near quantitative yield. **^{1}H-NMR** ($CDCl_3$): δ 6.19 (s, OOC-C**H**=C**H**-COO-, 2H), δ 4.11 (t, -CH_2-CH_2-COO-C**H_2**-, 2H), δ 4.58 (E-ester, =CH-**CH_2**-OCO-, 2H, s), δ 4.66 (Z-ester, =CH-**CH_2**-OCO-, 2H, s).

Synthesis of IIR-g-vinylbenzoate (IIR-VBA): 4-Vinylbenzoic acid (0.44 g, 3.0 mmol) was treated with a 1M solution of Bu_4NOH in methanol (3.0 ml, 3.0 mmol Bu_4NOH) to yield the desired Bu_4N carboxylate salt, which was isolated by removing methanol under vacuum. BIIR (10 g) and Bu_4NBr (0.77 g, 2.4 mmol) were dissolved in toluene (100 g) and heated to 85°C for 180 min. The Bu_4N carboxylate salt (1.16 g, 3.0 mmol) was added before heating the reaction mixture to 85°C for 60 min. The esterification product was isolated by precipitation from excess

acetone, purified by dissolution/precipitation using THF /acetone, and dried under vacuum to give IIR-g-vinylbenzoate (IIR-VBA) in near quantitative yield. **^{1}H-NMR** ($CDCl_3$), consistent with literature precedent [23]: δ 6.73 (dd,-CH_2=C**H**-Ar, 1H), δ 5.82 (dd, C**H_2**=CH-, 1H), δ 5.48 (dd, C**H_2**=CH-, 1H), δ 4.78 (E-ester, =CH-**CH_2**-OCO-, 2H, s), δ 4.81 (Z-ester, =CH-**CH_2**-OCO-, 2H, s).

Synthesis of IIR-g-acrylate (IIR-AA): Acrylic acid (0.21 g, 3.0 mmol) was treated with a 1M solution of Bu_4NOH in methanol (3.0 ml, 3.0 mmol Bu_4NOH) to yield the desired Bu_4N carboxylate salt, which was isolated by removing methanol under vacuum. BIIR (10 g) and Bu_4NBr (0.48 g, 1.5 mmol) were dissolved in toluene (100 g) and heated to 85°C for 180 min. The Bu_4N carboxylate salt (0.94 g, 3.0 mmol) was added before heating the reaction mixture to 85°C for 60 min. The esterification product was isolated by precipitation from excess acetone, purified by dissolution/precipitation using THF/acetone, and dried under vacuum to give IIR-g-acrylate (IIR-AA) in near quantitative yield. **^{1}H-NMR** ($CDCl_3$), consistent with literature precedent [23]: δ 6.12 (dd, CH_2=C**H**-COO-, 1H), δ 6.40 (dd, C**H_2**=CH-, 1H), δ 5.82 (dd, C**H_2**=CH-, 1H), δ 4.66 (E-ester, =CH-COO-**CH_2**-, 2H, s), δ 4.60 (Z-ester, =CH-COO-**CH_2**-, 2H, s).

Synthesis of IIR-g-vinylimidazolium bromide (IIR-VImBr): IIR-VImBr was prepared as previously described [66]. BIIR (20 g, 3.0 mmol allylic bromide) was dissolved in toluene (200 ml) and heated to 100 °C. 1-Vinylimidazole (1.69 g, 18.0 mmol, 6 eq.) was then added to the solution and the mixture was allowed to react for 50 h. The N-alkylation product was isolated by precipitation from excess acetone, purified by dissolution/precipitation using THF/acetone, and dried under vacuum to give IIR-g-vinylimidazolium bromide (IIR-VImBr) in near quantitative yield. **^{1}H-NMR** ($CDCl_3$ + 5 wt% CD_3OD), consistent with literature precedent: δ 11.53 (s, -N^+-

CH-N-, 1H), δ 7.61 (s, 1H, -N^+-CH=**CH**-N-), δ 7.42 (dd,1H, -N-**CH**=CH_2), δ 5.80 (dd, 1H, N-CH=CH-$\mathbf{H_{trans}}$), δ 5.41 (dd, 1H, N-CH=CH-$\mathbf{H_{cis}}$), found for the *Z*-isomer: δ 7.16 (s, 1H, *Z*, -N^+-**CH**=CH-N-), δ 5.69 (t, 1H, *Z*, CH_2-C=**CH**-CH_2) δ4.91 (s, 2H, -C-$\mathbf{CH_2}$-N^+), found for the *E*-isomer: δ 7.20 (s, 1H, *E*, -N^+-**CH**=CH-N-), δ 5.68 (t, 1H, *E*, CH_2-C=**CH**-CH_2), δ 4.84 (s, 2H, *E*, -C-$\mathbf{CH_2}$-N^+). ^{1}H-NMR for conjugated dienes: δ 5.98 (d, 1H, exo-diene), δ 5.92 (d, 1H, endo-diene). ^{1}H-NMR for residual isoprene mer: δ 5.04 (t, 1H, CH_3-C=CH-CH_2-).

Synthesis of IIR-g-allylimidazolium bromide (IIR-AlImBr): BIIR (20 g, 3.0 mmol allylic bromide) was dissolved in toluene (200 ml) and heated to 100 °C. 1-Allylimidazole (1.69 g, 18.0 mmol, 6 eq.) was then added to the solution and the mixture was allowed to react for 24 h. The N-alkylation product was isolated by precipitation from excess acetone, purified by dissolution/precipitation using THF/acetone, and dried under vacuum to give IIR-g-allylimidazolium bromide (IIR-AlImBr) in near quantitative yield. **^{1}H-NMR** ($CDCl_3$ + 5 wt% CD_3OD): δ 9.79 (s, -N^+-**CH**-N-, 1H), δ 7.21 (s, 1H, -N^+-CH=**CH**-N-), δ 6.00 (ddt,1H, -N-CH_2-**CH**=CH_2), δ 5.40 (dd, 1H, N-CH_2-CH=$\mathbf{CH_2}$), found for the *Z*-isomer: δ 7.12 (s, 1H, *Z*, -N^+-**CH**=CH-N-), δ 5.66 (t, 1H, *Z*, CH_2-C=**CH**-CH_2) δ4.85 (s, 2H, -C-$\mathbf{CH_2}$-N^+), found for the *E*-isomer: δ 7.14 (s, 1H, *E*, -N^+-**CH**=CH-N-), δ 5.62 (t, 1H, *E*, CH_2-C=**CH**-CH_2), δ 4.78 (s, 2H, *E*, -C-$\mathbf{CH_2}$-N^+). ^{1}H-NMR for conjugated dienes: δ 5.92 (d, 1H, endo-diene). ^{1}H-NMR for residual isoprene mer: δ 5.03 (t, 1H, CH_3-C=CH-CH_2-).

Synthesis of AOTEMPO: The synthesis and purification of 4-acryloyloxy-2,2,6,6-tetramethylpiperidine-N-oxyl (AOTEMPO) is described elsewhere [89].

Instrumentation and Analysis: ^{1}H-NMR spectra were acquired on a Bruker Avance-400 spectrometer. Mass spectra were obtained on an Applied Biosystems QStar XL QqTOF mass

spectrometer. Dynamic shear modulus measurements were recorded using an Alpha Technologies, Advanced Polymer Analyzer 2000. Pressed samples of elastomer were coated with the required amount of a stock solution of DCP in acetone, and allowed to dry prior to passing three times through a 2-roll mill. This mixed compound was cured at 160°C in the rheometer cavity at 3° oscillation arc and a frequency of 1 Hz.

2.3 Results and Discussion

2.3.1 Butyl Rubber Degradation

The challenge in working with isobutylene-rich elastomers is to overcome the susceptibility of the polymer backbone toward radical degradation [35]. Hydrogen atom abstraction from the polymer by dicumyl peroxide (DCP) derived radicals is regioselective for primary alkyl positions [90], yielding macro-macroradicals whose β-scission reduces molecular weight (Scheme 12). This fragmentation competes with macroradical combination, and can lead to bimodal molecular weight and branching distributions comprised of low molecular weight linear chains, and high molecular weight branched chain populations. In the context of macro-monomer design, radical oligomerization of pendant C=C functionality must dominate backbone fragmentation to the point that substantial polymer chains are incorporated in a covalent network of adequate cross-link density.

Scheme 12: DCP-initiated degradation of PIB

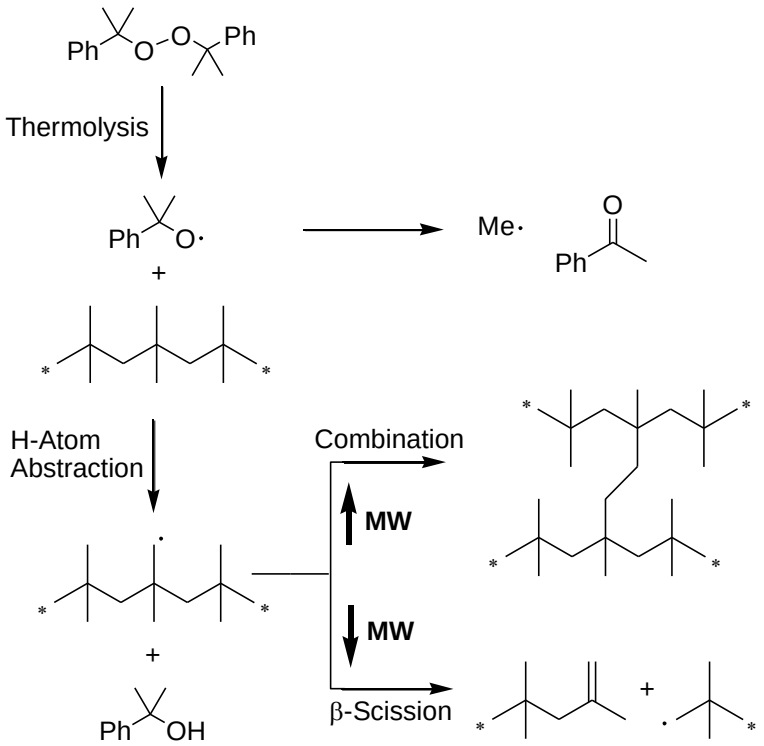

Chemical structure determinations of thermoset macro-monomers are complicated by the insolubility of cured products and the low functional group contents of the starting materials. Therefore, the standard means of monitoring the progress of a macromonomer cure involves measuring a formulation's dynamic storage modulus (G') at a fixed temperature, frequency, and shear strain amplitude. The sensitivity of polymer chain relaxation to changes in molecular weight and architecture translate into measureable changes in storage modulus (G') [4] [5]. Figure 3 provides plots of G' versus time recorded for samples of IIR that were mixed with varying amounts of DCP and heated to 160°C. The timescale of the degradation process is dictated by the first-order decomposition rate of the peroxide, whose 5.4 min half-life at 160°C [32] leads to an overall reaction time on the order of 40 min.

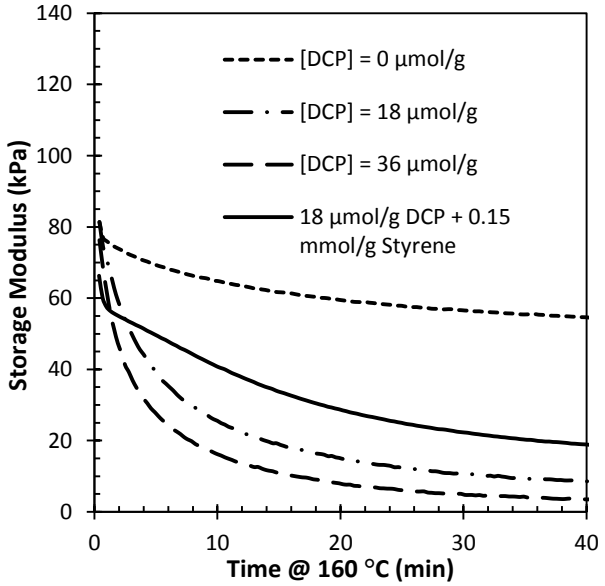

Figure 3: Dynamics of IIR degradation by DCP-initiated chain scission at increasing peroxide loadings, and in the presence of unbound styrene monomer

Note that IIR degradation dynamics and yields can be affected by the presence of a polymerizable monomer. Figure 3 also contains a plot of the storage modulus for an IIR compound containing DCP and a small amount of styrene. The presence of unbound styrene did not eliminate chain scission, but reduced its extent, presumably by shifting the radical population away from primary alkyl macroradicals and toward benzylic radical intermediates. By extension, polymerizable functional groups bound to macromonomer derivatives of BIIR may not eliminate backbone degradation, but affect the balance of cross-linking and scission that dictates the cure extent.

2.3.2 Peroxide-Initiated Cross-Linking Dynamics

The macromonomers illustrated in Scheme 11 were prepared by nucleophilic displacement of bromide from BIIR by the required carboxylate salt in toluene solution at 85°C [14] [15]. To reduce the time that potentially sensitive C=C groups were exposed to these conditions, the exo-allylic bromide functionality within the starting material was first reacted with TBAB to produce the corresponding E,Z-BrMe isomers, whose higher electrophilicity [15] serves to reduce

esterification times substantially. This two-step approach provided 100% allylic bromide conversion to the desired esters, without complications associated with BIIR dehydrohalogenation [12]. Therefore, all macromonomers contained 0.15 mmoles of reactive functionality per gram of elastomer that was distributed randomly within each polymer chain. Assuming a number average molecular weight of 400,000 g/mol for the starting material, about 60 functional groups per polymer chain were introduced, with an average molecular weight between functional groups (M_c) on the order of 6500 g/mol.

Note that instability towards auto-initiated cross-linking, even at room temperature, has been reported for closely related systems [23] [91] [92]. Our early work with IIR-MBA, IIR-VBA, and IIR-AA was similarly complicated by cross-linking over a period of days at ambient temperatures, and significant cross-linking activity was observed at 160°C, even when phenolic and nitroxyl radical traps were compounded into the material. However, purification by repeated dissolution/precipitation improved stability such that additive-free samples of IIR-AA and IIR-VBA could be stored for weeks at room temperature. The instability of IIR-MBA could not be overcome, however, and samples of this particular macromonomer were analyzed within hours of their preparation.

Figure 4 provides plots of G' versus time for macromonomer samples mixed with 18 μmole DCP/gram·polymer and heated to 160°C. As noted above, the half-life of DCP at 160°C is 5.4 min and, as such, the initiator reaches 98% conversion within the 30 min timescale of the plotted data. Note that peroxide cures of saturated polyolefins such as polyethylene are stoichiometric processes, and initiator thermolysis is the rate limiting step [93]. This means that each radical introduced into the system has the potential to produce only one cross-link. As a result, cross-linking dynamics mirror the first-order kinetics of initiator decomposition. The macromonomer

data presented in Figure 4 demonstrate altogether different behaviour, in that cure rates are not linearly proportional to initiator decomposition rates; they vary considerably depending on polymerizable group structure.

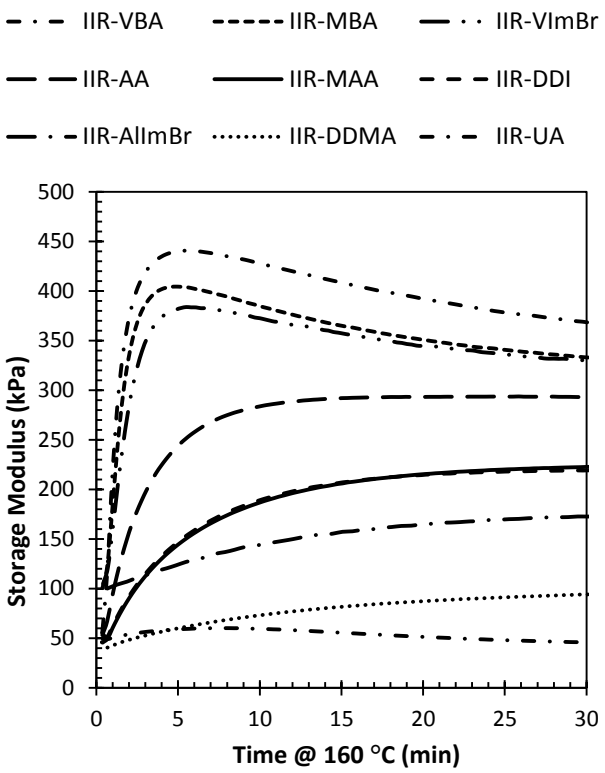

Figure 4: Dynamics of peroxide-initiated macromonomer cross-linking ([DCP] = 18 µmol/g; T = 160°C; t = 60 min)

The vinylbenzoate ester (IIR-VBA) was the most reactive, progressing from an initial storage modulus of 57 kPa to a maximum of 440 kPa ($\Delta G' = G'_{max} - G'_{min} = 383$ kPa) within just one initiator half-life. Cure reversion was observed beyond the 5.2 min mark of the process, at which point radical scission became the dominant molecular weight altering reaction. This post-cure loss of storage modulus occurs when macromonomer conversion to cross-links is no longer competitive with polymer backbone degradation, a shift that is likely due to the complete consumption of pendant monomer groups [23].

The storage modulus data plotted in Figure 4 show that IIR-VBA, IIR-MBA and IIR-VImBr provide similar cure dynamics, as they cross-link rapidly to full monomer conversion before undergoing significant post-cure reversion. These results are somewhat surprising, given that propagation rate constants for acrylates at moderate temperatures are greater than those generally reported for styrenics and maleimides [82]. The exceptional reactivity of IIR-VBA may be due to an electron withdrawing effect of the para-ester group, since the propagation rate constant for dodecyl-4-vinyl benzoate is known to exceed that of styrene [82] [94].

The reactivity of IIR-MBA may also benefit from an inductive effect of the N-aryl substituent, which would activate the reportedly moderate homopolymerizability of maleimide functionality. Note however, that maleimides copolymerize readily with electron-rich olefins and are effective co-curing agents for IIR [95] [43]. As such, residual unbrominated isoprene mers in BIIR could copolymerize with polymer-bound maleimide functionality to heighten cure activity. It is difficult to place the reactivity of IIR-VImBr into proper context, since reports of the polymerization of vinylimidazolium ionic liquids have not been accompanied by rate data [73] [69] [71].

The three acrylic macromonomers, IIR-AA, IIR-MAA, and IIR-DDI cross-linked more slowly and to a more moderate extent than those described above. The superior reactivity of IIR-AA over IIR-MAA is consistent with reported propagation rate constants [82], but the activity of the itaconate diester, IIR-DDI, is higher than expectations based on this data set. While reported k_p values at 60° for itaconate esters are an order of magnitude less than those of methacrylates, at the high temperature used in macromonomer cross-linking, the sterically hindered itaconate derivative (IIR-DDI) is no less reactive than its methacrylate analogue. The three remaining macromonomers, IIR-AlImBr, IIR-DDMA, and IIR-UA, were relatively unreactive, providing a

combination of low cross-linking rates and cure extents. Nonetheless, enough cross-linking activity was generated even by the unactivated α-olefin functionality within IIR-UA to counteract polymer backbone degradation.

Further analysis of the cure dynamics data revealed a relationship between the cross-link density provided by a macromonomer, as measured by the difference in storage modulus (ΔG), and the maximum rate of cross-linking ($dG'/dt\,|_{max}$). The latter is determined by taking the numerical derivative of G' versus time and reporting the highest rate observed throughout the curing reaction. Figure 5 presents a semi-log plot of ΔG' against $dG'/dt\,|_{max}$ that demonstrates the correlation between kinetic reactivity and cure extent. Since all macromonomers contained 0.15 mmol of reactive functionality per gram of polymer, they had the same potential to affect cross-linking. Nevertheless, IIR-VBA produced a higher cross-link density than did IIR-AA.

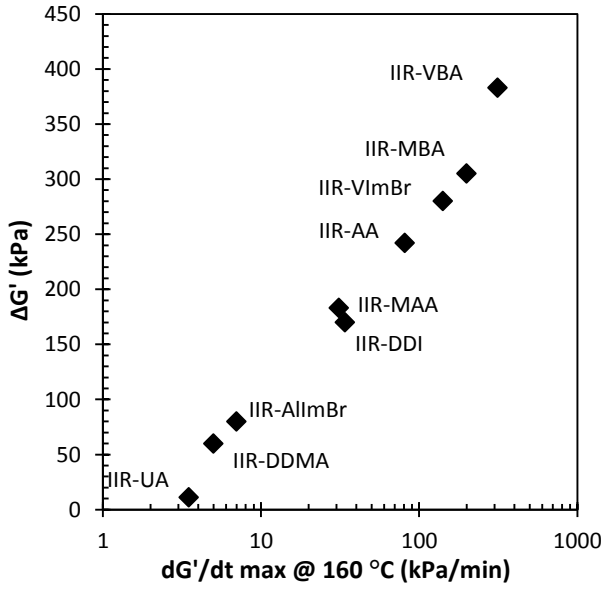

Figure 5: Cure yield versus maximum cure rate ([DCP] = 18 µmole/g; T = 160°C; t = 60 min)

One potential cause of this reactivity/yield connection is insufficient radical initiation. For example, a moderately reactive material such as IIR-MAA may need more than 18 μmole DCP/g to reach full monomer conversion at 160°C. However, the data plotted in Figure 6b show that doubling the peroxide concentration to 36 μmole DCP/g had little effect on the ultimate storage modulus, meaning that the ultimate cure extent of IIR-MMA is not the result of a "short-shot" polymerization, but a byproduct of its low kinetic reactivity.

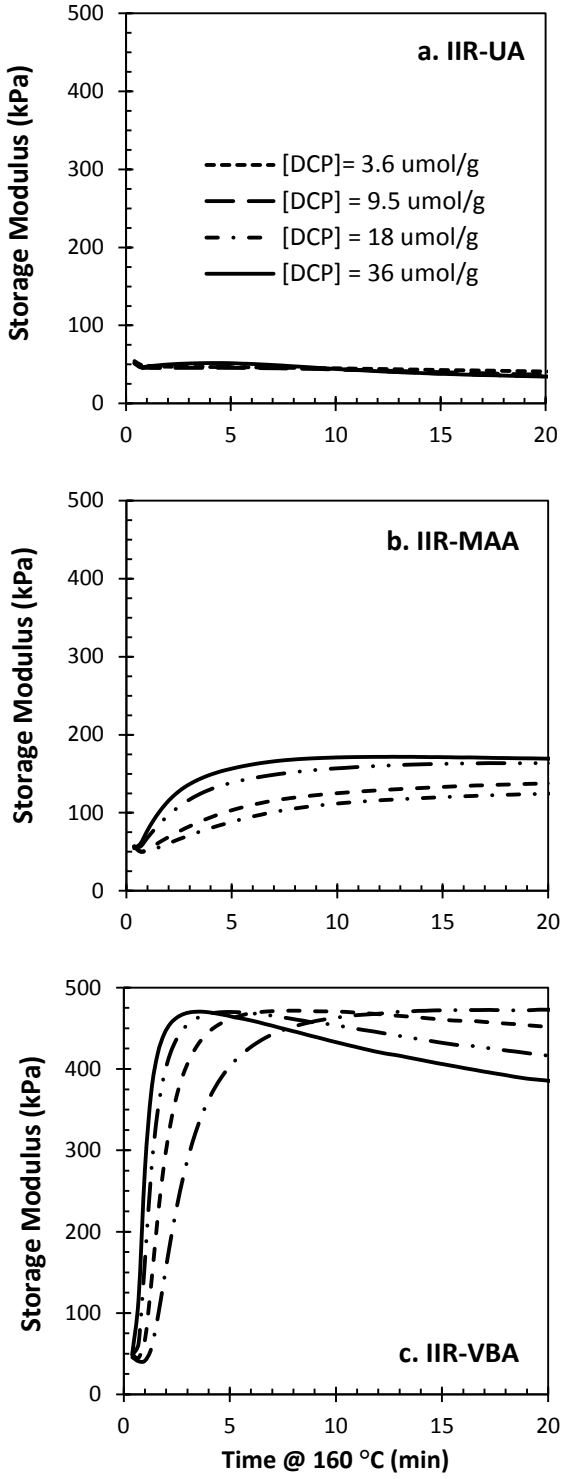

Figure 6: Cross-linking dynamics of (a) IIR-UA, (b) IIR-MAA, and (c) IIR-VBA with varying peroxide loadings

We propose that the observed relationship between cure rate and cure yield arises from a competition between ***interdependent*** cross-linking and degradation reactions. Note that if polymer degradation is kinetically favoured, then it will generate small chain fragments whose low molecular weight makes them more difficult to bring up to, and beyond, the gel point. As such, no matter how much initiator is charged to an inactive macromonomer, it cannot generate a tightly cross-linked thermoset. This is demonstrated in Figure 6a for the IIR-UA system, which fails to produce a measurable increase in G', irrespective of the peroxide loading employed.

Conversely, if cross-linking is favoured, then it will generate highly branched architectures whose molecular weight is relatively insensitive to chain scission. The storage modulus data illustrated in Figure 6c shows how IIR-VBA requires relatively few initiator-derived radicals to generate a highly elastic covalent polymer network. Once established, this network is more robust toward chain cleavage than a linear polymeric material. This phenomenon has been described in studies of biomaterial degradation, where a polymer's mass loss due to enzymatic [96] [97] [98], hydrolytic [96] [99], or thermal degradation [100] is strongly dependent on cross-link density, and that degradation is much slower in a cross-linked polymer compared to its linear parent material [99].

Hoffmann has presented a theoretical framework that captures the effect of chain architecture on its susceptibility to cleavage [101]. When a linear polymer chain of molecular weight $\overline{MW_0}$ is subjected to a fixed number of random scission events (Z), the average molecular weight ($\overline{MW}$) of the product can be expressed as follows.

Equation 1

$$\overline{MW} = \frac{\overline{MW_0}}{Z+1}$$

For example, a linear polymer chain incurring two chain scission events will have lost two thirds of its molecular weight (Figure 7a) [102] . In contrast, a scission event only affects the molecular weight of a cross-linked polymer when it frees a chain segment from the network. The number of effective scission events (Z_{eff}) is limited to those affecting chain segments that have just one point of attachment to the network, since scission between two cross-link nodes have no effect (Figure 7b). It stands to reason that Z_{eff} will be considerably less than Z highly cross-linked polymer architectures.

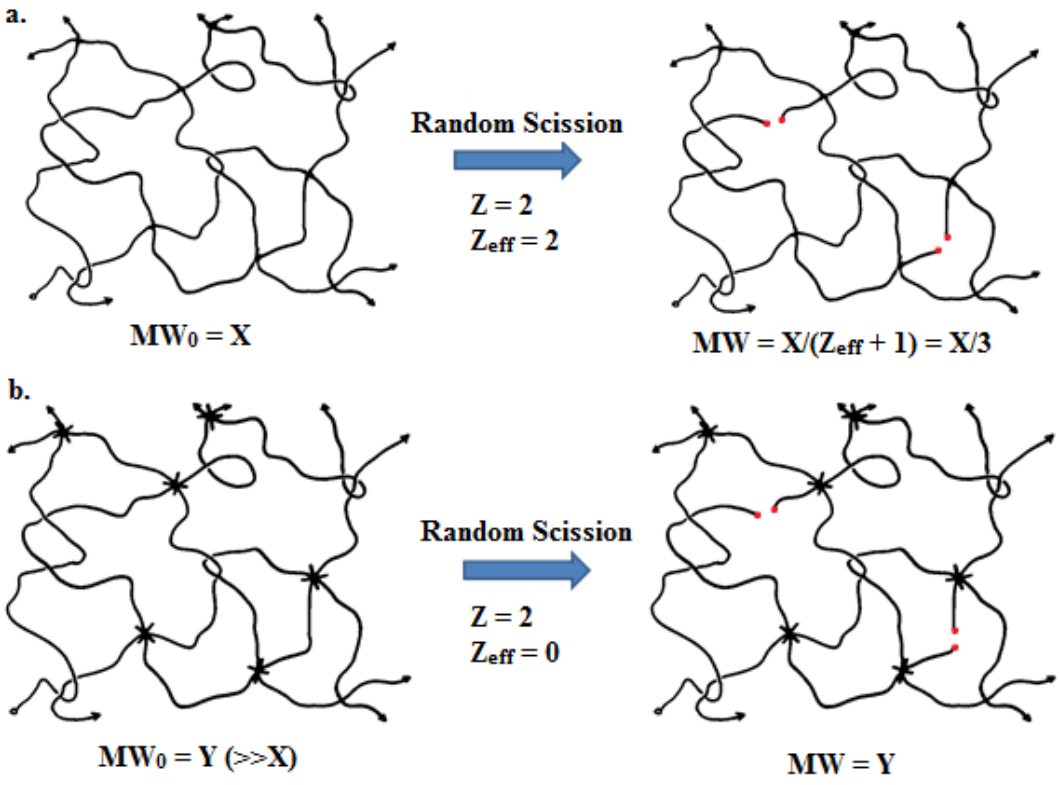

Figure 7: Effect of chain scission on molecular weight of linear (a) and cross-linked (b) polymers

In the context of IIR-based macromonomers, the most reactive materials quickly establish polymer networks that are more resistant to degradation than their linear parent materials. Therefore a material such as IIR-VBA can generate a high storage modulus at the 5 min mark of a

DCP cure, yielding a covalent network that resists large-scale degradation over the next 15 min, even though over 50% of the supplied peroxide remains active.

2.3.3 Delayed-Onset Macromonomer Cures

The macromonomer structure/reactivity data described above has shown that high cure yields are only obtained using highly reactive polymerizable functionality. However, extreme cross-linking rates in the early stages of a peroxide cure, a phenomenon known as scorch, can render the polymer thermoset before it can be molded into the desired shape. One means of delaying the onset of polymer cross-linking is to include a radical trap in the cure formulation to quench radical populations in the initial phase of the cure, thereby suppressing macro-radical combination. Nitroxyls such as TEMPO (Scheme 13) can be particularly effective, as they react with carbon-centered radicals at the diffusion limit of bimolecular reaction velocities [103] to yield spin-paired alkoxyamines [104] without trapping alkoxyl radicals generated by the peroxide initiator, [105] or affecting the rate of peroxide thermolysis [106]. This method has been previously explored in the scorch protection of polyolefins [104] and vinyl-functionalized polydimethylsiloxane [107].

Scheme 13: 2,2,6,6-tetramethylpiperidine-N-oxyl (TEMPO) and its acrylated analogue (AOTEMPO)

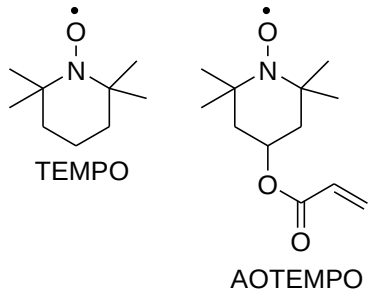

The data presented in Figure 8 demonstrate the ability of TEMPO, charged to the formulation at a concentration of 0.25 molar equivalents relative to DCP-derived cumyloxyl radicals, to suppress

IIR-VBA crosslinking for 5.1 minutes. Note that unlike controlled radical polymerizations involving nitroxyls and styrenic monomers, the intention is not to generate pseudo-living conditions, but to trap one quarter of initiator-derived radicals irreversibly. Ideally, an excess of nitroxyl relative to the initial alkyl radical population suppresses cross-linking entirely by producing stable alkoxyamines. This condition should persist until the entire 0.25 equivalents of TEMPO are consumed, at which point the residual peroxide should initiate macromonomer cross-linking unabated. At first glance, the IIR-VBA + TEMPO system appears to approach this ideal, in that a stable G' is maintained for a distinct induction period, after which rapid curing is observed to a high ultimate modulus. However, a closer examination reveals two significant deviations from ideality – the induction period is longer than anticipated, and the cure extent falls short of expectations.

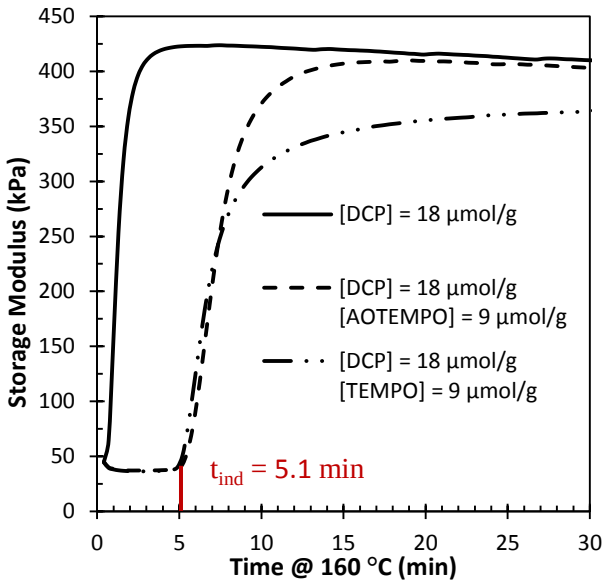

Figure 8: Cure dynamics of IIR-VBA in the presence of acrylated (AOTEMPO) and non-acrylated (TEMPO) nitroxyl anti-oxidants. [DCP] = 18 µmol/g, [Nitroxyl] = 9 µmol/g, trapping ratio = 0.25

Consider the length of the induction period. Given that TEMPO does not affect the first-order decomposition of a dialkyl peroxide [106], the time needed to consume the nitroxyl should be a

function of the initiator half-life ($t_{1/2}$) and the trapping ratio, which is defined as the ratio between the initial concentration of nitroxyl and cumyloxyl radicals. Previous studies of delayed-onset cures of polyethylene [108] and vinyl-functionalized polydimethylsiloxane [89] have shown that the induction phase of an ideal TEMPO-mediated cure abides by Equation 2.

Equation 2

$$t_{ind} = \frac{t_{1/2}}{\ln(1/2)} \ln\left(1 - \frac{[Nitroxyl]_0}{2[DCP]_0}\right)$$

$$= \frac{5.4 min}{\ln(1/2)} \ln\left(1 - \frac{9 \mu mol/g}{2(18 \mu mol/g)}\right) = 2.2\ min$$

Since the trapping ratio ($[TEMPO]_o/2[DCP]_o$) used to generate Figure 8 was 0.25, the induction period is predicted to be 2.2 min, as opposed to the observed value of 5.1 min.

It is conceivable that the cross-link density loss suffered by the IIR-VBA + TEMPO formulation is the result of insufficient radical initiator. However, sufficient residual DCP was available post-induction to convert 0.15 mmoles/g vinylbenzoate functionality. Figure 6c shows that IIR-VBA cures to the same extent when initiated by 3.6 µmol DCP/g polymer, as it does when 18 µmol/g is used. Based on a DCP half-life of 5.4 minutes at 160°C [32], at least 9 µmol/g of initiator should remain after the 5.1 min induction period. Therefore, we conclude that G' losses incurred by the use of TEMPO result from the non-productive consumption of a fraction of the macromonomer functionality in IIR-VBA.

Scheme 14 illustrates two pathways that may prolong the induction periods of TEMPO-mediated cross-linking while decreasing the ultimate cure yield. Both are based on the instability of benzylic alkoxyamines (**3**) at 160°C. The first is disproportionation to give TEMPOH + olefin [109], the kinetics and mechanism of which have been documented for small molecules [110]

[111] as well as controlled radical polymerization systems [112]. An early report by Li et al. describes the decomposition of 1-(2,2,6,6-tetramethylpiperidinyloxy)-1-phenylethane over the course of several hours at 140°C, while Ananchenko and Fischer conducted similar studies at 120°C, showing that alkoxyamine breakdown yields styrene, TEMPOH and 2,2,6,6-tetramethylpiperidine (TEMPH) [113]. The latter is believed to result from further reactions of TEMPOH. In the present context, disproportionation of the benzylic alkoxyamine (**3**) would yield a disubstituted styrenic adduct (**4**) and TEMPOH (**5**). The hydroxylamine could, in this case, regenerate TEMPO by H-atom transfer to initiator-derived alkyl or cumyloxyl radicals, or through air oxidation. Note that for this mechanism to significantly affect the induction time, the alkoxyamine decomposition at 160°C must be significantly faster than those previously reported for similar systems [110] [113].

Scheme 14: Proposed mechanism for the catalytic scorch protection of TEMPO on IIR-VBA

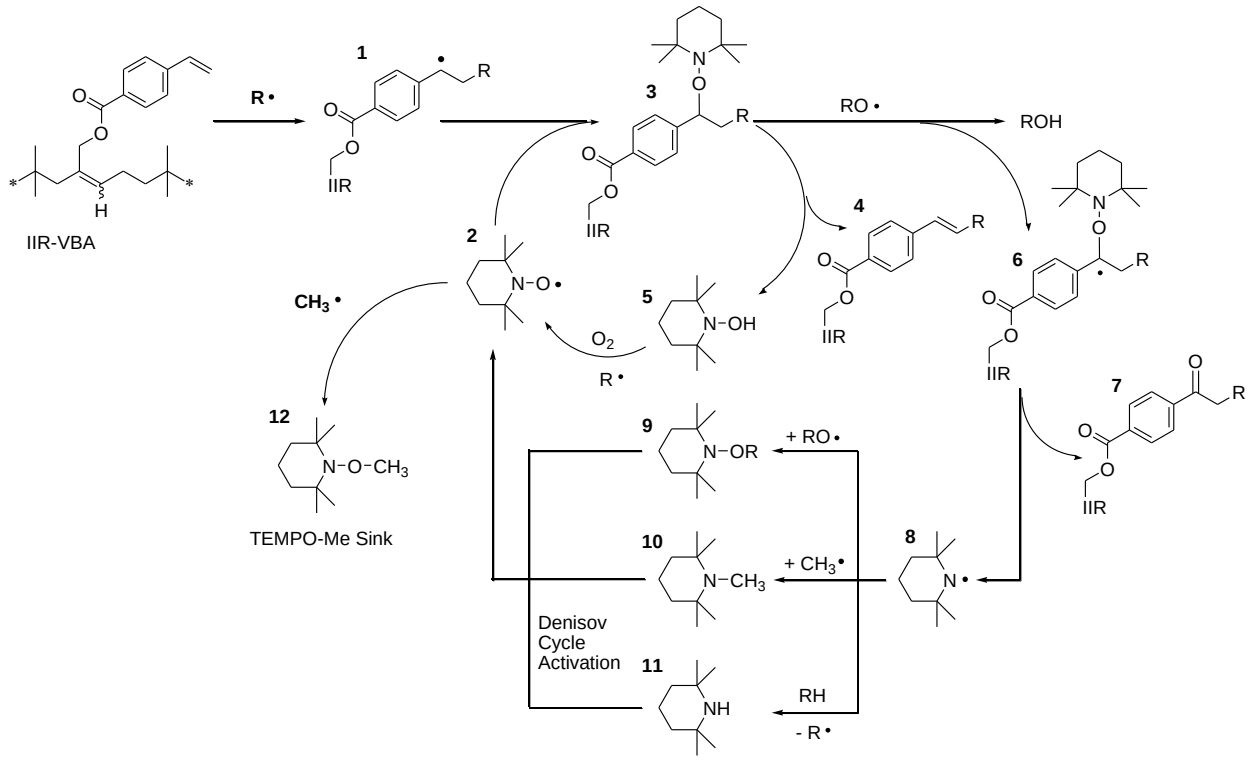

A second possible mechanism for TEMPO regeneration from **3** stems from literature that pertains to hindered amine light stabilizers, or HALS [114]. Although it is known that these alkoxyamines can protect polymer compositions from oxidative degradation, the mechanism through which they generate TEMPO free radical is presently unclear [115] [116]. Scheme 14 depicts a new a pathway suggested by Gryn'Ova et al. [117] that is based on β-hydrogen atom abstraction and subsequent disproportionation to form a ketone (**7**) and aminyl radical (**8**). Reaction of **8** with alkoxyl and alkyl radicals, as well as a suitable H-atom donor may give intermediates **9**, **10**, and **11** that are capable of producing TEMPO via established several pathways, including the Denisov cycle [118]. Note that regioselectivity could be important for the β-hydrogen atom abstraction required in this mechanism. No matter how thermodynamically favourable abstraction may be β to the alkoxyamine; it may be kinetically unlikely due the much larger concentration of abstraction sites along the polymer backbone.

Note that the product of methyl radical trapping by TEMPO, TEMPO-Me, is stable and its accumulation accounts for the eventual end of the induction time. Without a stable sink, the catalytic cycle proposed in Scheme 14 would continue indefinitely and not produce a post-induction time cure. This is clearly not the case, as IIR-VBA reaches high cross-link extents in the presence of nitroxyl. However, the proposed instability of alkoxyamine intermediates would transform vinylbenzoate groups into either unreactive ketones or less reactive 1,2-disubstituted derivatives that do not support the cure yield of their IIR-VBA precursor. One means of counteracting a loss of vinylbenzoate functionality is to use the acrylated nitroxyl, AOTEMPO (Scheme 13). Trapping of primary alkyl macroradicals generated as a result of IIR backbone activation yields acrylate macromonomer functionality, whose oligomerization can increase cure extent (Scheme 15) [89] [108]. Figure 8 demonstrates the efficacy of AOTEMPO, which provides the equivalent induction period of TEMPO while raising the ultimate storage modulus to that

provided by DCP alone. AOTEMPO provides a further advantage, in that methyl alkoxyamines created by nitroxyl trapping of cumyloxyl-derived methyl radicals (Scheme 12) can be copolymerized with macromonomer groups, thereby rendering them polymer bound. In contrast, the methyl alkoxyamines derived from of TEMPO are volatile organic compounds that can leach or be extracted from the thermoset article.

Scheme 15: Principle reactions underlying AOTEMPO-mediated IIR-VBA cross-linking

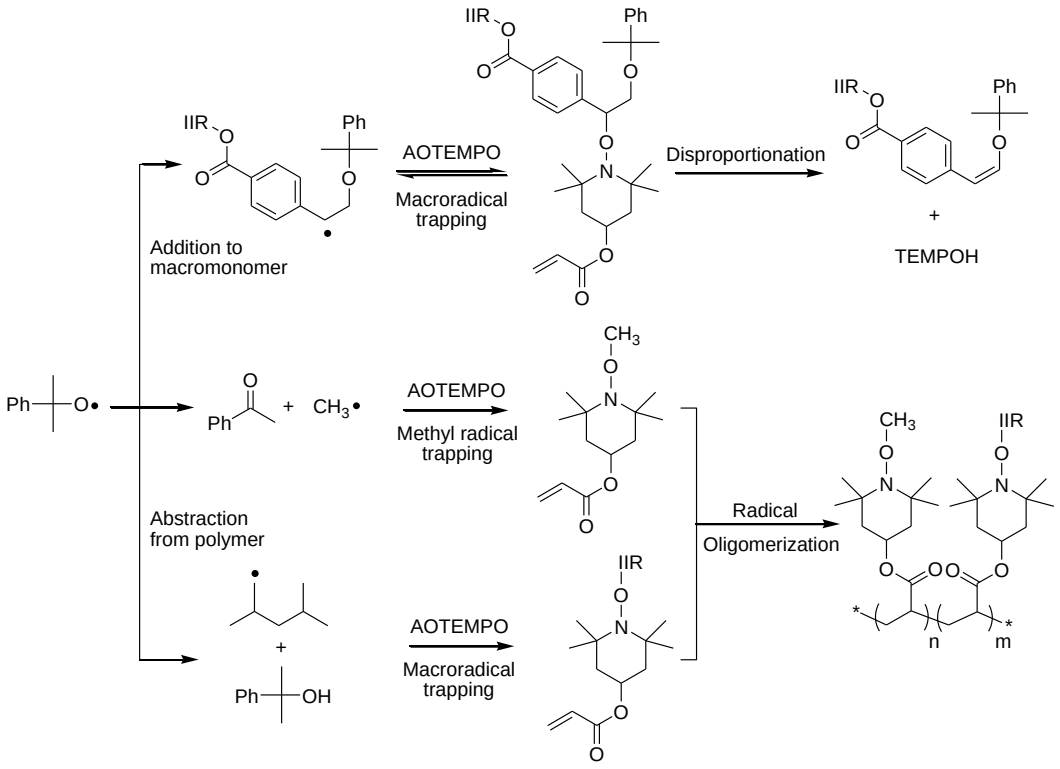

2.4 Conclusions

Macromonomer derivatives of BIIR undergo simultaneous cross-linking and degradation when activated by DCP at 160°C, with the competitive balance dictated by the reactivity of the oligomerizable group. Highly reactive styrenic, vinyl imidazolium, and maleimide functionalities rapidly produce a covalent polymer network that is resistant to chain scission, thereby generating exceptional ultimate cross-link densities. Acrylic-based macromonomers provided moderate cure rates and yields, while relatively unreactive maleate diester and allylic functionalized materials

proved incapable of generating high cross-link yields, irrespective of the amount of peroxide employed, due to the predominance of chain cleavage on polymer molecular weight.

Complications associated with the high initial cross-linking rate of IIR-VBA can be overcome using nitroxyls to quench radical activity in the early stages of the cure. Compared with ideal delayed-onset behaviour observed for the cross-linking of saturated polymers, the combination of IIR-VBA and TEMPO gives prolonged induction times and reduced cure extents. The latter can be obviated through the use of AOTEMPO to recover macromonomer functionality that is lost to undesired vinylbenzoate trapping reactions.

Chapter 3

Synthesis and Characterization of Rapidly Alkylated, Peroxide-Curable Imidazolium Bromide Derivatives of Brominated poly(isobutylene-*co*-para-methylstyrene)

3.1 Introduction

Isobutylene-rich elastomers are widely used in applications that require oxidative stability and gas impermeability [11]. Commercial grades of these materials are typically sulfur-cured, but interest in peroxide-curable grades has increased due to the superior stability of carbon-carbon cross-links over sulfide networks, and to the fewer cure by-products generated by peroxide cure chemistry. The development of peroxide-curable materials is complicated by the susceptibility of isobutylene-rich polymers toward radical degradation, as poly(isobutylene) and poly(isobutylene-co-isoprene) containing small amounts of residual isoprene unsaturation degrade when treated with peroxide initiators at standard cure temperatures [28] [35]. However, macromonomer derivatives of these materials bearing multiple acrylate, styrenic or maleimide groups per polymer chain can be cross-linked by radical oligomerization of their pendant functionality, yielding thermosets whose cross-link density scales linearly with functional group content [44] [45] [24] [23].

We have recently described a new class of macromonomer that contains a small amount (0.10 - 0.25 mmol/g) of 1-vinylimidazolium bromide functionality [66]. These reactive ionomers cure to high cross-link density when activated by standard peroxide initiators to give thermosets whose polymer network is comprised of carbon-carbon cross-links as well as aggregates of imidazolium bromide functionality. This hybrid ionic/covalent network provides unique physical properties,

owing to differences in the stress relaxation properties of the two network components. Furthermore, the ionic functionality within these materials confers antimicrobial properties to their thermosets, enhances their adhesion to high-energy surfaces, and improves their dispersion of siliceous fillers during elastomer compounding operations [56] [54] [65].

The most economical and environmentally responsible method of preparing these ionomers is a solvent-free process where a halogenated elastomer is mixed with the required imidazole nucleophile in a conventional polymer compounding device [65]. These processes seek full conversion of the electrophile to imidazolium bromide functionality in the shortest possible reaction time, using the least amount of nucleophile. Ozvald and Porter have studied the nucleophilic displacement of allylic halide from brominated poly(isobutylene-co-isoprene), or BIIR, by 1-butyl imidazole (BuIm) and 1-vinyl imidazole (VIm) under solvent–free and solvent-borne conditions [78] [119]. They reported significant differences in reaction rate between the two nucleophiles, with VIm requiring substantially longer times to reach equivalent conversions.

Although the resulting 1-vinylimidazolium bromide ionomer provided exceptional peroxide-cure reactivity and thermoset properties, the utility of this chemistry would be improved considerably by the development of an alternate functional imidazole nucleophile that is alkylated more rapidly to give an ionomer that cures at a more moderate rate. This development is the objective of the current work. A first step towards this objective involved moving from BIIR to brominated poly(isobutylene-*co*-para-methylstyrene) (BIMS). The benzylic bromide on BIMS provides a more electrophilic site for imidazole alkylation and has demonstrated faster alkylation rates. Furthermore, BIMS can alkylate imidazoles at higher temperatures without yield losses from complications attributed to dehydrohalogenation [12].

Scheme 16: Synthesis and peroxide initiated cross-linking of an N-vinylimidazolium bromide ionomer derivative of BIMS

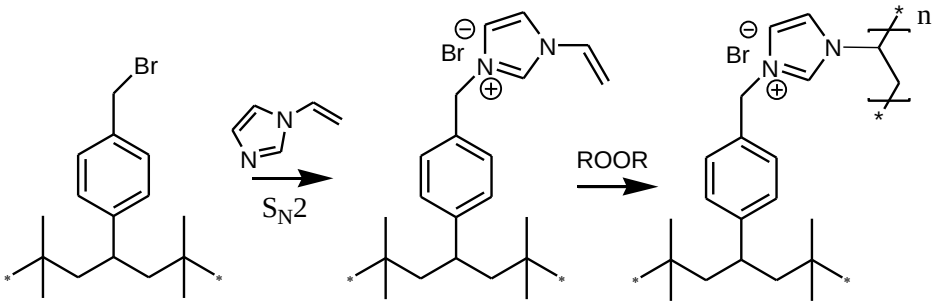

This work aims to find and characterize a functional imidazole containing unsaturation necessary for peroxide initiated oligomerization that is rapidly alkylated by BIMS. It is suspected from the previously collected rate data that electronic effects from the 1-vinyl moiety on VIm slow down the quaternization reaction. It is hypothesized that altering the electronic environment of the N-functional imidazole in question should strongly affect alkylation rate. Furthermore, it is suspected that introducing a slightly electron donating group on the 2 position on the heteroaromatic ring would increase electron density in the ring and enhance nucleophilicity, an effect observed by Salamone et al. [72]. To further explore the factors influencing quaternization of functional imidazoles by BIMS, the functional imidazoles depicted in Scheme 17 were synthesized and their respective alkylation rates with BIMS were evaluated.

Scheme 17: Imidazolium bromide ionomers included in this study

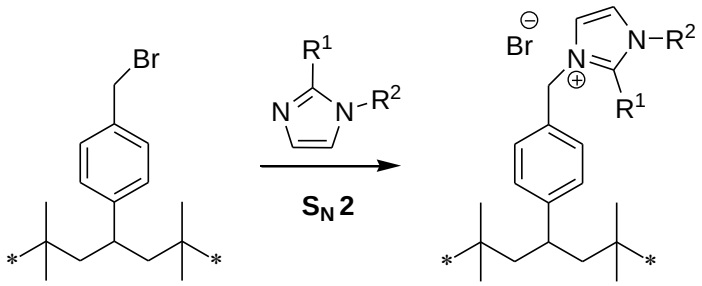

R^1	R^2	Nucleophile	Ionomer
H	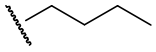	(1) 1-butylimidazole (BuIm)	(11) IMS-BuImBr
H		(2) 1-vinylimidazole (VIm)	(12) IMS-VImBr
H	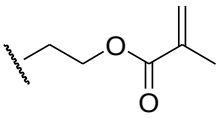	(3) 2-(1*H*-imidazol-1-yl)ethyl methacrylate (ImEMA)	(13) IMS-ImEMABr
H	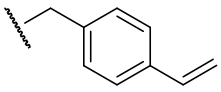	(4) 1-(4-vinylbenzyl)-1*H*-imidazole (VBIm)	(14) IMS-VBImBr
H	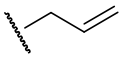	(5) 1-allylimidazole (AlIm)	(15) IMS-AlImBr
H	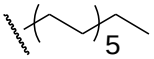	(6) 2-dodecyl-1*H*-imidazole (DDIm)	(16) IMS-DDImBr
H	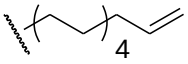	(7) 1-(10-undecen-1-yl**)**-1*H*-imidazole (UDIm)	(17) IMS-UDImBr
Et	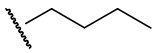	(8) 1-butyl-2-ethyl-1H-imidazole (EtBuIm)	(18) IMS-EtBuImBr
Et		(9) 1-vinyl-2-ethyl-1H-imidazole (EtVIm)	N/A
Et	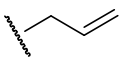	(10) 1-allyl-2-ethyl-1H-imidazole (EtAlIm)	N/A

This report describes the synthesis of the functional imidazole monomers shown in Scheme 17, and compares their respective alkylation rates by BIMS in both solvent-borne and solvent-free

syntheses. We then characterize each BIMS-derived ionomer's reactivity towards peroxide-initiated cross-linking by oscillatory rheometry. The physical properties of each novel ionomer thermoset are then tested to ensure they are in line with elastomeric ionomers previously studied. We conclude with an examination of the unique mechanism of allylimidazolium ionomer cross-linking based upon model compound studies.

3.2 Experimental

Materials: 1-Butylimidazole (BuIm, 98%), 1-vinylimidazole (VIm, 99+%), chloroform-*d* (99.8%D), methanol-*d4* (99.8%D), dicumyl peroxide (DCP, 98%) methacryloyl chloride (97.0%, ~0.02% 2,6-di-*tert*-butyl-4-methylphenol as stabilizer), 1-(2-hydroxyethyl)imidazole (97%), oxalic acid (98%), sodium carbonate (anhydrous, 99.5%, granular), 10-undecenoic acid (98%), 1M tetrabutylammonium hydroxide in methanol (Bu_4NOH), sodium hydroxide (NaOH, 97%, pellets), imidazole (99%), tetrabutylammonium bromide (TBAB, 98%), 11-bromo-1-undecene (95%), 1-bromododecane (97%), allyl bromide (97%, <1000 ppm propylene oxide as stabilizer), 2-ethylimidazole (98%), 1-bromobutane (99%), 1,2-dichloroethane (anhydrous, 99.8%), potassium hydroxide (KOH, 90%, flakes), potassium carbonate (K_2CO_3, 99%), hydroquinone (99.5%), benzyl bromide (98%), and vinylbenzyl chloride (VBCl, 97%) were used, as received, from Sigma-Aldrich (Oakville, Ontario). 2,6-Di-*tert*-butyl-4-methylphenol (BHT, 99%), and 1-allylimidazole (AlIm, 99%) were used, as received, from Alfa Aesar. Brominated poly(isobutylene-*co*-para-methylstyrene) (BIMS) (Exxpro 3745, 0.23 mmol benzylic bromide functionality/g BIMS) was used as supplied by Exxon Mobil Chemical (Baytown, Texas).

Solution Synthesis of IMS-VImBr: BIMS (10 g, 2.3 mmol benzylic bromide) was dissolved in chlorobenzene (100 mL) at 25 °C. The resulting cement was heated to 100 °C and VIm (**2**) (0.433 g, 4.6 mmol, 2 eq.) was added to the heated, stirring solution. Aliquots of the mixture (~0.3 g) were removed at regular intervals and characterized by ^{1}H-NMR for reaction dynamics data. The

final N-alkylation product, IMS-VImBr (**12**), was obtained after 30 hours in near quantitative yield by precipitation in excess acetone and purified by dissolution/precipitation using THF/acetone and dried *in vacuo*. **^{1}H-NMR** ($CDCl_3$ + 5 wt% CD_3OD): δ 10.41 (s, 1H, -N^+-C**H**-N-), δ 5.73 (dd, 1H, -N-CH=CH-**H_{trans}**), δ 5.51 (s, 2H, Ph-**CH_2**-N^+-), δ 5.41 (dd, 1H, -N–CH=CH–**H_{cis}**). Dynamics data acquired by ^{1}H-NMR integration of residual brominated para-methylstyrene mers: δ 4.49 (s, 2H), δ 4.45 (s, 2H).

Solid-State Synthesis of IMS-VImBr: BIMS (40 g, 9.2 mmol benzylic bromide) was mixed with VIm (**2**) (1.732 g, 18.4 mmol, 2 eq.), and BHT (0.008 g, 200 ppm) at 100 °C and 30 rpm using a Haake Polylab R600 internal batch mixer. Aliquots of the mixture (~0.3 g) were removed at regular intervals and characterized by ^{1}H-NMR for reaction dynamics data. The final product, IMS-VImBr (**12**), was obtained after 60 minutes in near quantitative yield. **^{1}H-NMR** ($CDCl_3$ + 5 wt% CD_3OD): δ 10.41 (s, 1H, -N^+-C**H**-N-), δ 5.73 (dd, 1H, -N-CH=CH-**H_{trans}**), δ 5.51 (s, 2H, Ph-**CH_2**-N^+-), δ 5.41 (dd, 1H, -N–CH=CH–**H_{cis}**). Dynamics data acquired by ^{1}H-NMR integration of residual brominated para-methylstyrene mers: δ 4.49 (s, 2H), δ 4.45 (s, 2H).

Synthesis of IMS-BuImBr: BIMS (10 g, 2.3 mmol benzylic bromide) was dissolved in chlorobenzene (100 mL) at 25 °C. The resulting cement was heated to 100 °C and BuIm (**1**) (0.571 g, 4.6 mmol, 2 eq.) was added to the heated, stirring solution. Aliquots of the mixture (~0.3 g) were removed at regular intervals and characterized by ^{1}H-NMR for reaction dynamics data. The N-alkylation product, IMS-BuImBr (**11**), was obtained after 7 hours in near quantitative yield by precipitation in excess acetone and purified by dissolution/precipitation using THF/acetone and dried *in vacuo*. **^{1}H-NMR** ($CDCl_3$ + 5 wt% CD_3OD): δ 9.99 (s, 1H, -N^+-C**H**-N-), δ 5.43 (s, 2H, Ph-**CH_2**-N^+-), δ 4.27 (t, 2H, -N-**CH_2**-CH_2-CH_2–CH_3). Dynamics data acquired by

^{1}H-NMR integration of residual brominated para-methylstyrene mers: δ 4.49 (s, 2H), δ 4.45 (s, 2H).

Solution Synthesis of IMS-AlImBr: BIMS (10 g, 2.3 mmol benzylic bromide) was dissolved in chlorobenzene (100 mL) at 25 °C. The resulting cement was heated to 100 °C and AlIm (**5**) (0.497 g, 4.6 mmol, 2 eq.) was added to the heated, stirring solution. Aliquots of the mixture (~0.3 g) were removed at regular intervals and characterized by ^{1}H-NMR for reaction dynamics data. The N-alkylation product, IMS-AlImBr (**15**), was obtained after 7 hours in near quantitative yield by precipitation in excess acetone and purified by dissolution/precipitation using THF/acetone and dried *in vacuo*. **^{1}H-NMR** ($CDCl_3$ + 5 wt% CD_3OD): δ 9.86 (s, 1H, -N^+-C**H**-N-), δ 6.00 (ddt, 1H, -N-CH_2-C**H**=CH_2), δ 5.43 (s, 2H, Ph-**CH_2**-N^+-), δ 5.43 (dd, 2H, -N-CH_2-CH=C**H_2**), δ 4.93 (d, 2H, -N-C**H_2**-CH=CH_2). Dynamics data acquired by ^{1}H-NMR integration of residual brominated para-methylstyrene mers: δ 4.49 (s, 2H), δ 4.45 (s, 2H).

Solid-State Synthesis of IMS-AlImBr: BIMS (40 g, 9.2 mmol benzylic bromide) was mixed with AlIm (**5**) (1.998 g, 18.4 mmol, 2 eq.) at 100 °C and 30 rpm using a Haake Polylab R600 internal batch mixer. Aliquots of the mixture (~0.3 g) were removed at regular intervals and characterized by ^{1}H-NMR for reaction dynamics data. The final product, IMS-AlImBr (**15**), was obtained after 60 minutes in near quantitative yield. **^{1}H-NMR** ($CDCl_3$ + 5 wt% CD_3OD): δ 9.86 (s, 1H, -N^+-C**H**-N-), δ 6.00 (m, 1H, -N-CH_2-C**H**=CH_2), δ 5.43 (s, 2H, Ph-**CH_2**-N^+-), δ 5.43 (dd, 2H, -N-CH_2-CH=C**H_2**), δ 4.93 (d, 2H, -N-C**H_2**-CH=CH_2). Dynamics data acquired by ^{1}H-NMR integration of residual brominated para-methylstyrene mers: δ 4.49 (s, 2H), δ 4.45 (s, 2H).

Synthesis of IMS-ImEMABr: 2-(1H-imidazol-1-yl)ethyl methacrylate (**3**) was synthesized as previously described [120]**.** 0.121g (1.076 mmol) 1-(2-hydroxyethyl)imidazole was dissolved in 5

mL DCM in a dry flask which was then purged with nitrogen gas. A 5 mL solution of DCM containing 0.169 g (1.614 mmol, 1.5 eq.) methacryloyl chloride was added dropwise to the flask at 25 °C. The mixture was stirred under nitrogen overnight at 25 °C and the DCM removed by rotary evaporation. The resulting imidazolium chloride salt was dissolved in water and acidified with oxalic acid. The water phase was then washed with ethyl acetate and basified with sodium carbonate. The pale yellow oil, ImEMA (**3**), was extracted with excess toluene and recovered in 42% yield after removing the solvent by vacuum. **^{1}H-NMR** ($CDCl_3$): δ 7.50 (s, 1H, -N-C**H**-N-), δ 7.07 (s, 1H, -N-C**H**=CH-N-), δ 6.95 (s, 1H, -N-CH=C**H**-N-), δ 6.08 (s, 1H, -OOC-C(CH_3)=CH-**H_{trans}**), δ 5.60 (s, 1H, -OOC-C(CH_3)=CH-**H_{cis}**), δ 4.38 (t, 2H, -N-C**H_2**-CH_2-COO-), δ 4.23 (t, 2H, -N-CH_2-C**H_2**-COO-), δ 1.92 (s, 3H, -OOC-C(C**H_3**)=CH_2).

BIMS (10 g, 2.3 mmol benzylic bromide) was dissolved in chlorobenzene (100 mL) at 25 °C. The resulting cement was heated to 100 °C and ImEMA (**3**) (0.829 g, 4.6 mmol, 2 eq.) was added to the heated, stirring solution. Aliquots of the mixture (~0.3 g) were removed at regular intervals and characterized by ^{1}H-NMR for reaction dynamics data. The N-alkylation product, IMS-ImEMABr (**13**), was obtained after 7 hours in near quantitative yield by precipitation in excess acetone and purified by dissolution/precipitation using THF/acetone and dried *in vacuo*. **^{1}H-NMR** ($CDCl_3$ + 5 wt% CD_3OD): δ 9.94 (s, 1H, -N^+-C**H**-N-), δ 6.08 (s, 1H, -OOC-C(CH_3)=CH-**H_{trans}**), δ 5.60 (s, 1H, -OOC-C(CH_3)=CH-**H_{cis}**), δ 5.39 (s, 2H, Ph-**CH_2**-N^+-), δ 4.70 (t, 2H, -N-C**H_2**-CH_2-COO-), δ 4.54 (t, 2H, -N-CH_2-C**H_2**-COO-). Dynamics data acquired by ^{1}H-NMR integration of residual brominated para-methylstyrene mers: δ 4.49 (s, 2H), δ 4.45 (s, 2H).

Synthesis of IMS-VBImBr: 1-(4-vinylbenzyl)-1*H*-imidazole (VBIm, **4**) was synthesized as previously described [121]. The product was obtained as a pale orange oil in 58% yield.**^{1}H-NMR** ($CDCl_3$), consistent with literature precedent: δ 6.85-7.71 (mult, 7H, aromatic), δ 6.65 (dd, 1H,

Ph-C**H**-CH_2), δ 5.71 (dd, 1H, Ph-CH-CH-$\mathbf{H_{trans}}$), δ 5.24 (d, 1H, Ph-CH-CH-$\mathbf{H_{cis}}$), δ 5.04 (s, 2H, N-C$\mathbf{H_2}$-Ph).

BIMS (10 g, 2.3 mmol benzylic bromide) was dissolved in chlorobenzene (100 mL) at 25 °C. The resulting cement was heated to 100 °C and VBIm (**4**) (0.847 g, 4.6 mmol, 2 eq.) was added to the heated, stirring solution. Aliquots of the mixture (~0.3 g) were removed at regular intervals and characterized by ^{1}H-NMR for reaction dynamics data. The N-alkylation product, IMS-VBImBr (**14**), was obtained after 7 hours in near quantitative yield by precipitation in excess acetone and purified by dissolution/precipitation using THF/acetone and dried *in vacuo*. **^{1}H-NMR** ($CDCl_3$ + 5 wt% CD_3OD): δ 10.15 (s, 1H, -N^+-C**H**-N-), δ 5.80 (dd, 1H, Ph-CH-CH-$\mathbf{H_{trans}}$), δ 5.50 (s, 2H, Ph-$\mathbf{CH_2}$-N^+-), δ 5.42 (s, 2H, N^+-C$\mathbf{H_2}$-Ph), δ 5.30 (d, 1H, Ph-CH-CH-$\mathbf{H_{cis}}$). Dynamics data acquired by ^{1}H-NMR integration of residual brominated para-methylstyrene mers: δ 4.49 (s, 2H), δ 4.45 (s, 2H).

Synthesis of IMS-UDImBr: NaOH (12.50 g, 312.5 mmol) was dissolved in water (12.50 g) and mixed with THF (60 mL). Imidazole (1.31 g, 19.8 mmol) and TBAB (0.606 g, 1.98 mmol) were added to the solution at 25 °C until all the solids were dissolved, prior to adding 11-bromo-1-undecene (4.35 g, 18.64 mmol) and heating to 60°C for 16 hours. Upon cooling, the THF was removed by rotary evaporation and the product extracted three times with DCM. The organic layer was dried with magnesium sulfate and the filtrate was concentrated by rotary evaporation. The resulting pale yellow oil, 1-(10-undecen-1-yl)-1*H*-imidazole (**7**), was obtained in 98% yield. **^{1}H-NMR** ($CDCl_3$): δ 7.40 (s, 1H, -N-C**H**-N-), δ 7.00 (s, 1H, -N-C**H**=CH-N-), δ 6.85 (s, 1H, -N-CH=C**H**-N-), δ 5.75 (ddt, 1H, -CH_2-C**H**=CH_2), δ 4.90 (dd, 2H, -CH_2-CH=C$\mathbf{H_2}$), δ 3.86 (t, 2H), δ 1.98 (dd, 2H), δ 1.71 (t, 2H), δ 1.22-1.32 (m, 12H). **^{13}C-NMR** ($CDCl_3$): δ 138.89, 136.837,

129.131, 118.556, 113.948, 46.805, 33.550, 30.865, 29.139, 29.114, 28.822, 28.657, 26.318. HRMS (EI): calculated for $C_{14}H_{24}N_2$ 220.1939, found 220.1935.

BIMS (40 g, 9.2 mmol benzylic bromide) was mixed with UDIm (**7**) (2.230 g, 1.1 eq.), at 100 °C and 30 rpm using a Haake Polylab R600 internal batch mixer for 1 hour. The product, IMS-UDImBr (**17**), was obtained in near quantitative yield. **^{1}H-NMR** ($CDCl_3$ + 5 wt% CD_3OD): δ 10.22 (s, 1H, -N^+-C**H**-N-), δ 5.80 (ddt, 1H, -CH_2-C**H**=CH_2), δ 5.48 (s, 2H, Ph-**CH_2**-N^+-), δ 4.95 (dd, 2H, -CH_2-CH=C**H_2**), δ 4.30 (dd, 2H, -N-C**H_2**-CH_2-CH_2-).

Synthesis of IMS-DDImBr: NaOH (12.50 g, 312.5 mmol) was dissolved in water (12.50 g) and mixed with THF (60 mL). Imidazole (1.31 g, 19.8 mmol) and TBAB (0.606 g, 1.98 mmol) were added to the solution at 25°C until all the solids were dissolved, prior to adding 1-bromododecane (4.65 g, 18.64 mmol) and heating to 60°C for 16 hours. Upon cooling, the THF was removed by rotary evaporation and the product was extracted three times with DCM. The organic layer was dried with magnesium sulfate and the filtrate was concentrated by rotary evaporation. The resulting oil, 2-dodecyl-1*H*-imidazole (**6**) was obtained in near quantitative yield. **^{1}H-NMR** ($CDCl_3$), consistent with literature precedent [122]: δ 7.44 (s, 1H, -N-C**H**-N-), δ 7.03 (s, 1H, -N-C**H**=CH-N-), δ 6.88 (s, 1H, -N-CH=C**H**-N-), δ 3.90 (t, 2H, N-C**H_2**-CH_2-), δ 1.75 (t, 2H, N-CH_2-C**H_2**-), δ 1.24 (m, 18H), δ 0.86 (t, 3H, -CH_2-CH_2-C**H_3**).

BIMS (40 g, 9.2 mmol benzylic bromide) was mixed with DDIm (3.720 g, 1.5 eq.), at 100 °C and 30 rpm using a Haake Polylab R600 internal batch mixer for 1 hour. The product, IMS-DDImBr (**16**), was obtained in near quantitative yield. **^{1}H-NMR** ($CDCl_3$ + 5 wt% CD_3OD): δ 10.93 (s, 1H, -N^+-C**H**-N-), δ 5.46 (s, 2H, Ph-**CH_2**-N^+-), δ 4.25 (t, 2H, -N-C**H_2**-CH_2-CH_2-).

Synthesis of IMS-EtBuImBr: 1-butyl-2-ethylimidazole was prepared as previously described [123]. The clear liquid product, EtBuIm (**8**), was recovered in 68% yield. **^{1}H-NMR** ($CDCl_3$), consistent with literature precedent: δ 6.76 (d, 1H, -N-C**H**=CH-N-), δ 6.65 (d, 1H, -N^+-CH=C**H**-N-), δ 3.66 (t, 2H, -N-C**H**$_2$-CH_2-), δ 2.51 (q, 2H, N^+-C-C**H**$_2$-CH_3), δ 1.55 (mult, 2H, -N-CH_2-C**H**$_2$-), δ 1.20 (dt, 2H, -N-CH_2-CH_2-C**H**$_2$-), δ 1.18 (t, 3H, N^+-CN-CH_2-C**H**$_3$), δ 0.79 (t, 3H, -CH_2-CH_2-CH_2-C**H**$_3$) .

BIMS (10 g, 2.3 mmol benzylic bromide) was dissolved in chlorobenzene (100 mL) at 25 °C. The resulting cement was heated to 100 °C and EtBuIm (**8**) (0.700 g, 4.6 mmol, 2 eq.) was added to the heated, stirring solution. Aliquots of the mixture (~0.3 g) were removed at regular intervals and characterized by ^{1}H-NMR for reaction dynamics data. The N-alkylation product, IMS-EtBuImBr (**18**), was obtained after 7 hours in near quantitative yield by precipitation in excess acetone and purified by dissolution/precipitation using THF/acetone and dried *in vacuo*. **^{1}H-NMR** ($CDCl_3$ + 5 wt% CD_3OD): δ 5.49 (s, 2H, Ph-**C**$\mathbf{H_2}$-N^+-), δ 4.23 (t, 2H, -N-**C**$\mathbf{H_2}$-CH_2-CH_2–CH_3), δ 3.24 (t, 2H, -C-**C**$\mathbf{H_2}$-CH_3 Dynamics data acquired by ^{1}H-NMR integration of residual brominated para-methylstyrene mers: δ 4.49 (s, 2H), δ 4.45 (s, 2H).

Synthesis of 1-allyl-2-ethyl-1H-imidazole: In 2mL acetonitrile was dissolved allyl bromide (0.665 g, 5.5 mmol), and 2-ethylimidazole (0.480 g, 5.0 mmol). NaOH (0.24 g, 6.0 mmol) was added and the mixture stirred at 25°C for 5 hours. The reaction mixture was then filtered, and the filtrate evaporated by rotary evaporation. The clear liquid product, EtAlIm (**10**), was recovered in 73% yield by Kugelrohr distillation (60°C, 0.6 mmHg). **^{1}H-NMR** ($CDCl_3$): δ 6.93 (d, 1H, -N-C**H**=CH-N-), δ 6.78 (d, 1H, -N-CH=C**H**-N-), δ 5.88 (ddt, 1H, -N-CH_2-C**H**=CH_2), δ 5.19 (dd, 1H, -N-CH_2-CH=CH-$\mathbf{H_{trans}}$), δ 4.98 (dd, 1H, -N-CH_2-CH=CH-$\mathbf{H_{cis}}$), δ 4.43 (dt, 2H, -N-**C**$\mathbf{H_2}$-CH=CH_2), δ 2.62 (q, 2H, -C-C**H**$_2$-CH_3), δ 1.30 (t, 3H, -C-CH_2-C**H**$_3$). **^{13}C-NMR** ($CDCl_3$): δ

149.26, 132.95, 127.12, 119.25, 117.40, 47.98, 19.98, 12.03. HRMS (EI): calculated for $C_8H_{12}N_2$ 136.1000, found 136.1005.

Synthesis of 1-vinyl-2-ethyl-1H-imidazole: EtVIm (**9**) was prepared as previously described [124]. 2-ethylimidazole (1.442 g, 15.0 mmol) was added to a stirring mixture of 1,2-dichloroethane (40mL), TBAB (0.104 g, 0.32 mmol), KOH (5.6 g, 100 mmol), and K_2CO_3 (4.42 g, 32 mmol). The mixture was stirred at 50 °C for 5 hours, cooled, filtered, and the organic solution washed with water (2 x 10 mL). The organic phase was then dried with magnesium sulfate and the solvent removed by rotary evaporation. The clear liquid product, 2-ethyl-1-chloroethyl-1*H*-imidazole, was purified and isolated in 41% yield by Kugelrohr distillation (60°C, 0.6 mmHg). **^{1}H-NMR** ($CDCl_3$), consistent with literature precedent: δ 6.90 (d, 1H, -N-C**H**=CH-N-), δ 6.82 (d, 1H, -N-CH=C**H**-N-), δ 4.12 (d, 2H, -N-CH_2-C**H_2**-Cl), δ 3.65 (d, 2H, -N-C**H_2**-CH_2-Cl), δ 2.64 (q, 2H, -C-C**H_2**-CH_3), δ 1.29 (t, 3H, -C-CH_2-C**H_3**).

A mixture of 2-ethyl-1-chloroethyl-1*H*-imidazole (0.98 g, 6.18 mmol), potassium hydroxide (1.38 g, 24.6 mmol), and hydroquinone (30 mg) were added to isopropyl alcohol (40 mL) and refluxed for 2 hours. Upon cooling and filtering, the alcohol was removed by rotary evaporation, water (20 mL) was added to the reaction mixture and the organic material was extracted with DCM (3 x 20 mL). The organic phase was dried with magnesium sulfate, filtered and the solvent removed by rotary evaporation. The dehydrohalogenation product, EtVIm (**9**), was purified and isolated in 53% yield by Kugelrohr distillation (60°C, 0.6 mmHg). **^{1}H-NMR** ($CDCl_3$), consistent with literature precedent: δ 7.02 (d, 1H, -N^+-C**H**=CH-N-), δ 6.84 (d, 1H, -N^+-CH=C**H**-N-), δ 6.77 (dd, 1H, -N-C**H**=CH_2), δ 5.01 (dd, 1H, -N-CH=CH-**H_{trans}**), δ 4.75 (dd, 1H, -N-CH=CH-**H_{cis}**), δ 2.63 (q, 2H, -C-C**H_2**-CH_3), δ 1.21 (t, 3H, -C-CH_2-C**H_3**).

General procedure for the synthesis of imidazolium bromide ionic liquids: The appropriate 3-alkyl-1*H*-imidazole compound (8 mmol) and benzyl bromide (1.368 g, 8 mmol) were dissolved in THF (12 mL) and stirred at 25 °C overnight. The viscous ionic liquid settled to the bottom of the stirred flask and the organic phase was decanted. The ionic liquid was washed and decanted three times with additional THF and any residual solvent removed by rotary evaporation.

3-benzyl-1-allyl-1H-imidazol-3-ium bromide: **DSC**: T_g = -48 °C. **IR** (film) ν = 3427(s), 3130(s), 3068(s), 1625(m), 1560(s), 1497(m), 1454(s), 1341(m), 1155(s), 994(m), 947(m), 757(s), 713(s) cm^{-1}. **^{1}H-NMR** ($CDCl_3$): δ 10.43 (s, 1H, N^+-C**H**-N), δ 7.29-7.46 (m, 7H, aromatics), δ 5.95 (ddt, 1H, -N-CH_2-C**H**=CH_2), δ 5.56 (s, 2H, Ph-**CH_2**-N^+-), δ 5.38 (dd, 2H, -N-CH_2-CH=C**H_2**), δ 4.93 (d, 2H, -N-C**H_2**-CH=CH_2). **^{13}C NMR** ($CDCl_3$): δ 136.5, 129.8, 129.3, 129.0, 122.7, 122.3, 122.2, 53.2, 52.1. HRMS (EI): calculated for $C_{13}H_{15}N_2$ 199.1227, found 199.1235.

3-benzyl-1-vinyl-1H-imidazol-3-ium bromide: **DSC:** T_g = N/A. **IR** (film) ν = 3429(s), 3127(s), 3082(s), 1651(s) 1550(s), 1497(w), 1455(m), 1369(m), 1163(s), 958(m), 922(m), 719(s) cm^{-1}. **^{1}H-NMR** ($CDCl_3$): δ 10.68 (s, 1H, -N^+-C**H**-N-), δ 7.17-7.91 (m, 7H, aromatics), δ 7.22 (dd, 1H, -N-C**H**=CH_2), δ 5.89 (dd, 1H, -N-CH=CH-**H_{trans}**), δ 5.52 (s, 2H, Ph-**CH_2**-N^+-), δ 5.16 (dd, 1H, -N–CH=CH–**H_{cis}**). HRMS (ESI): calculated for $C_{12}H_{13}N_2$ 185.1078, found 185.1079.

3-benzyl-2-ethyl-1-allyl-1H-imidazol-3-ium bromide: **^{1}H-NMR** ($CDCl_3$): δ 7.66 (d, 1H, -N^+-C**H**=CH-N-), δ 7.59 (d, 1H, -N^+-CH=C**H**-N-), δ 7.34 (m, 5H, phenylic), δ 5.98 (ddt, 1H, -N-CH_2-C**H**=CH_2), δ 5.57 (s, 2H, Ph-**CH_2**-N^+-) δ 5.38 (dd, 1H, -N-CH_2-CH=CH-**H_{trans}**), δ 5.29 (dd, 1H, -N-CH_2-CH=CH-**H_{cis}**), δ 4.93 (dt, 2H, -N-**CH_2**-CH=CH_2), δ 3.19 (q, 2H, -C-C**H_2**-CH_3), δ 1.01 (t, 3H, -C-CH_2-C**H_3**). HRMS (ESI): calculated for $C_{15}H_{19}N_2$ 227.1548, found 227.1540.

General procedure for the peroxide initiated polymerization of N-functional imidazolium bromide ionic liquids: A mixture of imidazolium bromide ionic liquid (2.4 mmol) and dicumyl peroxide (52.1 mg, 0.19 mmol) were stirred in a 1mL Wheaton vial and heated in a heating block at 160°C for 1 hour. The resulting mixture was taken up in $CDCl_3$ and to it was added TBAB (0.193 g, 0.60 mmol) as an external standard for ^{1}H-NMR analysis. To isolate the microparticles, the mixture was taken up in water (5mL), centrifuged, and decanted. The washing process was repeated 3 times and the purity of the insoluble particles verified by ^{1}H-NMR.

PhAlImBr-XL: **DSC**: T_g = N/A. **IR** (film) ν = 3395(m), 3962(m), 2929(m), 1627(m), 1496(w), 1454(m), 1357(w), 1261(m), 1157(s), 1096(m), 1027(m), 800(m), 703(m) cm^{-1}.

PhVImBr-XL: **DCS**: T_g = N/A. **IR** (ATR-ZnSe) ν = 3402(s), 3124(m), 3060(s), 1632(m), 1549(s), 1497(w), 1454(m), 1209(w), 1151(s), 1109(w), 711(s).

Preparation of Cured Macrosheets: A 35 g batch of purified ionomer was coated with the required amount of a solution of DCP in acetone and allowed to dry before being passed through a two roll mill ten times. The compounded sample was then sheeted in the mill and compression molded at 160°C and 20 MPa for 60 min [125]. The sheeted product had a thickness of 2.00 ± 0.2 mm.

Analysis: NMR characterization was done on a Bruker AM400 instrument with chemical shifts (δ) reported relative to tetramethylsilane in ppm. Mass spectra were obtained on an Applied Biosystems QStar XL QqTOF mass spectrometer. Rheological characterization was performed with an Advanced Polymer Analyzer 2000 from Alpha Technologies operating in a biconical disk configuration. A 5.0 g sample of the uncured material was coated with 0.5 wt% of a solution of

DCP in acetone and allowed to dry for ten minutes before being passed through a two roll mill ten times. The mixed compound was cured in the rheometer cavity at 160°C for 60 min, at a 3° oscillation arc and a frequency of 1 Hz. Stress relaxation measurements were conducted at 100 °C with a strain of 2° for 5 min. Temperature sweeps were conducted from 100 °C to 200 °C at a frequency of 1 Hz and a 3° oscillation arc.

Tensile strength data were acquired using an INSTRON Series 3360 universal testing instrument, operating at a crosshead speed of 500 mm/min at 23 ± 1 °C [126]. Young's modulus was found by calculating the slope of the stress (MPa) vs. strain (mm/mm) curve from 0 mm to 0.2 mm extension. Dog bones were cut from the specimen cutter described in ASTM D4482 [127]. Five replicate measurements were made for each sample.

3.3 Results and Discussion

3.3.1 Solution State N-Alkylation Dynamics

Careful studies of solvent-free reaction dynamics are complicated by the difficulty in maintaining constant temperatures within a conventional polymer processing device, as well as the increased sensitivity to experimental error incurred by shorter reaction times. More precise assessments of reaction rates can be gained from the solvent-borne data of the type illustrated in Figure 9. These results were acquired using 10 wt% solutions of BIMS in chlorobenzene that contained two molar equivalents of nucleophile relative to benzylic bromide functionality. ^{1}H-NMR analysis of samples withdrawn at specific intervals showed no evidence of undesirable side-reactions that might compromise reaction yields, as all N-alkylations proceeded to full conversion given sufficient time.

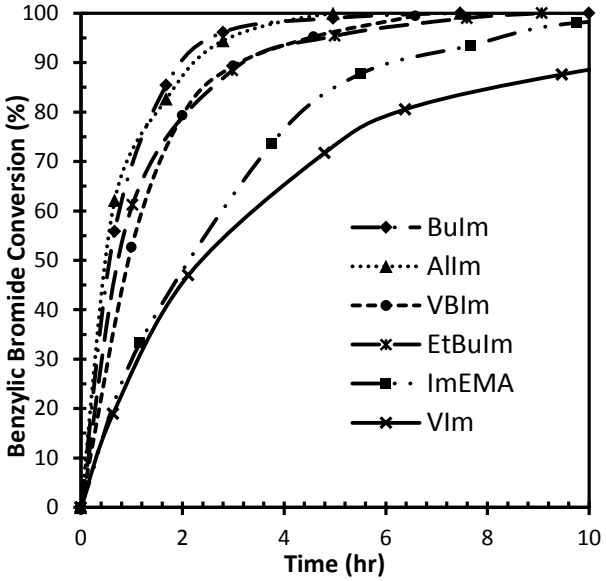

Figure 9: N-alkylation dynamics of imidazole nucleophiles by BIMS in chlorobenzene (100°C, 2 eq.)

Substantial differences in the N-alkylation rates of BuIm and VIm demonstrate the extent to which substituents can affect the nucleophilicity of a functional imidazole (Figure 9). Salamone et al. observed improved nucleophilicity for imidazoles bearing alkyl substituents at the 2-position [72], leading us to assess the reactivity of 2-ethyl-1-butyl imidazole (EtBuIm, **8**). The reaction conversion data showed no improvement when compared to BuIm, suggesting that this approach may not be applicable to the system of interest. Furthermore, it was found that introducing an ethyl substituent to the otherwise stable VIm system increased the monomer's susceptibility to auto-initiated cross-linking at high temperature. Even in the presence of anti-oxidants, (2-ethyl-1-vinylimidazole (EtVIm, **9**) produced insoluble gel early in the BIMS alkylation, and as a result, withdrawn samples could not be fully dissolved and ^{1}H-NMR data could not be collected at high conversion. As such, conversion data was collected for the reaction of EtVIm with benzyl bromide in acetone as a model system for BIMS. These reaction rate data confirmed that

introducing 2-alkyl substituents to functional imidazoles does not increase alkylation rate by benzylic bromides.

To overcome potential electronic effects associated with an N-vinyl substituent, 2-(1*H*-imidazol-1-yl)ethyl methacrylate (ImEMA, **3**) was synthesized and alkylated by BIMS. The effect of distancing the polymerizable functionality from the heteroaromatic nucleophile was significant, but did not match the reactivity observed for BuIm. This could be due to residual inductive effects from the electron withdrawing oxygen. To further mitigate electronic effects, 1-(4-vinylbenzyl)-1*H*-imidazole (VBIm, **4**) was synthesized and similarly alkylated by BIMS. This again increased alkylation rate but at the expense of high temperature stability as high gel content product with limited solubility was invariably recovered. Nevertheless, ^{1}H-NMR reaction rate data was collected from the soluble portion of each aliquot.

1-Allylimidazole (AlIm) was synthesized as a final candidate to further increase alkylation rate. It was hypothesized that allylic unsaturation would produce a different electronic environment around the imidazole ring than vinyl unsaturation. Unique peroxide cross-linking potential also exists as allylic systems have very low bond dissociation energies [128] and have demonstrated good activity towards hydrogen atom abstraction and combination [87] [129] . Furthermore, non-ionic allylic systems are known to possess some free radical oligomerization activity [86] and have even been used in a cross-linking paradigm by Oie et al. to peroxide cross-link polybenzoxazines [130]. It was found that the N-alkylation rate of AlIm with BIMS in solution was statistically identical to that of BuIm, an encouraging result going forward. Note that even the ostensibly less reactive allylic moiety became unstable upon the introduction of the 2-ethyl substituent (**10**) and, similarly to **9,** formed insoluble gel early in the alkylation reaction.

3.3.2 Peroxide-Initiated Cure Dynamics

Because of the challenges in characterizing the chemical structure of polymer thermosets, the extent of polymer cross-linking must be inferred from rheological measurements of a formulation's storage modulus (G') [5]. This is accomplished using an oscillating biconical disc rheometer operating at fixed temperature, frequency and strain amplitude to give data such as those plotted in Figure 10. These results confirm that IMS-BuImBr, which contains no oligomerizable functional groups, degrades when mixed with 0.5 wt% dicumyl peroxide (DCP) and heated to 160°C. Note that the benzylic site adjacent to the imidazolium ion pair within IMS-BuImBr has a relatively low BDE, and could promote cross-linking by H-atom abstraction followed by benzylic radical combination. However, the observed loss of G' shows that this mechanism is not competitive with polymer chain scission, resulting in a net loss of molecular weight.

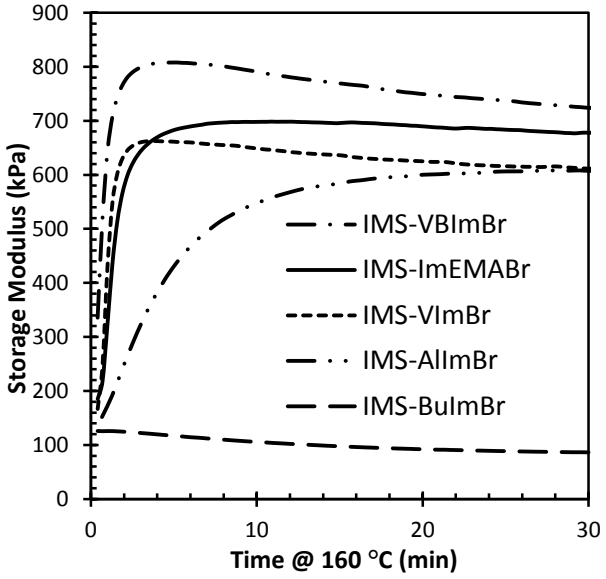

Figure 10: Peroxide cross-linking dynamics of various imidazolium ionomers of BIMS ([DCP]=18 µmol/g, 160°C, 1 Hz, 3° arc)

Consistent with the report of Ozvald et al. [78], IMS-VImBr attained its maximum storage modulus before DCP reached its first half-life (5.4 min at 160°C) [32]. The subsequent decline in G' marks the transition between vinyl imidazolium bromide conversion to cross-links, and peroxide-initiated degradation of the polymer backbone. Both the acrylate functionalized ionomer (**13**), and its styrenic analogue (**14**), also cured at similarly exceptional reaction velocities. Note, however, that high cross-linking rates can be problematic for some applications, as the material may be rendered thermoset before taking the shape of a compression mold cavity, a phenomenon known as scorch. As such, a macromonomer bearing less reactive pendant functionality may be of considerable utility. Furthermore, extreme reactivity can also produce the synthesis and storage instability observed for IMS-VBImBr, which cross-links to some extent during synthesis or storage even in the presence of conventional anti-oxidants. The IMS-VBImBr product is a high gel content rubber similar to the isobutylene/isoprene/divinylbenzene terpolymer invented in 1969 by Oxley and Wilson, which possessed diminished processing characteristics and high initial modulus (330 kPa in this case), though still able to further cross-link under peroxide initiation [44].

Interestingly, the allylic ionomer (**15**) produced a comparable ultimate modulus to its very reactive counterparts, but at a much slower cure rate. In general, allylic monomers are not viewed as highly polymerizable, due to degradative chain transfer to monomer [87] [86]. For example, radical polymerizations of propylene and allyl benzoate generally produce low yields of oligomeric materials, because allylic H-atom abstraction competes with radical addition to the C=C bond. In the context of an isobutylene-rich macromonomer cure, low functional group reactivity usually correlates with low cure extent, since polymer backbone degradation competes with cross-linking through oligomerization of pendant C=C functionality. The unique

combination of moderate cure rate and high cure yield provided by IMS-AlImBr is, therefore, of considerable fundamental and technological interest.

Insight into the differences between IMS-VImBr and IMS-AlImBr was gained by comparing their response to peroxide concentration. Macromonomers whose functionality oligomerizes with high kinetic chain length require relatively little initiator to reach full C=C conversion. This is the case for IIR-VImBr, which needed only 3.6 μmole DCP/g to reach a storage modulus plateau of 660 kPa (Figure 11a). In contrast, IMS-AlImBr is much less reactive, as it required several times more DCP to achieve this ultimate cure extent (Figure 11b). It is important to note, however, that the IMS-AlImBr system does, in fact, reach an upper limit to the storage modulus. Peroxide cures of fully saturated polymers such as linear low density polyethylene are purely stoichiometric processes involving H-atom abstraction from the polymer followed by combination of the resulting macroradicals. In these simple cure systems, the cross-link density is always proportional to the initiator loading. This is clearly not the case for IMS-AlImBr, whose response to DCP concentration is consistent with a macromonomer whose limited reactivity requires higher initiator loadings to fully convert its pendant functional groups.

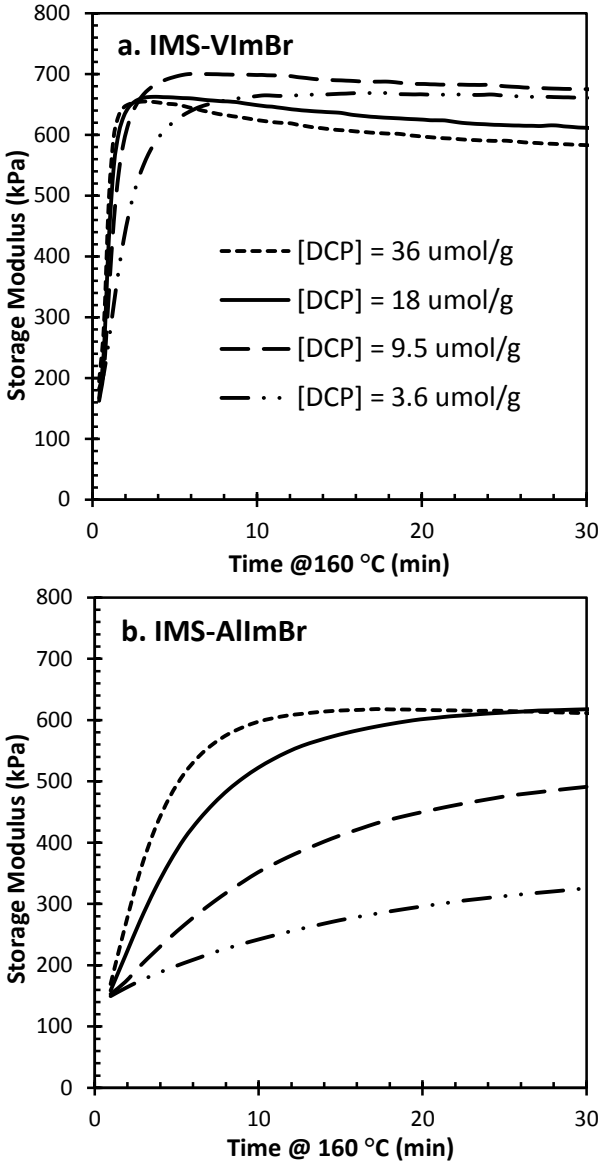

Figure 11: Peroxide cure dynamics of (a) IMS-VImBr and (b) IMS-AlImBr with increasing peroxide loading (160°C, 1 Hz, 3° arc)

What distinguishes IMS-AlImBr from other macromonomers that suffer from poor kinetic reactivity is its potential to achieve high extents of cross-linking. Consider the rheology data plotted in Figure 12, in which IMS-AlImBr is compared with an allyl-functionalized imidazolium ionomer, IMS-UDImBr (**17**), whose reactive functional group is remote from the imidazolium group, and a completely saturated ionomer, IMS-DDImBr (**16**). The results confirm that the allyl

group within IMS-AlImBr is activated by the heteroaromatic ring, which differentiates it from standard α-olefin functionality. Unfortunately, literature reports on allylimidazolium polymerization are limited to a study 1-allyl-3-methyl imidazolium chloride copolymerization with acrylonitrile, wherein observed reactivity ratios simply demonstrated the relatively low reactivity of the allyl monomer [131].

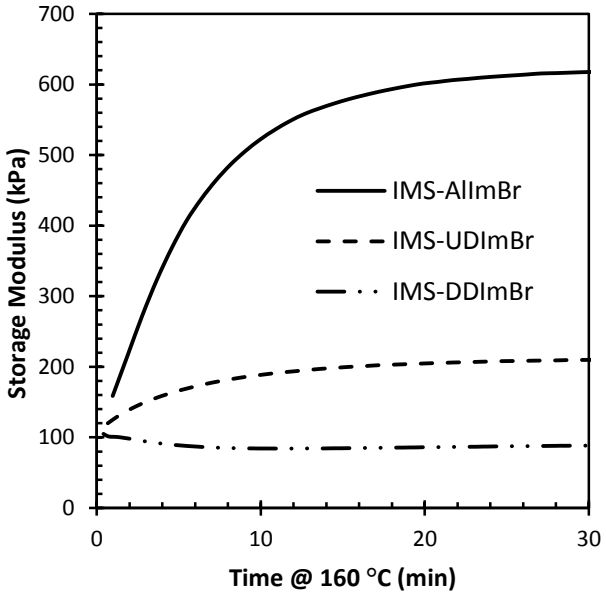

Figure 12: Peroxide cure dynamics of allylic, terminally unsaturated, and saturated imidazolium bromide ionomers of BIMS ([DCP] = 18 μmol/g, 160°C, 1 Hz, 3° arc)

The susceptibility of an activated allylic monomer toward H-atom abstraction is likely to underlie its unique cure reactivity / cure yield performance. Scheme 18 illustrates two distinct mechanisms for DCP-initiated cross-linking. Highly reactive materials such as IMS-VImBr cure through radical addition to the C=C bond, yielding an oligomeric macroradical that can be quenched by chain transfer and/or radical-radical termination. An allylic monomer can also be activated by H-atom transfer, yielding a resonance-stabilized allyl radical that prefers termination by combination to propagation through monomer addition. This H-atom abstraction is commonly referred to as degradative chain transfer, in that both polymerization rate and degree of

polymerization are reduced. However, in the context of an isobutylene-rich macromonomer cure, labile allylic H-atoms may promote cross-linking by reducing the extent of polymer backbone degradation.

Scheme 18: Proposed IMS-AlImBr cross-linking mechanism

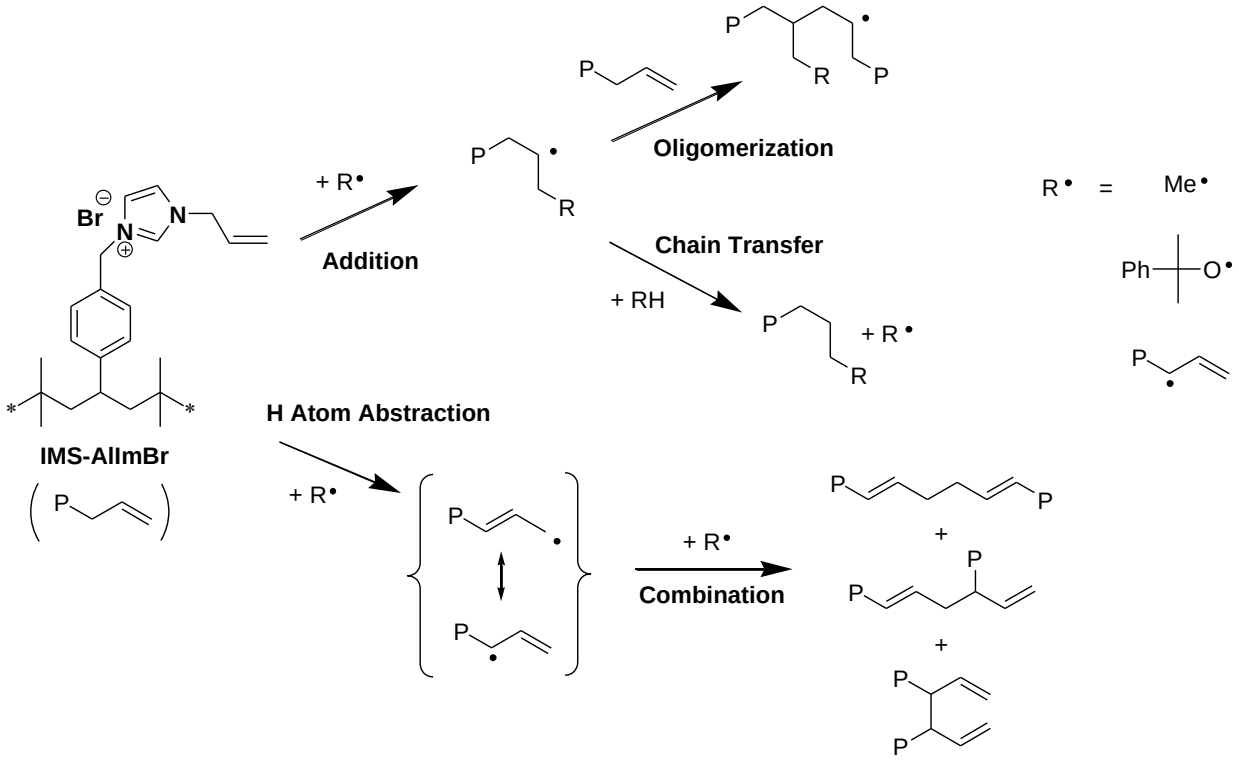

Note that the molecular weight losses suffered by poly(isobutylene) result from H-atom abstraction from methyl groups, followed by cleavage of the resulting primary macro-radical [35] [90]. The IMS-AlImBr system provides 0.23 mmole of allylic groups, which are far more reactive H-atom donors than methyl groups. As such, activation of allyl imidazolium functionality by H-atom transfer and/or addition shifts the radical population away from the polymer backbone, thereby suppressing the degradation process that competes with macromonomer cross-linking. According to this proposed mechanism, allylic H-atom abstraction hinders the oligomerization process, but protects the backbone from radical scission. Furthermore, the possible products of allyl radical combination contain residual unsaturation, some of which able to oligomerize to

some extent by typical vinyl addition, further reducing the chain breaking effects of H-atom abstraction in this system. These factors combine in IMS-AlImBr to produce a slow cure rate with high final modulus.

To gain a better understanding of the radical reactivity of allylimidazolium bromides, a model compound, PhAlImBr (**21**), was reacted with DCP under solvent-free conditions that mimic the aggregated state of ion-pairs in the ionomer (Scheme 19). The 0.5 wt% peroxide loading used throughout the cure studies corresponds to 13 mol% DCP relative to the imidazolium bromide content of IMS-AlImBr. Therefore, 13 mol% DCP was decomposed within PhAlImBr for 1 hour at 160°C. ^{1}H-NMR analysis of the reaction mixture in both acetone-d_6 and $CDCl_3$ revealed only starting material (**21**) and acetophenone, the latter resulting from the β-scission of the cumyloxyl radicals derived from DCP. However, the PhAlImBr conversion was 31%, indicating that reaction products were insoluble in either solvent.

Scheme 19: Solvent-free imidazolium halide model compound cures

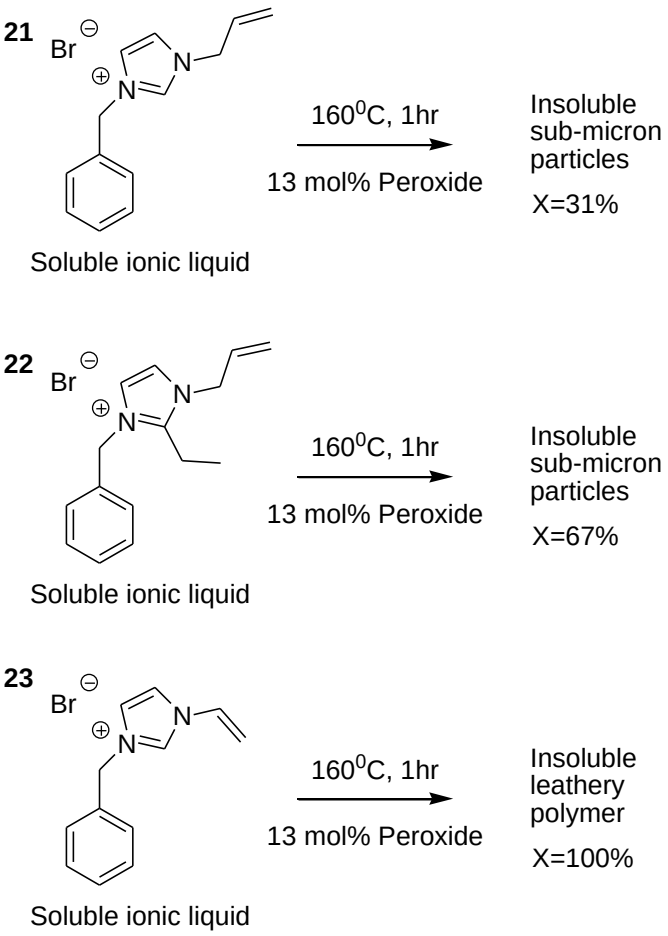

Furthermore, it is known that vinylimidazolium (VIm) halide ionic liquids can be polymerized via free radical polymerization to produce highly conductive poly(ionic liquid)s (PILs) [132] [69] [71]. It has even been observed that VIm halide ionic liquids are more reactive towards free radical polymerization than their non-ionic vinyl imidazole analogues [76]. Typically, the conditions for these polymerization reactions mimic conventional free radical polymerization conditions and involve moderate temperatures (around 60 °C) and 1-2 mol% initiator [72] [70].

Work-up of the PhAlImBr (**21**) reaction mixture in water revealed a fine suspension that was sonicated and centrifuged before decanting fluid from the solid product. SEM analysis of the resulting insoluble material revealed sub-micron spheres of relatively uniform diameter (Figure

13). The complete insolubility of these particles is consistent with a highly cross-linked architecture, as opposed to a linear PIL that would be water soluble. DSC analysis of the solids found no apparent T_g, unlike the starting material which exhibited a distinct glass transition temperature of -48°C. FT-IR analysis revealed clear differences between the monomer and its solid products.

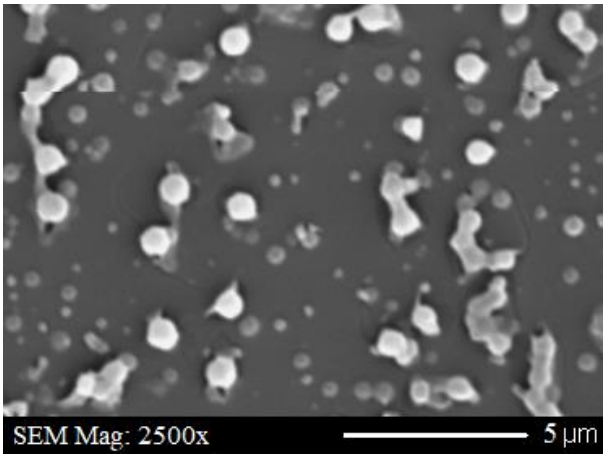

Figure 13: SEM image of solids derived from PhAlImBr + DCP reaction

Variations of this model compound experiment placed these PhAlImBr results in better context. The conversion of 2-ethyl-1-allyl imidazolium bromide (PhEtAlImBr, **22**) to insoluble product was 67%, indicating that an alkyl substituent at the 2-position of the imidazolium cation increases its radical reactivity. Recall that gelation was observed during the alkylation of EtAlIm by BIMS, indicating that cross-linking during the ionomer preparation is difficult to overcome. A model compound for the IMS-VImBr ionomer, PhVImBr (**23**), generated a leathery polymer in 100% yield. This material was insoluble in water or non-polar solvents, and was distinctly different from the intractable cross-linked particles produced by the allylic monomers.

The formation of highly cross-linked particles from the PhAlImBr model compound is evidence of the multi-functional nature of allylic systems. Whereas simple radical addition polymerizations

generate linear polymer chains, a mixture of radical addition and H-atom transfer chemistry can produce the observed cross-linked architecture within model compound solids and IMS-AlImBr thermosets. It is proposed that contributions from both monomer activating pathways support the observed combination of low cross-linking rates and high final cross-link densities.

3.3.3 Solid State N-Alkylation

It is both economical and environmentally advantageous to synthesize ionomers in a one-step solvent free process, which on a commercial scale would involve reactive extrusion using residence times on the order of a few minutes. In this respect, the higher nucleophilicity of AlIm relative to that of VIm, as observed in the solution borne alkylation reactions described above, would make the allylic system attractive from the both a synthetic standpoint, as well as radical cross-linking dynamics and yields. Figure 14 is a plot of the benzylic bromide conversion to imidazolium bromide functionality within BIMS that was mixed with 2 eq. of nucleophile at 100°C in a Haake Polylab mixing bowl. The alkylation of AlIm reached 100% conversion in just 20 minutes, compared to 60 minutes for VIm. These results indicate that AlIm is better suited for ionomer product through a continuous extrusion process.

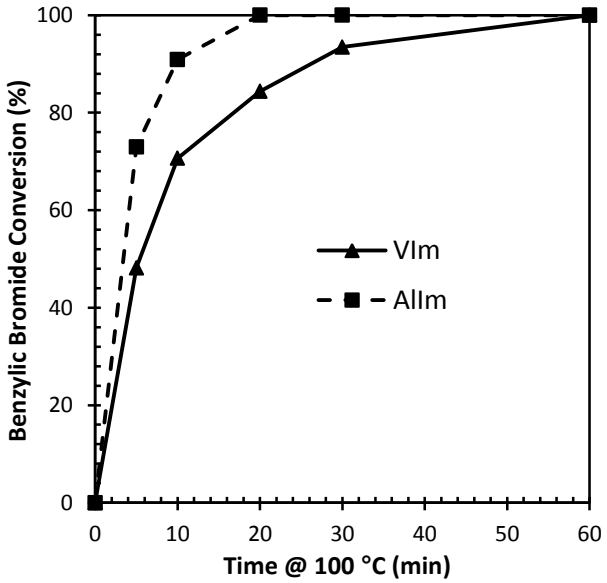

Figure 14: Solvent-free N-alkylation dynamics of VIm and AlIm by BIMS (100°C, 30 rpm, 2 eq.)

It should be noted that significant amounts of residual monomer present after the solvent-free synthesis had a detrimental effect on the ensuing peroxide cure. This could simply be due to unbound monomer using up the initiator by oligomerizing within the polymer without creating cross-links. As such, devolatilization of the alkylated article to remove residual monomer is important to achieve good peroxide cure activity. Further note that solid-state alkylation of VBIm proceeded even more rapidly than AlIm, reaching full conversion after just five minutes. The product, though, again displayed a high gel content, limited solubility and worsened processability.

3.3.4 Physical Properties of Cross-Linked Reactive Ionomers

3.3.4.1 Stress Relaxation

Previous studies of imidazolium bromide thermoset derivatives of BIIR have demonstrated the unique physical properties provided by a hybrid ionic/covalent network [66]. Because the ionic network is labile and polymer chains are able to move past each other, stress relaxation is a

significant problem observed in conventional ionomers containing no covalent cross-links. In a thermoset elastomer, the polymer chains can no longer move past one another and the static modulus (G) remains constant with applied stress. The thermoset ionomers studied in this report display many of the unique properties attributed to the hybrid ionic/covalent network that have previously been characterized, the first being resistance to stress relaxation. As can be seen in Figure 15, both BIMS and IMS-BuImBr stress relax quickly, although IMS-BuImBr takes longer to do so because of the ionic network contribution.

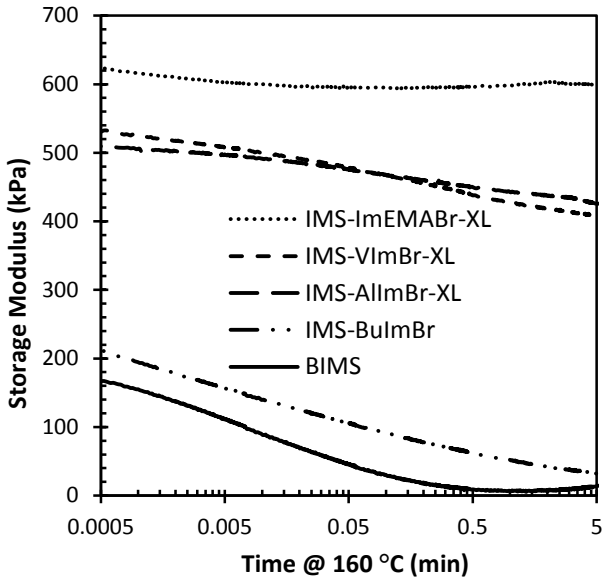

Figure 15: Stress relaxation of cross-linked imidazolium bromide ionomer derivatives of BIMS (100 °C, 2° strain)

All of the cross-linked ionomers, IMS-VImBr-XL, IMS-ImEMA-XL, and IMS-AlImBr-XL, demonstrated a hybrid effect of covalent and ionic networks. Since the covalent network does not stress relax and the ionic network does, the relative contribution of each network on G' can be estimated by the amount with which the modulus decreases over the course of the experiment. For IMS-VImBr-XL, the change in modulus (ΔG) in five minutes contributes 160 kPa, or 28% of the total modulus. i.e. 28% of the total modulus observed in the cross-link ionomer can be

attributed to the ionic aggregates. IMS-AlImBr-XL displayed similar properties wherein the ionic network contributed 150 kPa, or 26% of the total modulus. The IMS-ImEMABr graft, which cured to very high extent, displayed only a very small stress relaxation of 60 kPa, or 10% of the total modulus. This indicates that it is possible to over-cure the ionomer to the point where the stress realization of the ionic network is no longer significant. This problem has been addressed previously by producing a mixed alkylation product of BuIm and VIm in order to reduce the final modulus [78].

3.3.4.2 Temperature Sweeps

The physical characteristics of the cured ionomers can be further evaluated by analyzing the temperature sweep data in Figure 16. This test assesses the modulus of the hybrid ionic/covalent network in a temperature range between 100°C and 200°C. Ideally, a commercially viable elastomer should have a wide range of operating temperatures in which its physical properties stay relatively constant.

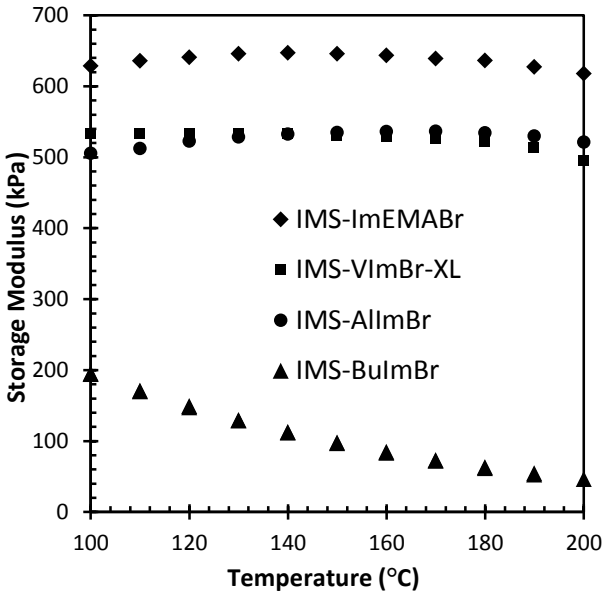

Figure 16: Temperature sweep of cross-linked imidazolium bromide ionomer derivatives of BIMS between 100°C and 200°C (1Hz, 3° arc)

In line with other uncross-linked elastomeric ionomers, the storage modulus of IMS-BuImBr decreases with increasing temperature owing to a reduction in the ionic network strength [26]. For thermoset elastomers however, the standard model predicts an increase in G' with increasing temperature because entropically-driven elasticity responds with greater restorative force as temperature increases [133] . The relatively constant value of G' for the cross-linked ionomers can be explained by a combination of both effects; strengthening of the covalent network and weakening of the ionic network with increasing temperature.

Although, for clarity, Figure 16 shows only the data points collected during the heating cycle from 100°C to 200°C, data was also collected for the cooling cycle. These data points overlapped very well with those in the heating phase indicating that the integrity of the networks did not show any signs of irreversible degradation upon heating. These results suggest that cross-linked ionic elastomers do not degrade at temperatures up to 200°C and that their moduli remain stable over a wide range of temperatures, two properties which could make them very useful as engineering materials.

3.3.4.3 Tensile Strength

Table 1 shows the tensile properties of dogbones cut from a cured macrosheet of IMS-AlImBr. As was expected, based on the exceptionally high storage modulus observed from rheometry, IMS-AlImBr-XL showed both high modulus and low elongation at break. This combination of properties is generally not valued in an engineering thermoset elastomer as high modulus can be achieved by adding filler and low elongation at break limits utility. It has previously been shown, though, that tensile properties can be improved by mixed alkylating the unreactive BuIm with VIm [78]. Decreasing VIm content produced a favourable decrease in modulus and an increase in elongation at break. Because alkylation rates for AlIm and BuIm so similar, this strategy could be easily investigated to produce better tensile properties for the cross-linked IMS-AlImBr system.

Table 1: Tensile properties of cross-linked IMS-AlImBr

	Freshly Cured Sample		**After 48 days @ 110 °C**	
Physical Property	Mean	Std. Dev.	Mean	Std. Dev.
Maximum Tensile Stress (MPa)	1.48	0.287	1.74	0.163
Young's Modulus (MPa)	1.15	0.063	1.32	0.035
Elongation at Break (%)	142	12.8	142	10.7

Table 1 also shows tensile data for dogbones cut from the same macrosheet after being left in a 110°C oven for 48 days. This was meant as an accelerated test of long-term oxidative and temperature stability. The results show no difference in elongation at break and only a slight increase in Young's modulus consistent with oxidative hardening. The difference in tensile properties, though, is small and suggests good oxygen and heat resistance for IMS-AlImBr-XL.

3.4 Conclusions

A novel isobutylene-rich elastomeric ionomer bearing N-allyl imidazolium bromide functionality has been synthesized able to cross-link by peroxide activation. AlIm is rapidly alkylated by BIMS in a one-step solvent free process and cures at a relatively slow rate to high extent with minimal peroxide in the formulation. This phenomenon is likely due to the unique radical reactivity of allyl imidazolium moieties to create highly branched architectures. The cross-linked ionomer displays physical properties associated with a hybrid ionic/covalent network and is not limited by stress relaxation issues that plague typical elastomeric ionomers.

Chapter 4

Conclusions and Future Work

4.1 BIIR-Derived Macromonomers

Whereas commercial grades of isobutylene-rich elastomers do not cure under the action of peroxides, macromonomers bearing oligomerizable C=C functionality can be cured to high extent. In this work, the effect of the nature of the C=C functionality on the rate and extent of cure has been studied. It was found that these materials undergo simultaneous cross-linking and degradation when activated by radical initiators, with the competitive balance being dictated by the reactivity of the oligomerizable group. The highly reactive vinylbenzoate, vinyl imidazolium, and acrylate functionalities cured quickly and to a high extent, whereas the over-reactivity and instability observed for the maleimide graft was never overcome. Methacrylate and itaconate grafts were found to cure to moderate extent with the latter displaying particular interest because of the potential for further functionalization. The maleate ester, allylic and unactivated terminally unsaturated groups were unable to significantly counteract the degradation mechanism and do not afford any appreciable cross-link density.

The high rate of cure for the very reactive moieties could make these materials prone to scorch, the phenomenon where rubber articles become thermoset during compounding or before their desired end shape is reached. Nitroxyls were found to efficiently mitigate free radical cure activity in the early parts of the highly reactive macromonomer cures. Furthermore, an acrylated adduct AOTEMPO was able to recover more of the cross-link density that would otherwise be lost to irreversible free radical coupling. It was also found that these nitroxyls produced induction times longer than what would be expected from simple macroradical coupling. This effect is likely due to the catalytic nature of TEMPO when alkoxyamine instability is significant.

4.2 BIMS-Derived Reactive Ionomers

A suite of novel isobutylene-rich elastomeric ionomers bearing N-functional imidazolium bromide functionality has been synthesized in order to investigate their BIMS N-alkylation dynamics as well as the subsequent peroxide cure activity of the reactive ionomers. A highly reactive methacrylate imidazole provided very good cure activity but did not significantly improve N-alkylation speed with respect to the previously studied N-vinyl imidazole system. Furthermore, a 4-vinylbenzyl imidazole provided very good N-alkylation rate, but at the expense of a thermally and oxidatively stable product. N-Allylimidazole provided the best alkylation rate by BIMS, making this technology attractive for commercialization by reactive extrusion. Furthermore, the N-allylimidazolium bromide ionomer is able to cross-link by peroxide activation, counteracting the degradation mechanism otherwise observed for isobutylene-rich elastomers. This functional ionomer displays unique cure dynamics and cross-links at a relatively slow rate but to a high final modulus. This phenomenon is likely due to the unique free radical reactivity of allyl imidazolium moieties, able to create highly branched architectures within the elastomers. The cross-linked ionomer displays many of the beneficial physical properties associated with a hybrid ionic/covalent network including good resistance to stress relaxation, and thermal stability.

4.3 Future Work

Future work in the BIIR macromonomer field should involve steps towards commercialization of these products. It has already been shown that some highly reactive moieties can provide good cross-link density at a high rate and can be scorch protected effectively by a functional nitroxyl. Solid-state syntheses should be optimized for the macromonomers discussed in this work in order to improve productivity. Furthermore, physical characterization of these species has been limited thus far and should be investigated in more detail. These characterizations include stress

relaxation and compression set, thermal stability tests as well as dynamics properties such as fatigue failure and hysteresis.

The mechanism by which TEMPO produces an extended induction time for these macromonomers should be further experimentally investigated. Model benzylic and acrylic alkoxyamines similar to those created *in situ* in these systems should be synthesized, and their effect on peroxide cures at 160°C studied. These alkoxyamines can even be doped into LLDPE/peroxide cures, otherwise known to cross-link stoichiometrically, and their mitigating effect on cross-linking can be assessed in order to corroborate the catalytic mechanism proposed in this work.

With regards to the reactive ionomers of BIMS, future work should examine the effect of anion metathesis on the cure and physical properties of the material. Several opportunities for further chemistry are possible including large, functional, or even reactive anions. Furthermore, although BIMS is ideal for the simple synthesis of imidazolium bromide reactive ionomers, it is a specialty elastomer and thus BIIR is more attractive as a starting material. It was found that allylimidazole does not provide cure activity in BIIR as it does in BIMS and the reason for this should be further investigated. In particular, model compound work to assess the significance of residual unbrominated para-methylstyrene on BIMS-derived ionomers should be conducted.

Because the 4-vinylbenzyl imidazole (VBIm) was found to alkylate quickly, but produce an unstable ionomeric product, the alpha-methyl version shown below should be synthesized.

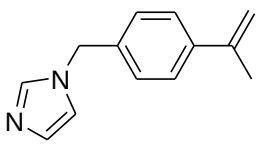

It is suspected that this functional imidazole should also alkylate quickly but not be as susceptible to thermal or oxidative cross-linking as VBIm.

Lastly, mixed-alkylations of allylimidazole and butylimidazole by BIMS should be conducted to determine the effect of allylimidazolium bromide content on cure dynamics and resulting mechanical properties. This technique was used to improve the mechanical properties of cross-linked IMS-VImBr, and should be further investigated with the allylimidazolium species, whose alkylation rate is very similar to that of butylimidazole.

5.0 Works Cited

[1] A. Y. Coran, "Vulcanization," in *Science and Technology of Rubber, 3rd edition*, Boston, Elsevier Academic Press, 2005, pp. 321-364.

[2] R. H. Boyd and P. V. Krishna Pant, "Molecular packing and diffusion in polyisobutylene," *Macromolecules,* vol. 24, no. 25, pp. 6325-6331, 1991.

[3] P. J. Flory, "Principle of polymer chemistry," in *Chap 11.*, New York, Cornell University Press, 1953.

[4] R. Brown, Physical Testing of Rubber, New York: Springer, 2006.

[5] F. C. Auluck and D. S. Kothari, "The kinetic theory of rubber," *The Journal of Chemical Physics,* vol. 11, no. 8, pp. 387-392, 1943.

[6] R. M. Thomas, I. E. Lightbown, W. J. Sparks, P. K. Frolich and E. V. Murphree, "Butyl Rubber: A New Hydrocarbon Product," *Industrial and Engineering Chemistry,* vol. 32, no. 10, pp. 1283-1292, 1940.

[7] C. Y. Chu and R. Vukov, "Determination of the structure of butyl rubber by NMR spectroscopy," *Macromolecules,* vol. 18, pp. 1423-1430, 1985.

[8] R. T. Morrissey, "Butyl-type polymers containing bromide," *Industrial and Engineering Chemistry,* vol. 47, pp. 1562-1569, 1955.

[9] I. Kuntz and K. W. Powers, "Halomethylated aromatic interpolymers". US Patent US 4074035 A, 22 Apr 1975.

[10] W. K. Powers and H.-C. Wang, "Para-alkylstyrene/isoolefin copolymers". European Patent Patent EP19890305395, 26 Ma7 1989.

[11] T. Shaffer, A. Tsou and R. Webb, "Butyl Rubber," in *Kirk-Othmer Encyclopedia of Chemical Technology*, John Wiley and Sons, 2003.

[12] S. M. Malmberg, J. S. Parent, D. A. Pratt and R. A. Whitney, "Isomerization and elimination reactions of brominated poly(isobutylene-co-isoprene)," *Macromolecules,* vol. 43, pp. 8456-8461, 2010.

[13] J. S. Parent, D. J. Thom, G. White, R. A. Whitney and W. Hopkins, "Thermal stability of brominated poly(isobutylene-co-isoprene)," *Journal of Polymer Science: Part A: Polymer Chemistry,* vol. 39, pp. 2019-2026, 2001.

[14] J. K. McLean, S. A. Guillen-Castellanos, J. S. Parent and R. A. Whitney, "Phase-transfer catalyzed esterification of brominated poly(isobutylene-co-isoprene)," *Industrial and Engineering Chemistry Research ,* vol. 48, pp. 10759-10764, 2009.

[15] J. S. Parent, S. Malmberg, J. K. McLean and R. A. Whitney, "Nucleophlic catalysis of halide displacement from brominated poly(isobutylene-co-isoprene)," *European Polymer Journal,* vol. 46, pp. 702-708, 2010.

[16] J. S. Parent, G. D. F. White and R. A. Whitney, "Synthesis of thioether derivatives of brominated poly(isobutylene-co-isoprene): Direct coupling chemistry for silica reinforcement," *Journal of Polymer Science: Part A: Polymer Chemistry,* vol. 40, pp. 2937-2944, 2002.

[17] J. S. Parent, G. D. F. White, D. J. Thom, R. A. Whitney and W. Hopkins, "Sulfuration and reversion reactions of brominated poly(isobutylene-co-isoprene)," *Journal of Polymer Science: Part A: Polymer Chemistry,* vol. 41, pp. 1915-1926, 2003.

[18] P. A. Callais, "Understanding organic peroxides to obtain optimal crosslinking performance," *Rubber World,* vol. 229, pp. 35-41, 2003.

[19] R. F. Ohm, "Rubber Chemicals," in *Kirk-Othmer Encyclopedia of Chemical Technology*, 2000.

[20] W. L. Guess and R. K. O'Leary, "Toxicity of a Rubber Accelerator," *Toxicology and Applied Pharmacology,* vol. 14, pp. 221-231, 1969.

[21] S. A. Guillen-Castellanos, J. S. Parent and R. A. Whitney, "Synthesis and characterization of ether derivatives of brominated poly(isobutylene-co-isoprene)," *Macromolecules,* vol. 44, pp. 983-992, 2006.

[22] S. A. Guillen-Castellanos, J. S. Parent and R. A. Whitney, "Synthesis of ester derivatives of brominated poly(isobutylene-co-isoprene): Solvent-free phase transfer catalysis," *Macromolecules,* vol. 39, pp. 2514-2520, 2006.

[23] S. Xiao, J. S. Parent, R. A. Whitney and L. K. Knight, "Synthesis and Characterization of poly(isobutylene-co-isoprene)-derived Macro-monomers," *Journal of Polymer Science Part A: Polymer Chemistry,* vol. 48, pp. 4691-4696, 2010.

[24] H. C. Wang, J. V. Fusco and P. Hous, "Acrylate ester modifications of isobutylene/paramethylstyrene copolymer," *Rubber World,* pp. 37-41, 1994.

[25] J. S. Parent, G. D. F. White and R. A. Whitney, "Amine Substitution Reactions of Brominated Poly(isobutylene-co-isoprene): New Chemical Modification and Cure

Chemistry," *Macromolecules,* vol. 35, pp. 3374-3379, 2002.

[26] A. Eisenberg and J. S. Kim, Introduction to Ionomers, New York: Wiley, 1998.

[27] K. Takenaka, M. Suzuki, H. Takeshita, M. Miya, T. Shiomi, K. Tamamitsu and T. Konda, "Synthesis of peroxide-curable butyl rubber via Suzuki-Miyaura coupling of halogenated butyl rubber with 4-vinylphenylboronic acid," *Journal of Polymer Science: Part A: Polymer Chemistry,* vol. 50, pp. 659-664, 2011.

[28] P. R. Dluzneski, "Peroxide Vulcanization of Elastomers," *Rubber Chemistry and Technology,* vol. 74, no. 3, pp. 451-493, 2001.

[29] A. Y. Coran, "Chapter 7," in *Science and Technology of Rubber*, New York, Academic Press, 1978.

[30] H. L. Fisher, "Vulcanization of rubber," *Industrial and Engineering Chemistry,* vol. 31, no. 11, pp. 1381-1389, 1939.

[31] P. R. Dluzneski, "The chemistry of peroxide vulcanization," *Rubber World,* vol. 224, pp. 34-37, 2001.

[32] Technical Bulletin, *Atofina Chemicals,* 2001.

[33] M. J. Gibian and R. C. Corley, "Organic radical-radical reactions, disproportionation vs. combination," *Chemical Reviews,* vol. 73, pp. 441-464, 1973.

[34] D. K. Thomas, "The Degradation of polyisobutylene by Dicumyl Peroxide," *Transactions of the Faraday Society,* vol. 57, pp. 511-517, 1961.

[35] L. D. Loan, "The reaction between dicumyl peroxide and butyl rubbers," *Jounal of Polymer Science: Part A: Polymer Chemistry,* vol. 2, pp. 2127-2134, 1964.

[36] E. H. Farmer and C. G. Moore, "Radical mechanisms in saturated and olefinic systems. Part 1. Liquid-Phase Reaction of the tert.-butoxy-radical with olefins and with cycloHexane," *Journal of the Chemical Society,* pp. 131-141, 1951.

[37] E. H. Farmer and C. G. Moore, "Radical mechanisms in saturated and olefinic systems. Part II. Disubstitutive carbon-carbon cross-linking by tert.-alkoxy-radicals in isoprenic olefins and rubber," *Journal of the Chemical Society,* pp. 142-148, 1951.

[38] E. H. Farmer and C. Moore, "Radical mechanisms in saturated and olefinic systems. Part III. The reaction of hydroxyl radicals with olefins," *Journal of the Chemical Society,* pp. 149-

153, 1951.

[39] B. M. E. van der Hoff, "Reactions between peroxide and polydiolefins," *Industrial and Engineering Chemistry Product Research and Development,* vol. 2, no. 4, pp. 273-278, 1963.

[40] A. Baignee, J. A. Howard, J. C. Scaiano and L. C. Stewart, "Absolute rate constants for reactions of cumyloxy in solution," *Journal of the American Chemical Society,* vol. 105, no. 19, pp. 6120-6123, 1983.

[41] G. Moad, "The synthesis of polyolefin graft copolymers by reactive extrusion," *Progress in Polymer Science,* vol. 24, no. 1, pp. 81-142, 1999.

[42] I. Kuntz and K. D. Rose, "Copolymerization of Isobutylene with 1,4-C-Isoprene," *Journal of Polymer Science: Part A: Polymer Chemistry,* vol. 27, pp. 107-124, 1989.

[43] K. V. S. Shanmugam, J. S. Parent and R. A. Whitney, "Design, synthesis, and characterization of bismaleimide co-curing elastomers," *Industrial & Engineering Chemistry Research,* vol. 51, no. 26, pp. 8957-8965, 2012.

[44] C. E. Oxley and G. J. Wilson, "A peroxide curing butyl rubber," *Rubber Chemistry and Technology,* vol. 42, pp. 1147-1154, 1969.

[45] T. Crockett, A. Gronowski and A. Osman, "Peroxide vulcanizable butyl compositions useful for rubber articles". WO Patent WO2006060896 A1, 15 June 2006.

[46] J. S. Kim, "Ionomers," in *Kirk-Othmer Encyclopedia of Chemical Technology*, John Wiley & Sons Inc., 2005.

[47] J. S. Parent, A. M. Porter, M. R. Kleczek and R. A. Whitney, "Imidazolium Bromide Derivatives of poly(isobutylene-co-isoprene): A New Class of Elastomeric Ionomers," *Polymer,* vol. 52, no. 24, pp. 5410-5418, 2011.

[48] A. Eisenberg, B. Hird and R. B. Moore, "A new multiplet-cluster model for the morphology of random ionomers," *Macromolecules,* vol. 23, no. 18, pp. 4098-4107, 1990.

[49] W. J. MacKnight and T. R. Earnest, *Journal of Polymer Science: Macromolecular Reviews,* vol. 16, pp. 41-122, 1981.

[50] J. J. Fitzgerald and R. A. Weiss, *Journal of Macromolecular Science - Reviews in Macromolecular Chemistry and Physics ,* vol. C28, pp. 99-185, 1988.

[51] W. J. MacKnight and R. D. Lundberg, *Rubber Chem Technol,* vol. 57, pp. 652-663, 1984.

[52] S. K. Prince Antony, "Ionomeric Polyblends of Zinc Salts of Maleated EPDM Rubber and poly(ethylene-co-acrylic acid)," *Journal of Applied Polymer Science,* vol. 71, no. 8, pp. 1247-1256, 1999.

[53] S. Bagrodia, M. R. Tant, G. L. Wilkes and J. P. Kennedy, "Sulphonated polyisobutylene telechelic ionomers: 12. Solid-state mechanical properties," *Polymer,* vol. 28, pp. 2207-2226, 1987.

[54] J. S. Parent, A. Penciu, S. A. Guillen-Castellanos, A. Liskova and R. A. Whitney, "Synthesis and Characterization of Isobutylene-Based Ammonium and Phosphonium Bromide Ionomers," *Macromolecules,* vol. 37, pp. 7477-7483, 2004.

[55] M. Colonna, C. Berti, E. Binassi, M. Fiorini, S. Sullalti, F. Acquasanta, M. Vannini, D. Di Gioia and I. Aloisio, "Imidazolium poly(butylene terphthalate) ionomers with long-term antimicrobial activity," *Polymer,* vol. 53, pp. 1823-1830, 2012.

[56] J. S. Parent, A. Liskova and R. Resendes, "Isobutylene-Based Ionomer Composites: Siliceous Filler Reinforcement," *Polymer,* vol. 45, pp. 8091-8096, 2004.

[57] M. Charnley, M. Textor and C. Acikgoz, "Designed Polymer Structures With Antifouling-Antimicrobial Properties.," *Reactive and Functional Polymers ,* vol. 71, no. 3, pp. 329-334, 2011.

[58] M. Gurian, "An Evaluation of the Effectiveness of Anti-Microbial Finishes and Additives to Healthcare Interior Textiles," *Journal of Industrial Textiles,* vol. 25, no. 1, pp. 13-23, 1995.

[59] P. Arjunan, H.-C. Wang and J. A. Olkusz, "New options for chemical modification of polyolefins: Part 1. Synthesis and properties of novel phosphonium ionomers from poly(isobutylene-co-4-bromomethylstyrene)," *ACS Symposium Series,* vol. 704, no. Chapter 14, pp. 199-216, 1998.

[60] A. H. Tsou, I. Duvdevani and P. K. Agarwal, "Quaternary ammonium elastomeric ionomers by melt-state conversion," *Polymer,* vol. 45, pp. 3163-3173, 2004.

[61] J. E. Gordon, "Fused organic salts. III. Chemical stability of molten tetra-n-alkylammonium salts. Medium effects on thermal R4N+X- decomposition. RBr + I- = RI + Br- equilibrium constant in fused salt medium," *Journal of the American Chemical Society,* vol. 87, pp. 2760-2763, 1965.

[62] B. Lin, L. Qiu, B. Qiu, Y. Peng and F. Yan, "A soluble and conductive polyfluorene ionomer with pendant imidazolium groups for alkaline fuel cell applications," *Macromolecules,* vol.

44, pp. 9642-9649, 2011.

[63] B. S. Aitken, F. Buitrago, J. D. Heffley, M. Lee, H. W. Gibson, K. I. Winey and K. B. Wagener, "Precision ionomers: synthesis and thermal/mechanical characterization," *Macromolecules,* vol. 45, pp. 681-687, 2012.

[64] J. S. Parent, A. M. J. Porter, M. R. Kleczek and R. A. Whitney, "Imidazolium Bromide Derivatives of poly(isobutylene-co-isoprene): A New Class of Elastomeric Ionomers," *Polymer,* vol. 52, no. 24, pp. 5410-5418, 2011.

[65] J. S. Parent, S. M. Malmberg and R. A. Whitney, "Auto-catalytic chemistry for the solvent-free synthesis of isobutylene-rich ionomers," *Green Chemistry,* vol. 13, pp. 2818-2824, 2011.

[66] A. Ozvald, J. S. Parent and R. A. Whitney, "Hybrid ionic/covalent polymer networks derived from functional imidazolium ionomers," *Journal of Polymer Science: Part A: Polymer Chemistry,* vol. 51, pp. 2438-2444, 2013.

[67] J. E. Gordon, "Fused Organic Salts.," *Journal of Organic Chemistry,* vol. 30, no. 8, pp. 2760-2763, 1965.

[68] J. Dugal-Tessier, P.-S. Kuhn, G. R. Dake and D. P. Gates, "Synthesis of Functional Phosphines with Ortho-Substituted Aryl Groups," *Heteroatom Chemistry,* vol. 21, no. 5, pp. 355-360, 2010.

[69] J. Yuan and M. Antonietti, "Poly(ionic liquid) latexes prepared by dispersion polymerization of ionic liquid monomers," *Macromolecules,* vol. 44, pp. 744-750, 2011.

[70] C. Damas, S. Baggio, A. Brembilla and P. Lochon, "Microstructure study of new amphiphilic copolymers from 3-alkyl-1-vinylimidazolium salts," *European Polymer Journal,* vol. 33, no. 8, pp. 1219-1224, 1997.

[71] H. Mori, M. Yahagi and T. Endo, "RAFT polymerization of N-vinylimidazolium salts and syntehsis of thermoresponsive ionic liquid block copolymers," *Macromolecules,* vol. 42, pp. 8082-8092, 2009.

[72] J. C. Salamone, S. C. Israel, P. Taylor and B. Snider, "Synthesis and homopolymerization studies of vinylimidazolium salts," *Polymer,* vol. 14, pp. 639-644, 1973.

[73] M. Hiaro, K. Ito and H. Ohno, "Preparation and polymerization of new organic molten salts; N-alkylimidazolium salt derivatives," *Electrochimica Acta,* vol. 45, pp. 1291-1294, 2000.

[74] H. L. Ngo, K. LeCompte, L. Hargens and A. B. McEwen, "Thermal properties of imidazolium ionic liquids," *Thermochimica Acta,* Vols. 357-358, pp. 97-102, 2000.

[75] B. K. M. Chan, N.-H. Chang and M. R. Grimmett, "The synthesis and thermolysis of imidazole quaternary salts," *Australian Journal of Chemistry,* vol. 30, pp. 2005-2013, 1977.

[76] K. L. Petrak, "Reactivity of some vinylimidazoles towards other vinyl monomers in radical copolymerization," *Journal of Polymer Science: Polymer Letters Edition,* vol. 16, no. 8, pp. 393-399, 1978.

[77] R. Marcilla, J. A. Blasquez, J. Rodriguez, J. A. Pomposo and D. Mecerreyes, "Tuning the solubility of polymerized ionic liquids by simple anion-exchange reactions," *Journal of Polymer Science: Part A: Polymer Chemistry,* vol. 42, pp. 208-212, 2004.

[78] A. M. Ozvald, *Reactive Ionomers: N-vinylimidazolium Bromide Derivatives of Poly(isobutylene-co-isoprene) and Poly(isobutylene-co-para-methylstyrene),* Kingston, Ontario: Unpublished Manuscript, Queen's University, 2012.

[79] K. Ito, "Polymeric design by macromonomer technique," *Progress in Polymer Science,* vol. 23, pp. 581-620, 1998.

[80] V. Percec and J. H. Wang, "Free radical copolymerization of w-(p-vinylbenzyl ether) macromonomer of poly(2,6-dimethyl-1,4-phenylene oxide) with methyl methacrylate in the presence of different initiators," *Journal of Macromolecular Science: Part A - Chemistry,* vol. 28, no. S3, pp. 221-231, 2006.

[81] J. Ryan, F. Aldabbagh, P. B. Zetterlund and B. Yamada, "Nitroxide-mediated controlled/living radical copolymerizations with macromonomers," *Reactive and Functional Polymers,* vol. 68, pp. 692-700, 2008.

[82] K. Matyjaszewski and T. P. Davis, Handbook of Radical Polymerization, Hoboken, NJ: John Wiley and Sons, Inc., 2002, p. 534.

[83] L. Wojnarovits and E. Takacs, "Rate coefficients of the initial steps of radiation induced oligomerization of acrylates in dilute aqueous solutions," *Radiation Physics and Chemistry,* vol. 55, pp. 639-644, 1999.

[84] J. D. Druliner, "Polymerization of acrylates and methacrylates to make homopolymers and block copolymers initiated by N-alkoxyphthalimides and succinimides," *Journal of Physical Organic Chemistry,* vol. 8, pp. 316-324, 1995.

[85] T. Otsu and N. Toyoda, "Monomer-isomerization polymerization of dialkyl maleates by radical mechanism," *Die Makromolekulare Chemie, Rapid Communications,* vol. 2, pp. 79-

81, 1981.

[86] C. E. Schildknecht, Allyl Compounds and Their Polymers (Including Polyolefins), New York: John Wiley & Sons, 1973.

[87] W. Wu, J. S. Parent, S. S. Sengupta and B. I. Chaudhary, "Preparation of crosslinked microspheres and porous solids from hydrocarbon solutions: A new variation of precipitation polymerization chemistry," *Journal of Polymer Science: Part A: Polymer Chemistry,* vol. 47, pp. 6661-6670, 2009.

[88] R. A. Prasath and S. Ramakrishnan, "Synthesis, characterization, and utilization of itaconate-based polymerizable surfactants for the preparation of surface-carboxylated polystyrene latexes," *Journal of Polymer Science: Part A: Polymer Chemistry,* vol. 43, pp. 3257-3267, 2005.

[89] D. K. Hyslop and J. S. Parent, "Functional nitroxyls for use in delayed-onset polyolefin cross-linking," *Macromolecules,* vol. 45, pp. 8147-8154, 2012.

[90] G. E. Garrett, *On the regioselectivity of H-atom abstraction from model polyolefins by alkoxyl radicals,* Kingston, Ontario: Master's Thesis, Queen's University, 2011.

[91] S. A. Canary and M. P. Stevens, "Thermally reversible crosslinking of polystyrene via the furan-maleimide Diels-Alder reaction," *Journal of Polymer Science: Part A: Polymer Chemistry,* vol. 30, pp. 1755-1760, 1992.

[92] D. J. T. Hill, L. Y. Shao, P. J. Pomery and A. K. Whittaker, "The radical homopolymerization of N-phenylmaleimide, N-n-hexylmaleimide and N-cyclohexylmaleimide in tetrahydrofuran," *Polymer,* vol. 42, pp. 4791-4802, 2001.

[93] J. Liu, W. Yu, C. Zhao and C. Zhou, "EPR/rheometric studies on radical kinetics in melt polyolefin elastomer initiated by dicumyl peroxides," *Polymer,* vol. 48, pp. 2882-2891, 2007.

[94] H. S. Bisht, S. S. Ray, D. Pandey, C. D. Sharma and A. K. Chatterjee, "Copolymerization of dodecyl-4-vinyl benzoate and dodecyl acrylate by conventional, atom transfer, and nitroxide-mediated free-radical polymerization," *Journal of Polymer Science: Part A: Polymer Chemistry,* vol. 40, pp. 1818-1830, 2002.

[95] K. V. S. Shanmugam, J. S. Parent and R. A. Whitney, "C-H bond addition and copolymerization reactions of N-arylmaleimides: Fundamentals of coagent-assisted polymer cross-linking," *European Polymer Journal,* vol. 48, pp. 841-849, 2012.

[96] O. Jeon, S. J. Song, K.-J. Lee, M. H. Park, S.-H. Lee, S. K. Hahn, S. Kim and B.-S. Kim, "Mechanical properties and degradation behavios of hyaluronic acid hydrogels cross-linked at various cross-linking densities," *Carbohydrate Polymers,* vol. 70, no. 3, pp. 251-257, 2007.

[97] G. Imparato, F. Urciuolo, C. Casale and P. A. Netti, "The role of microscaffold properties in controlling the collagen assembly in 3D dermis equivalent using modular tissue engineering," *Biomaterials,* vol. 34, pp. 7851-7861, 2013.

[98] G. J. M. de Koning, H. M. M. van Bilsen, P. J. Lemstra, W. Hazenberg, B. Witholt, H. Preusting, J. G. van der Galien, A. Schirmer and D. Jendrossek, "A biodegradable rubber by crosslinking poly(hydroxyalkanoate) from pseudomonas oleovorans," *Polymer,* vol. 35, no. 10, pp. 2090-2097, 1994.

[99] K. A. George, T. V. Chirila and E. Wentrup-Byrne, "Effects of crosslink density on hydrolytic degradation of poly(L-lactide)-based networks," *Polymer Degradation and Stability,* vol. 97, pp. 964-971, 2012.

[100] V. V. Krongauz, "Crosslink density dependence of polymer degradation kinetics: Photocrosslinked acrylates," *Thermochimica Acta,* Vols. 503-504, pp. 70-84, 2010.

[101] M. Hoffmann, "Determination of network structure by extraction and random degradation, 1a)," *Die Makromolekulare Chemie,* vol. 183, pp. 2191-2211, 1982.

[102] W. Schnabel, Polymer Degradation: Principles and Practical Applications, Muenchen: Hanser International, 1981, p. 21.

[103] J. Chateauneuf, J. Lusztyk and K. U. Ingold, "Absolute rate constants for the reactions of some carbon-centered radicals with 2,2,6,6-tetramethylpiperidine-N-oxyl," *Journal of Organic Chemistry,* vol. 53, pp. 1629-1632, 1987.

[104] B. I. Chaudhary, L. Chopin and J. Klier, "Nitroxyls for scorch suppression, cure control, and functionalization in free-radical crosslinking of polyethylene," *Polymer Engineering and Science,* vol. 47, no. 1, pp. 50-61, 2006.

[105] A. L. J. Beckwith, V. W. Bowry and M. Graeme, "Kinetics of the coupling reactions of the nitroxyl radical 1,1,3,3-tetramethylisoindoline-2-oxyl with carbon-centered radicals," *Journal of Organic Chemistry,* vol. 53, pp. 1632-1641, 1988.

[106] S. M. Kabun and A. L. Buchachenko, "A study of the decomposition of tertiary alkyl and aralkyl peroxides by means of stable nitrogen oxide radicals," *Bulletin of the Academy of Sciences of the USSR, Divison of chemical science,* vol. 15, no. 8, pp. 1430-1431, 1966.

[107] S. Mani, P. Cassagnau, M. Bousmina and P. Chaumont, "Cross-linking control of PDMS rubber at high temperatures using TEMPO nitroxide," *Macromolecules,* vol. 42, pp. 8460-8467, 2009.

[108] D. K. Hyslop and J. S. Parent, "Dynamics and yields of AOTEMPO-mediated polyolefin cross-linking," *Polymer,* vol. 54, pp. 84-89, 2013.

[109] C. J. Hawker, A. W. Bosman and E. Harth, "New polymer synthesis by nitroxide mediated living radical polymerizations," *Chemical Reviews,* vol. 101, pp. 3661-3688, 2001.

[110] I. Li, B. A. Howell, K. Matyjaszewski, T. Shigemoto, P. B. Smith and D. B. Priddy, "Kinetics of decomposition of 2,2,6,6-tetramethyl-1-(1-phenylethoxy)piperidine and its implications on nitroxyl-mediated styrene polymerization," *Macromolecules,* vol. 28, pp. 6692-6693, 1995.

[111] K. Ohno, Y. Tsujii and T. Fukuda, "Mechanism and kinetics of nitroxide-controlled free radical polymerization. Thermal decomposition of 2,2,6,6-tetramethyl-1-polystyroxypiperidines," *Macromolecules,* vol. 30, pp. 2503-2506, 1997.

[112] D. Greszta and K. Matyjaszewski, "Mechanism of controlled/"living" radical polymerization of styrene in the presence of nitroxyl radicals. Kinetics and simulations," *Macromolecules,* vol. 29, pp. 7661-7670, 1996.

[113] G. S. Ananchenko and H. Fischer, "Decomposition of model alkoxyamines in simple and polymerizing systems. 1. 2,2,6,6-tetranmethylpiperidinyl-N-oxyl-based compounds," *Journal of Polymer Science: Part A: Polymer Chemistry,* vol. 39, pp. 3604-3621, 2001.

[114] P. Gijsman, "Photostabilization of Polymer Materials," in *Photochemistry and Photophysics of Polymer Materials*, Weinheim, Germany, Wiley, 2010, pp. 627-679.

[115] F. Gugumus, "Current trends in mode of action of hindered amine light stablizers," *Polymer Degradation and Stability,* vol. 40, pp. 167-215, 1993.

[116] J. Pospisil, "Aromatic and Heterocyclic Amines in Polymer Stabilization," in *Advances in Polymer Science*, vol. 124, 1995, pp. 87-189.

[117] G. Gryn'ova, K. U. Ingold and M. L. Coote, "New insights into the mechanism of amine/nitroxide cycling during the hindered amine light stabilizer inhibited oxidative degradation of polymers," *Journal of the American Chemical Society,* vol. 134, pp. 12979-12988, 2012.

[118] N. S. Allen, "Recent advances in the photo-oxidation and stabilization of polymers," *Chemical Society Reviews,* vol. 15, pp. 373-404, 1986.

[119] A. M. J. Porter, *Imidazolium Ionomer Derivatives of Poly(isobutylene-co-isoprene),* Master's Thesis: Queen's University, Kingston, Canada, 2011.

[120] Y. Masahiro, "Method for producing high-purity imidazole compound containing (meth)acryloyl group". Japan Patent 2010-260850, 18 11 2012.

[121] M. D. Green, D. Wang, S. T. Hemp, J.-H. Choi, K. I. Winey, J. R. Heflin and T. E. Long, "Synthesis of imidazolium ABA triblock copolymers for electromechanical transducers," *Polymer,* vol. 53, pp. 3677-3686, 2012.

[122] R. S. Varma and V. V. Namboodiri, "An expeditious solvent-free route to ionic liquids using microwaves," *Chemical Communications,* no. 7, pp. 643-644, 2001.

[123] M. S. Hindman, A. D. Stanton, C. A. Irvin, D. A. Wallace, J. D. Moon, K. R. Reclusado, H. Liu, K. A. Belmore, Q. Liang, M. S. Shannon, C. H. Turner and J. E. Bara, "Synthesis of 1,2-dialkyl-, 1,4(5)-dialkyl-, and 1,2,4(5)-trialkylimidazoles via a one-pot method," *Industrial and Engineering Chemistry Research,* vol. 52, pp. 11880-11887, 2013.

[124] D. Bogdal and K. Jaskot, "Synthesis of vinyl monomers with active azaaromatic groups. Phase-transfer catalytic approach.," *Synthetic Communications,* vol. 30, no. 18, pp. 3341-3352, 2000.

[125] ASTM International, "Designation: D3182 - 07. Standard Practice for Rubber - Materials, Equipment, and Procedures for Mixing Standard Compounds and Preparing Standard Vulcanized Sheets," 1 May 2012. [Online]. Available: http://enterprise2.astm.org/DOWNLOAD/D3182.144734-1.pdf. [Accessed 24 July 2013].

[126] ASTM International, "Designation: D412 - 06a. Standard Test Methods for Vulcanized Rubber and Thermoplastic Elastomers - Tension," 1 January 2013. [Online]. Available: http://enterprise2.astm.org/DOWNLOAD/D412.144734-1.pdf. [Accessed 24 July 2013].

[127] ASTM International, "Designation: D4482 - 11. Standard Test Method for Rubber Property - Extension Cycling Fatigue," 1 May 2011. [Online]. Available: http://enterprise2.astm.org/DOWNLOAD/D4482.144734-1.pdf. [Accessed 24 July 2013].

[128] A. Stanger, "A simple and intuitive description of C-H bond energies," *European Journal of Organic Chemistry,* vol. 34, pp. 5717-5725, 2007.

[129] B. I. Chaudhary, J. M. Cogen and J. S. Parent, "Thermal analyses of organic powders made from precipitation polymerization of triallyl monomers," *Journal of Thermal Analysis and Calorimetry ,* vol. 105, pp. 279-285, 2011.

[130] H. Oie, A. Sudo and T. Endo, "Synthesis of networked polymers by crosslinking reactions of polybenzoxazines bearing allyl group in the side chain," *Journal of Polymer Science: Part A: Polymer Chemistry,* vol. 51, no. 9, pp. 2035-2039, 2013.

[131] G. Zhang, X. Liu, B. Li and Y. Bai, "Solution copolymerization of acrylonitrile with 1-allyl-3-methyl-imidazolium," *Acta Polymerica Sinica,* vol. 3, pp. 216-221, 2009.

[132] M. Hirao, K. Ito and H. Ohno, "Preparation and polymerization of new organic molten salts; N-alkylimidazolium salt derivatives," *Electrochimica Acta,* vol. 45, pp. 1291-1294, 2000.

[133] J. Gao and J. H. Weiner, "Range of Validity of the Entropic Spring Concept in Polymer Melt Relaxation," *Macromolecules,* vol. 25, pp. 3462-3467, 1992.

[134] A. V. Lubnin, I. Orszagh and J. P. Kennedy, "The Microstructure of poly(isobutylene-co-p-methylstyrene) by NMR Spectroscopy," *Journal of Macromolecular Science,* vol. 32, no. 11, pp. 1809-1830, 1995.

Appendix A

Supporting Spectra for Chapter 2

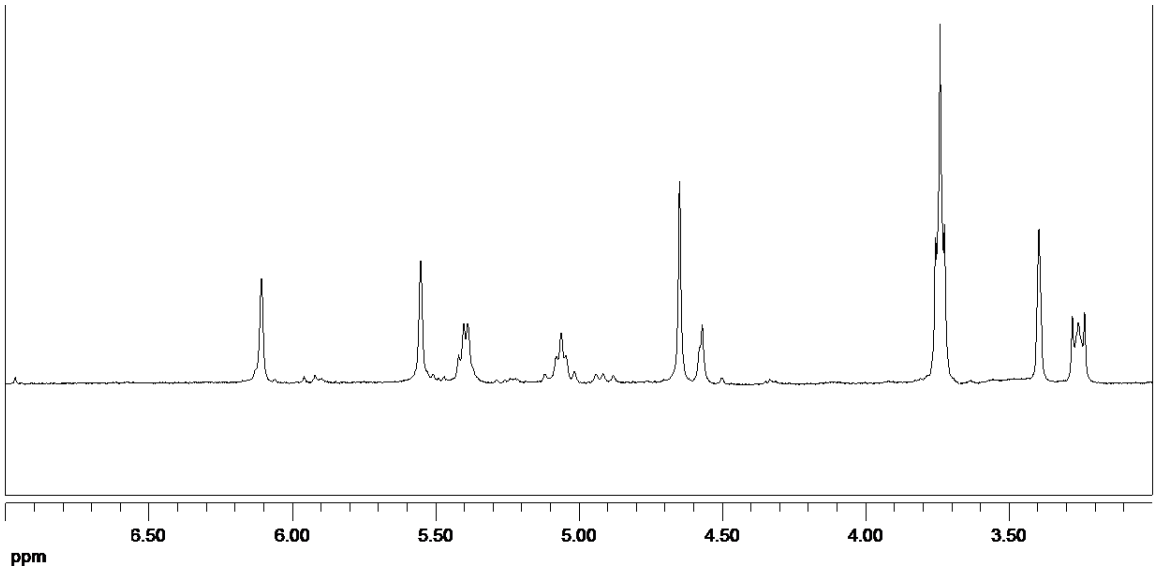

Figure 17: Downfield region of ^{1}HNMR spectrum of IIR-MAA

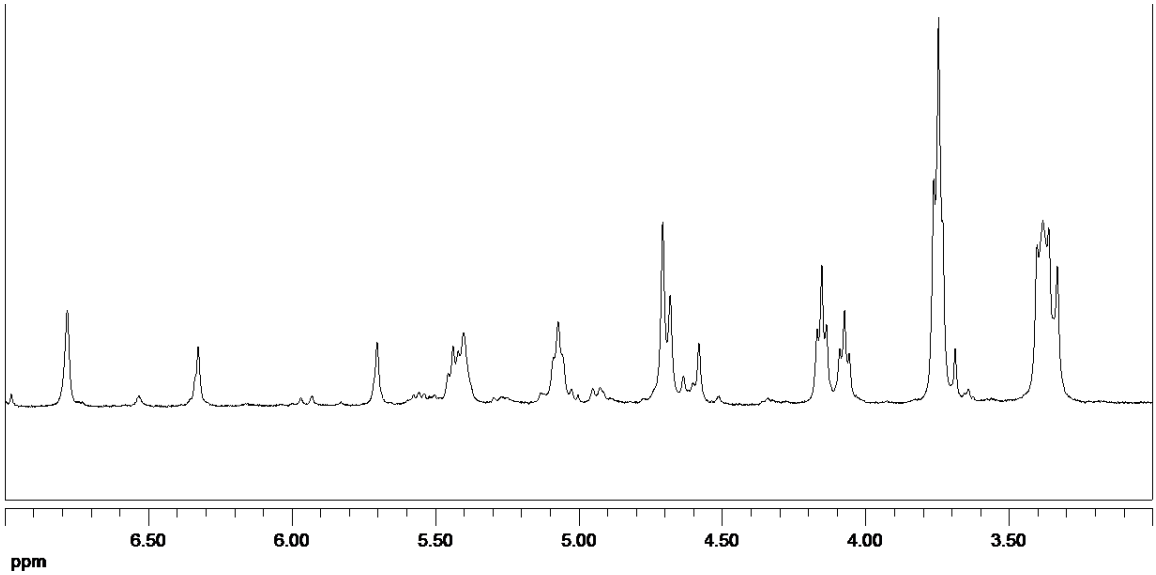

Figure 18: Downfield region of ^{1}HNMR spectrum of IIR-DDI

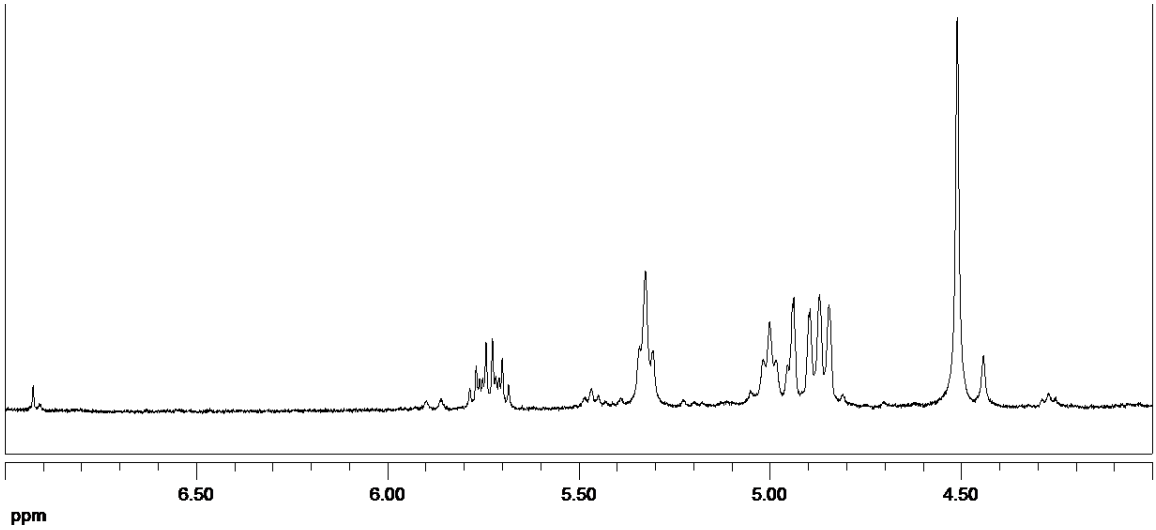

Figure 19: Downfield region of ^{1}HNMR spectrum of IIR-UA

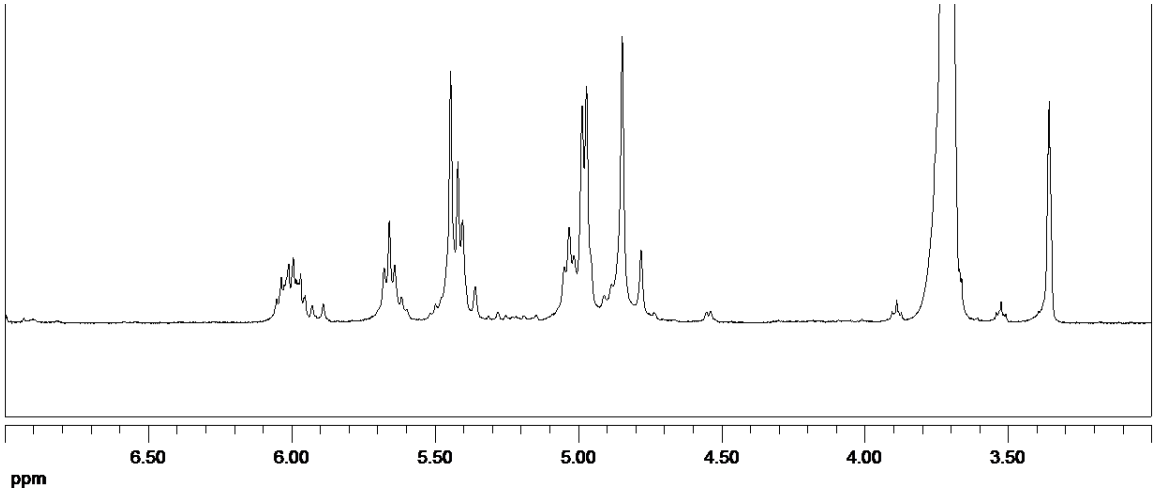

Figure 20: Downfield region of ^{1}HNMR spectrum of IIR-AlImBr

Appendix B

Supporting Spectra for Chapter 3

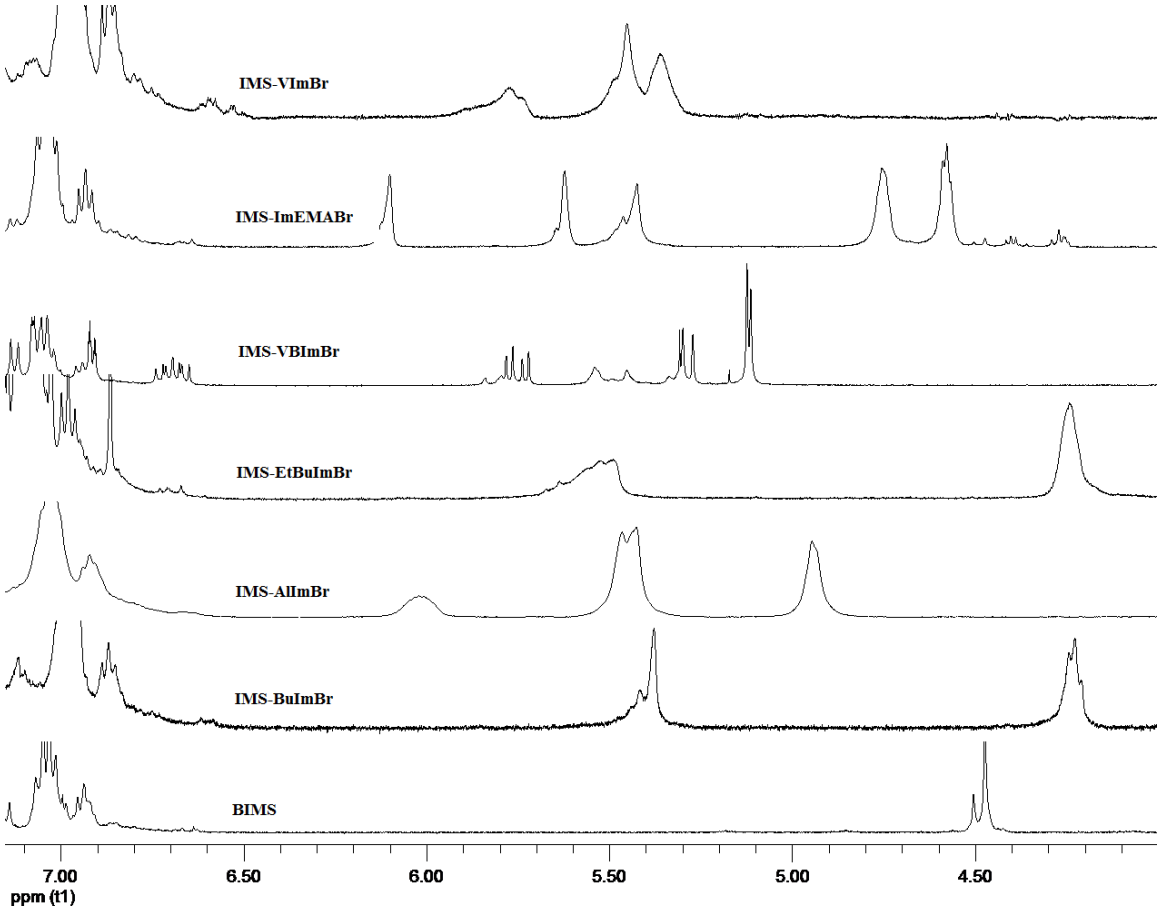

Figure 21: Downfield region of ^{1}HNMR spectra for each fully converted ionomer included in this study. Conversion data collected by comparing integration of BIMS benzylic bromide protons (appearing as two singlets at 4.50ppm [134]) to product ionomer benzylic protons.

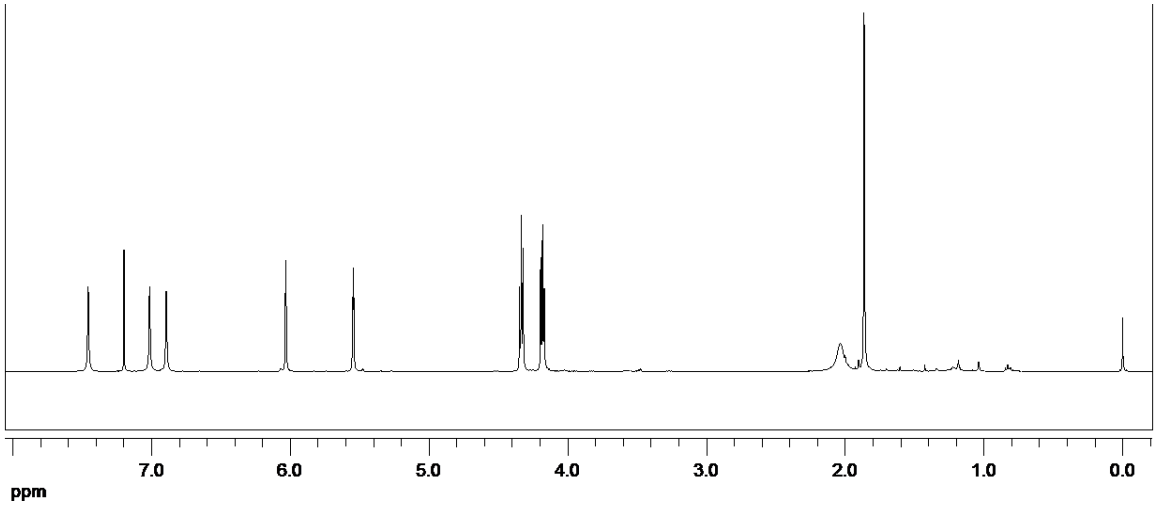

Figure 22: ^{1}HNMR spectrum of ImEMA

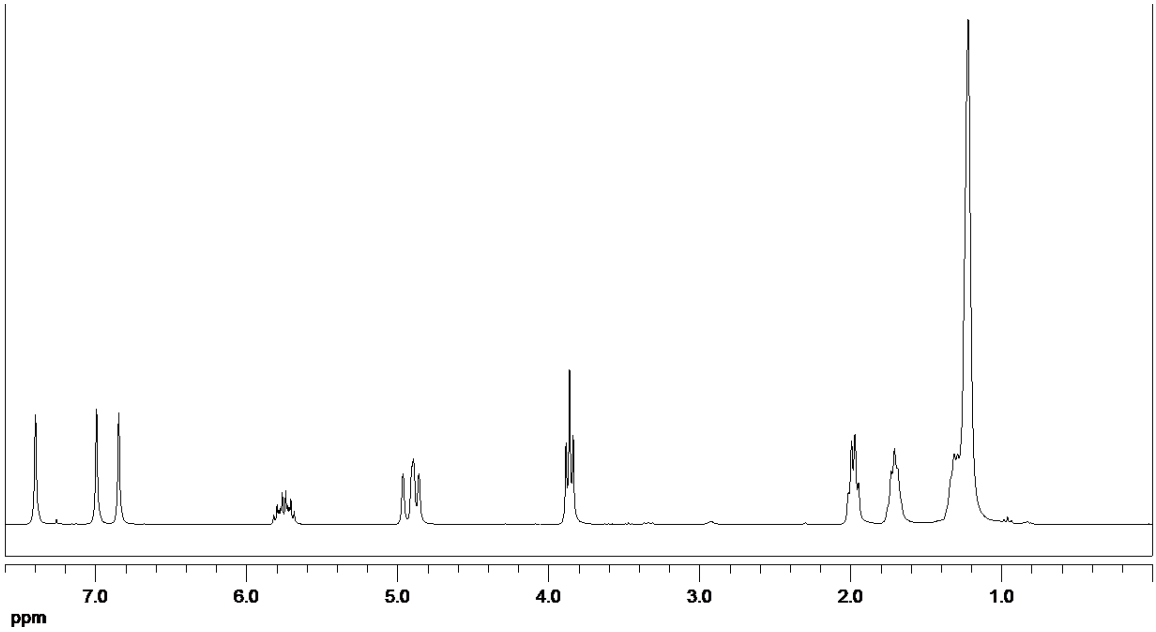

Figure 23: ^{1}HNMR spectrum of UDIm

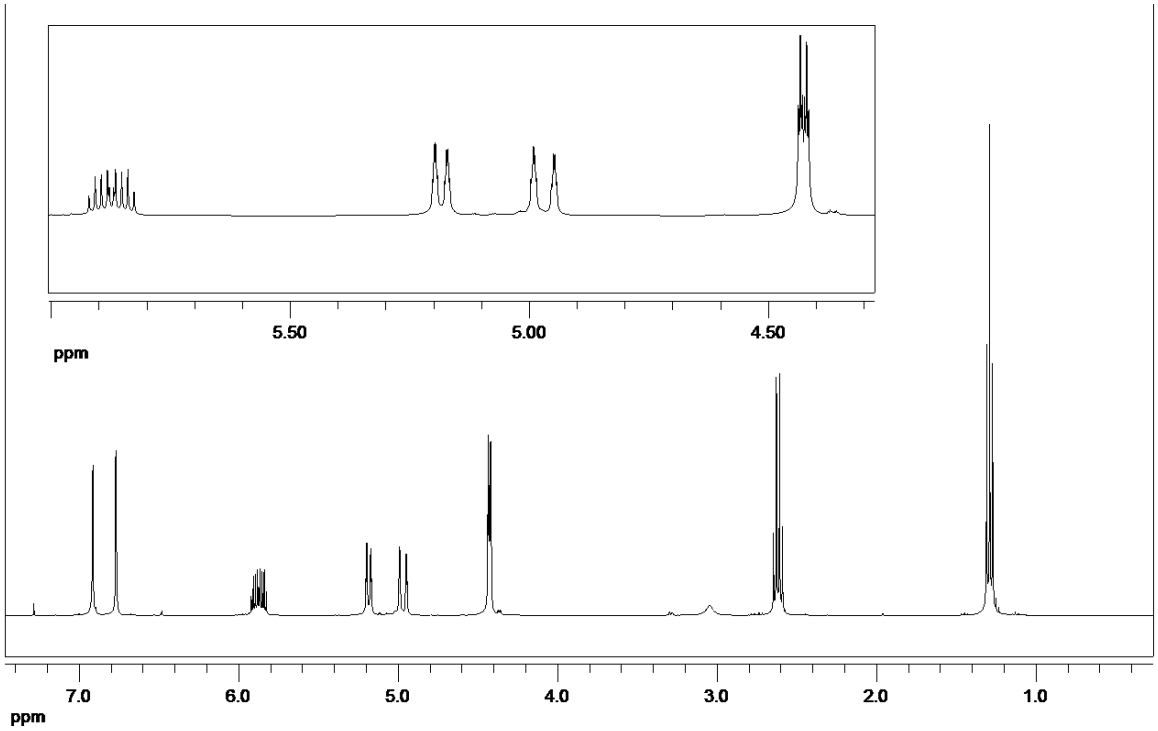

Figure 24: ^{1}HNMR spectrum of EtAlIm

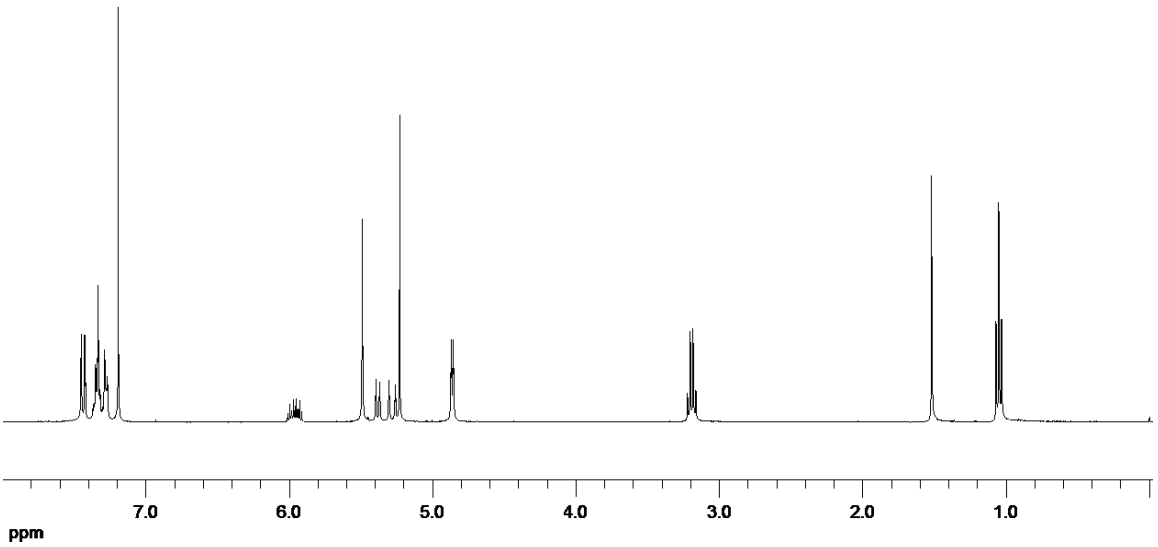

Figure 25: ^{1}HNMR spectrum of PhEtAlImBr

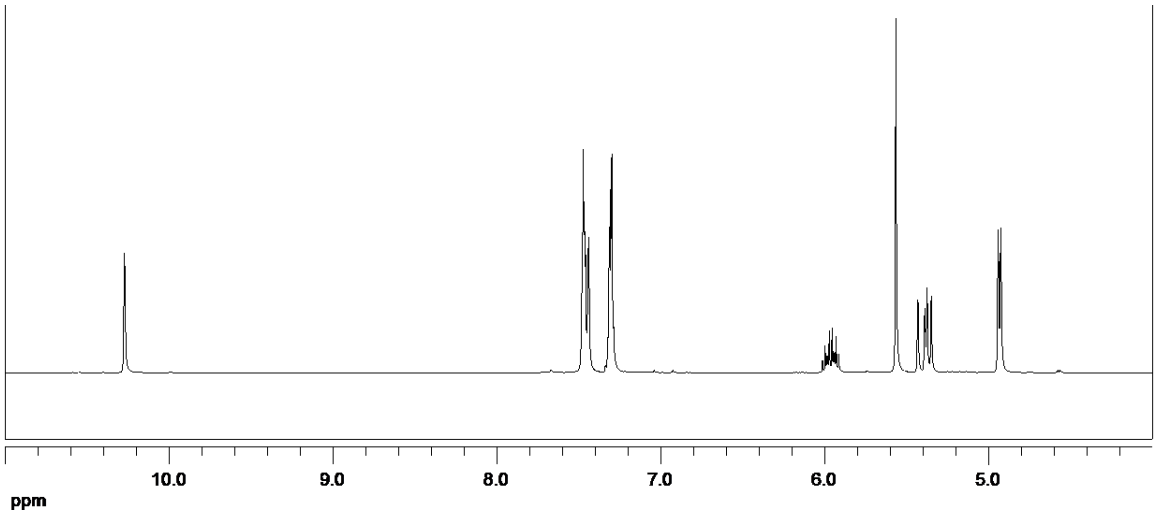

Figure 26: ^{1}HNMR spectrum of PhAlImBr

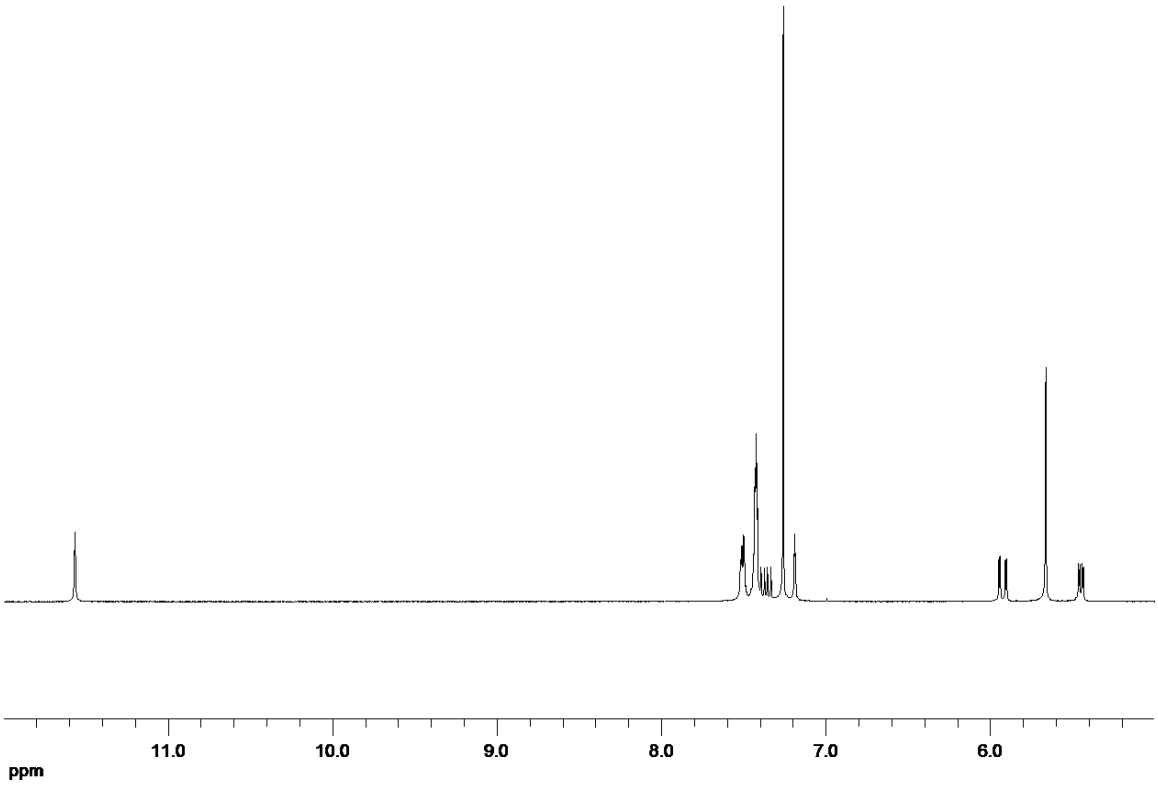

Figure 27: ^{1}HNMR spectrum of PhVImBr